Synthesis and NMR Structure Determination of Bis-Amino Acid Oligomers

by

Paul M. Morgan

B.S., California University of Pennsylvania, 1993

Submitted to the Graduate Faculty of

Arts and Sciences in partial fulfillment

of the requirements for the degree of

Doctor of Philosophy

University of Pittsburgh

2007

UNIVERSITY OF PITTSBURGH

Department of Chemistry

This thesis was presented

by

Paul M. Morgan

It was defended on

August 8, 2006

and approved by

Dr. Paul Floreancig, Department Chemistry

Dr. Angela Gronenborn, Department of Structural Biology

Dr. Megan Spence, Department of Chemistry

Thesis Director: Dr. Christian Schafmeister,Department of Chemistry

Synthesis and NMR Structure Determination of Bis-Amino Acid Oligomers

Paul M. Morgan, PhD

University of Pittsburgh, 2007

I present the complete synthesis of 3 bis-amino acid monomers. The *pro3* class monomer was designed to create a sharp turn in bis-peptide oligomeric sequences. The *pro3*(2S4S) monomer was synthesized, but had an unexpected tendency to epimerize when incorporated into an oligomer. The synthesis of two pip5 class monomers was complete.

I present the first use of residual dipolar couplings (RDCs) in the solution structure determination of a bis-peptide oligomer. This technique allows the determination of bond orientations with respect to the magnetic field of a nuclear magnetic resonance (NMR) spectrometer. I showed that the information gained from the measurement of RDCs can be used to filter a library conformational models to select the best fit model to the RDC data. The best fit model was found to be the lowest energy conformation of the bis-peptide oligomer.

TABLE OF CONTENTS

LIST OF TABLES

LIST OF FIGURES

LIST OF SCHEMES

PREFACE

I would like to thank Dr. Chris Schafmeister for years of advice and support. I would like to thank the members of my thesis committee for their time and talent in guiding my research.

I would like to thank the members of the University of Pittsburgh Chemistry Department. The faculty for your knowledge, and the staff for your helpfulness.

Lastly, I would like to thank the person without whom I could not have done this, my wife, my life, Sherry Lesako.

1.0 INTRODUCTION

Nature's primary tools are proteins. These nanoscale (on the order of 10^{-9} meters in size) machines serve such diverse purposes within organisms as energy transduction and utilization, motion and catalysis. Currently no technology outside of the biological realm has been developed to work as efficiently and diversely on the nanoscale as proteins.

The ability for science to understand how to mimic the capabilities of proteins is hampered by the complexity of the protein folding problem. Proteins are chains of amino acids that undergo a complex and poorly understood folding process in order to attain a well defined and functional three-dimensional structure. Folded proteins place multiple functional groups in precise three-dimensional arrangements and it is such precise location of functional groups that enables proteins to carry out their molecular recognition and catalytic functions. A synthetic approach to create macromolecules that could mimic this placement of functional groups but would avoid the complex process of folding would be a great advance towards the creation of designed nanostructured devices and would allow us to learn a great deal about the relationship between function and structure in macromolecules[1].

1.1 FOLDAMERS

Several groups have developed unnatural oligomers termed "Foldamers" that adopt well defined secondary structures with very short sequences. Gellman has coined the term foldamer "to describe any polymer with a strong tendency to adopt a specific compact conformation"[2]. A goal of foldamer research efforts is the development of molecules which can adopt designed three-dimensional structures and perform designed functions[3].

Diverse foldamers have been developed with a wide range of monomer structures and non-covalent interactions employed to achieve the designed oligomer shape (Figure 1)[3]. While

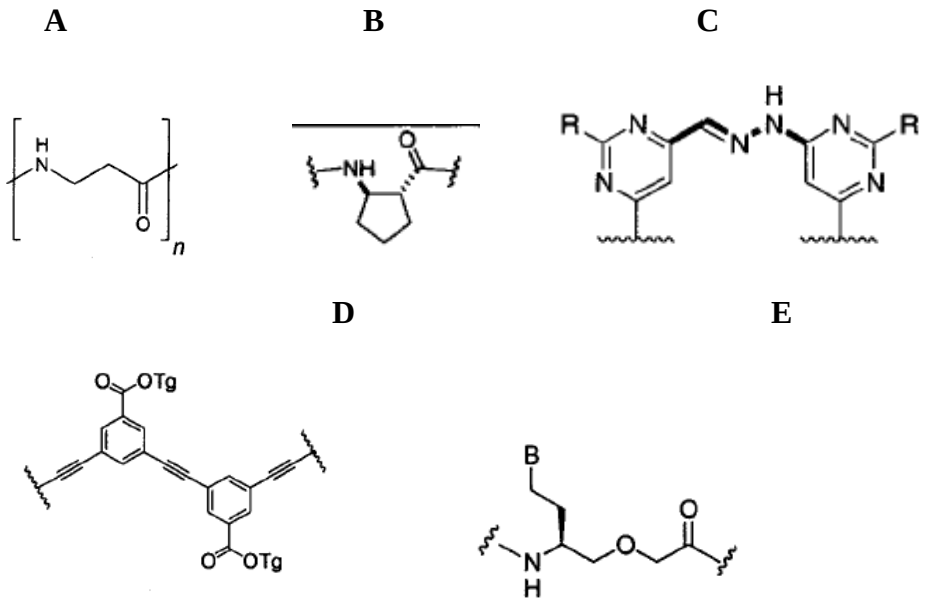

From top left: Seebach (A) and Gellman's (B) β-peptide monomers, Lehn's pyridine-pyrimidine oligomers (C), Moore's phenylene ethynylene oligomers (D), and Nieslen's peptide nucleic acids (PNA's) (E). Each of these monomer types forms a helical structure. Copied from ref. 3.

Figure 1. Sample of Diverse Foldamer Monomer Structures

many unnatural oligomers adopt well defined helical secondary structures, it remains outside of our ability to rationally design foldamers that adopt well defined tertiary structure (Figure 2).

1.2 BIS-PEPTIDE APPROACH TO MACROMOLECULAR SYNTHESIS

In the bis-peptide approach to macromolecular design developed in our lab[4-8], we avoid the use of non-covalent interactions to achieve three-dimensional structure and instead create

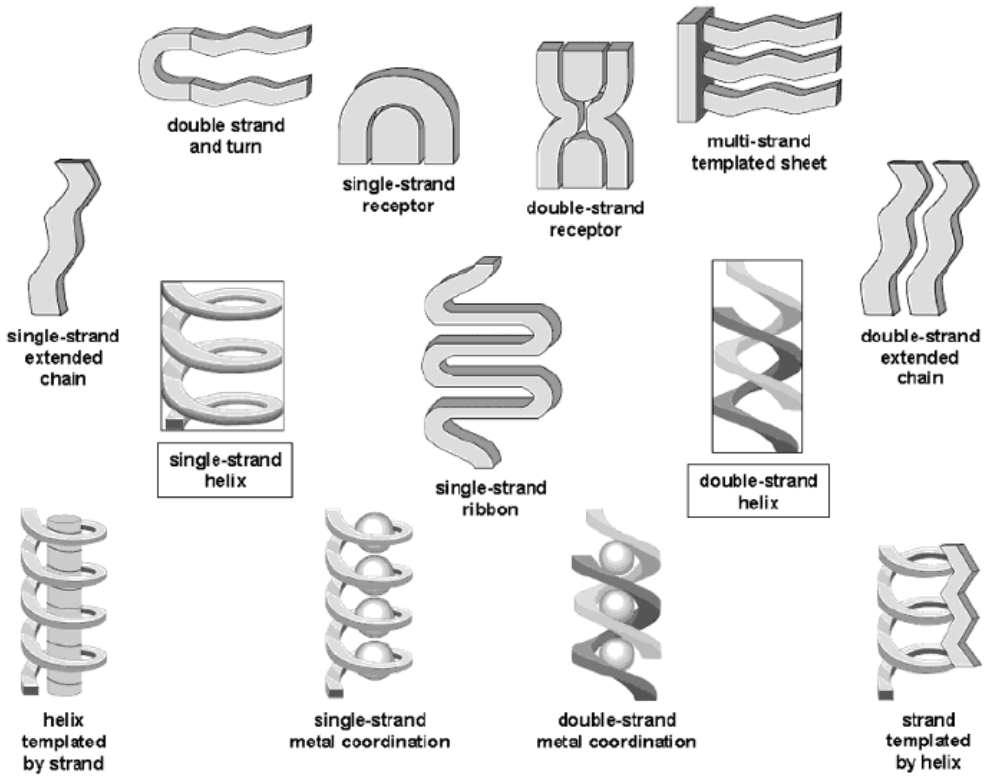

Common structures adopted by foldamers. Copied from reference 3.

Figure 2. Range of Common Shapes Seen in Foldamers

structure by coupling cyclic monomers to each other through pairs of bonds to create spiro-ladder oligomers (Figure 3a).

In our bis-peptide approach, monomers contain two amino acid functionalities displayed on a cyclic framework (Figure 4). We connect the monomers together through pairs of amide bonds forming a 2,5-diketopiperazine linkage as indicated in red in Figure 3a. The diketopiperazine linked oligomers have limited conformational freedom as there are no freely rotating bonds in the oligomer backbone. The three-dimensional shape of bis-peptide oligomers is defined by synthetically controlled features including the structures of the monomer rings, the stereochemical configuration of the stereocenters within each monomer, and the monomer sequence within the oligomer.

A.)

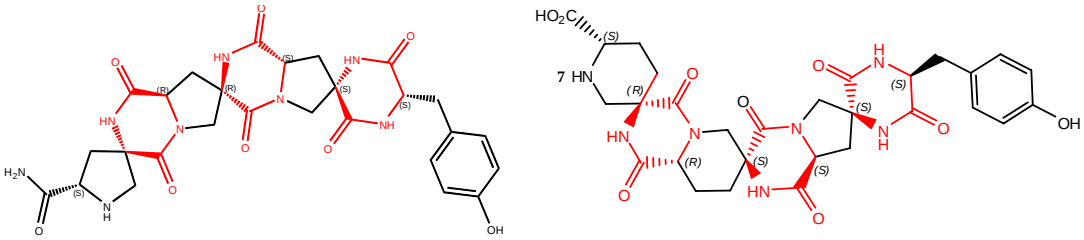

B.)

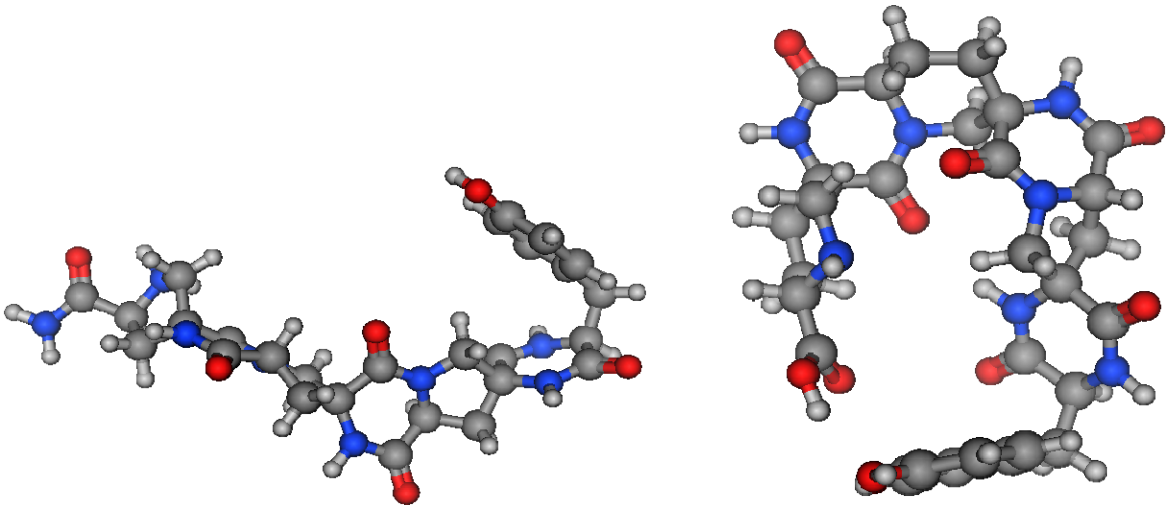

Two bis peptide oligomers shown at top as chemical structures. The solved solution phase NMR structures (Chapter 4) of these compounds.

Figure 3. Example of Two Bis-Peptide Trimers

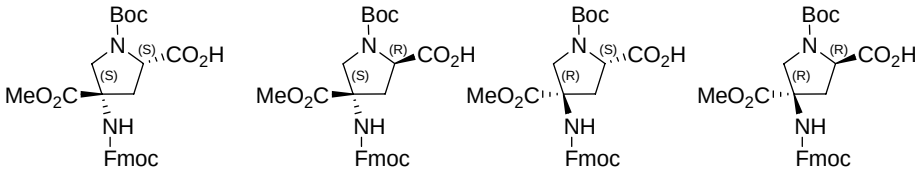

pro4(2S4S) pro4(2R4S) pro4(2S4R) pro4(2R4R)

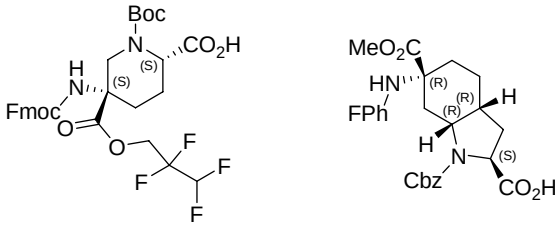

pip5(2S5S) hin(2S4R7R9R)

Figure 4. Currently Developed Bis Amino Acid Monomers

In working to expand our ability to synthesize more complex bis-peptide oligomers, I developed a new class of bis-amino acid monomer that we called the “pro3” monomer class (cf Chapter 2) and I also worked on developing the “pip4” monomer class (cf Chapter 3). In order to better determine the three-dimensional structures of bis-peptides I developed the use of residual dipolar couplings as additional NMR constraints for NMR solution structure determination (cf Chapter 4).

2.0 3-HYDROXY-PROLINE DERIVED MONOMER SYNTHESIS

To develop bis-peptide oliogmers capable of carrying out molecular recognition and biomimetic catalysis, the development of bis-amino acid monomers capable of producing tight turns within these macromolecules is required. We designed a 3-hydroxy-proline derived monomer class (*pro3* class) that, based on modeling in the computer program MOE[9] with the AMBER 94 Force Field[10], would provide such a turn (Figure 5). This chapter details my synthesis of two versions of the *pro3* monomer and my work to incorporate it into a short oligomer. I found that both version of the *pro3* monomer performed poorly in solid phase peptide synthesis with other bis-amino acid monomers and once incorporated into an oligomer, I found that the *pro3* monomer had an unexpected tendency to spontaneously epimerize at the C2 position.

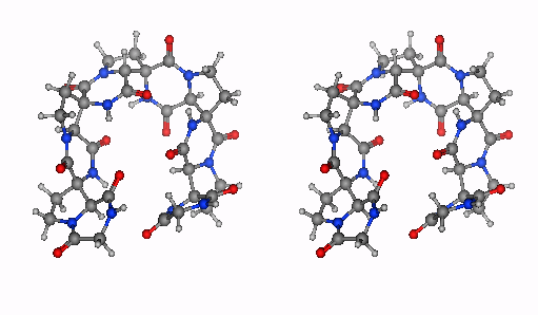

Stereoview of a sequence of 5 *pro3* class monomers sequence Gly-*pro3*(2S3S)-*pro3*(2S3S)-*pro3*(2S3S)-*pro3*(2S3R)-*pro3*(2S3S)-*pro3*(2R3S)-Gly that creates a tightly turned oligomer.

Figure 5. Curved Structure Containing *pro3* Class Monomers

2.1 SYNTHETIC OUTLINE UTILIZING THE BUCHERER-BERGS REACTION

The original retrosynthetic analysis of the *pro3* class monomer synthesis involved the installation of a second α–amino acid functionality on C3 of the pyrrolidine ring through a Bucherer-Bergs[11,12] reaction from the ketone **3** (Scheme 1). β–Ketoester **3** could only be realized in a stereopure manner when the risk of deprotonation at the proline α–carbon was effectively eliminated. We envisioned that a bulky 9-phenyl-9-fluorenyl (PhF)[13] protecting group, **6,** on the secondary amine of **3** would protect the α-proton from epimerization. After the PhF protection, oxidation could be performed to yield the β-ketoester **3** with reduced risk of epimerization[13,14].

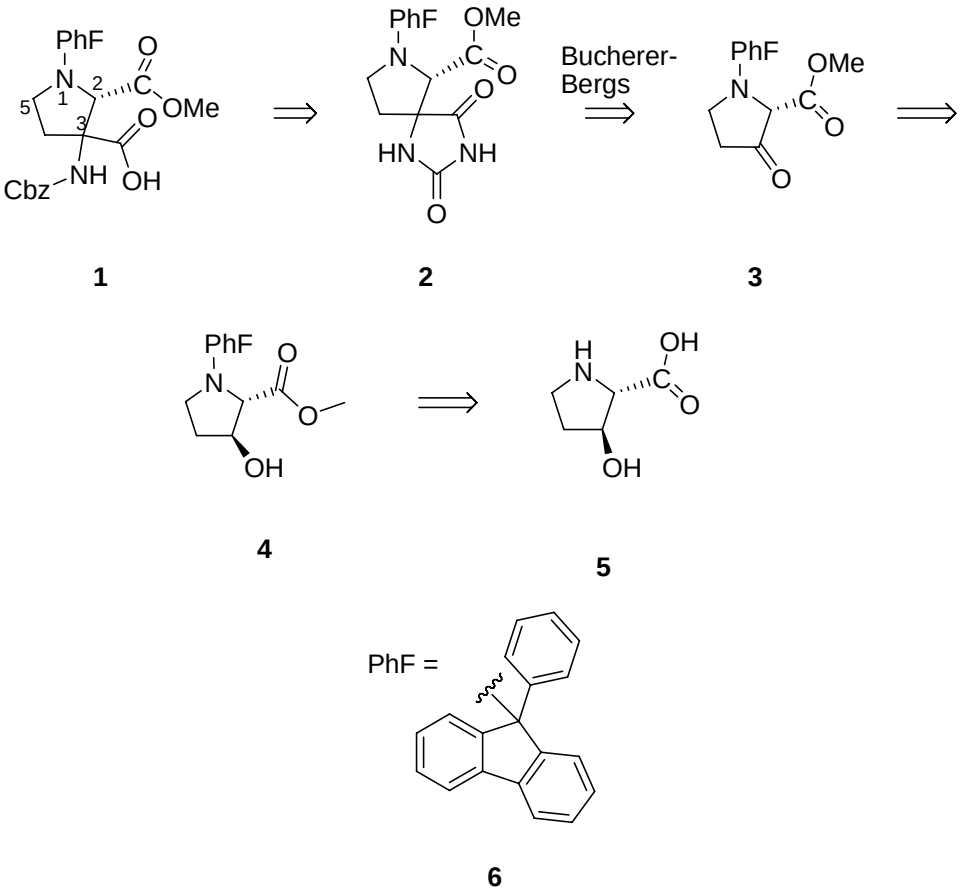

Scheme 1. Retrosynthesis of Monomer via Bucherer-Bergs Reaction.

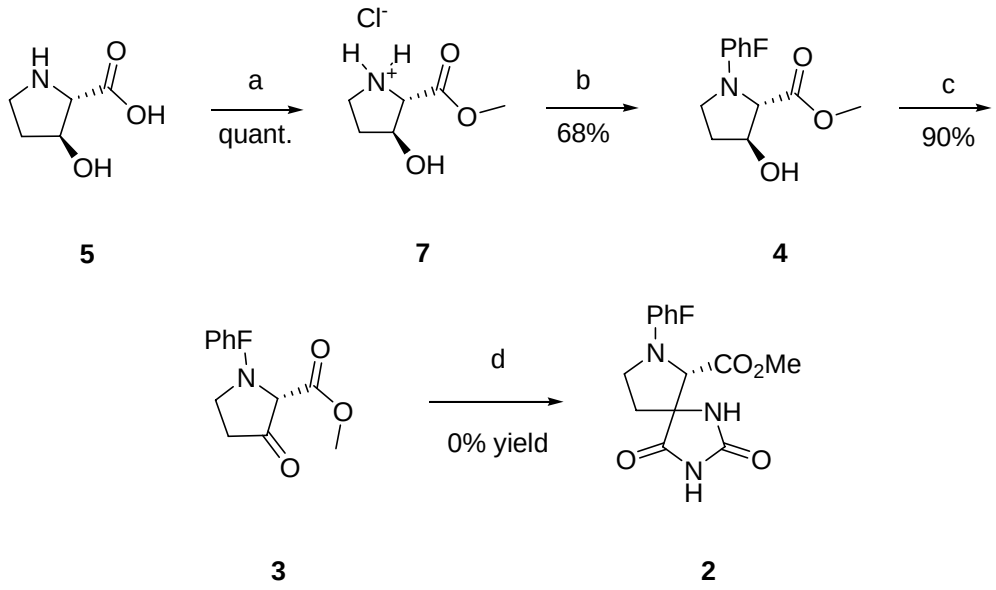

a.) MeOH, HCl (g). b.) i.) 2 eq. TMSCl, DIPEA, DCM, reflux. ii.) 0.9 eq. MeOH, DCM 0 ^{O}C-rt. iii.) PhFBr, $Pb(NO_3)_2$, DIPEA. iv) 10% (w/v) citric acid/MeOH. c.) TPAP, NMO, DCM, 4A M.S d.) KCN, $(NH_4)CO_3$, DMF, H_2O, 60^{o}C

Scheme 2. Synthesis of the β–Ketoester

2.2 RESULTS OF THE BUCHERER-BERGS SYNTHETIC APPROACH

Formation of the methyl ester hydrochloride salt **7** of (2*S*,3*S*)-3-hydroxy–proline, **5,** was accomplished in quantitative yield by Fischer esterification in methanolic hydrogen chloride (Scheme 2).

We were able to protect the secondary nitrogen atom of **7** as the 9-phenyl-fluorenyl amine, **4,** in a one pot, four step process. The amine and hydroxyl groups of **7** were first masked with two equivalents of chlorotrimethylsilane (TMSCl), and the trimethylsilyl (TMS) group on the amine was selectively removed with 0.9 equivalents of methanol. The amine was then reacted with 9-bromo-9-phenyl-fluorene[15] in the presence of lead nitrate to install the PhF protecting group. A solution of 10% citric acid in methanol was used to remove the trimethylsilyl group from the alcohol to form **4** in 68% overall yield from **7**.

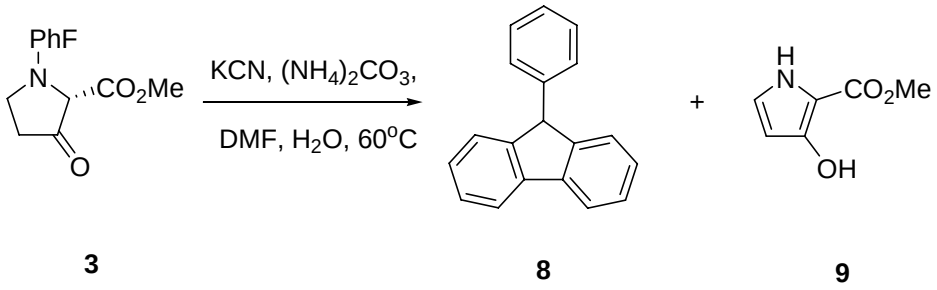

Figure 6. Bucherer-Bergs Reaction Products

Subsequently, **4** was converted to the β-ketoester **3** by oxidation with TPAP (tetrapropylammonium perruthenate) and NMO (4-methyl-morpholine *N*-oxide) in 90% yield. The ketone **3** was subjected to the conditions of the Bucherer-Bergs reaction (KCN, $(NH_4)_2CO_3$, DMF (N,N-dimethylformamide), H_2O, 60°C), but no spirohydantoin **2** could be isolated from the reaction. The isolated products were 9-phenyl-9*H*-fluorene **8** and 3-hyroxy-pyrrole-2-methyl ester, **9** (Figure 6).

Pyrrolidine ring aromatization has been observed by Marcotte and Lubell[16] in 9-phenyl-fluoren-9-yl-3-oxo-proline derivatives, such as **3**, but the exact mechanism has not been determined. An E_1Cb mechanism has been proposed for the transformation and appears in Figure 7[16].

2.3 SYNTHESIS BASED ON A MODIFIED COREY-LINK REACTION

A modified Corey-Link[17,18] reaction was next employed to install the amino acid functionality at C3 of the pyrrolidine ring. This approach (Scheme 3) allowed the synthesis of a *pro3* monomer, with the second amine functionality masked as an azide **10**.

The conversion of the ketone **3** into the trichlorocarbinol diastereomers **11a** and **11b** was accomplished by deprotonation of chloroform at -78°C in THF with LHMDS (lithium

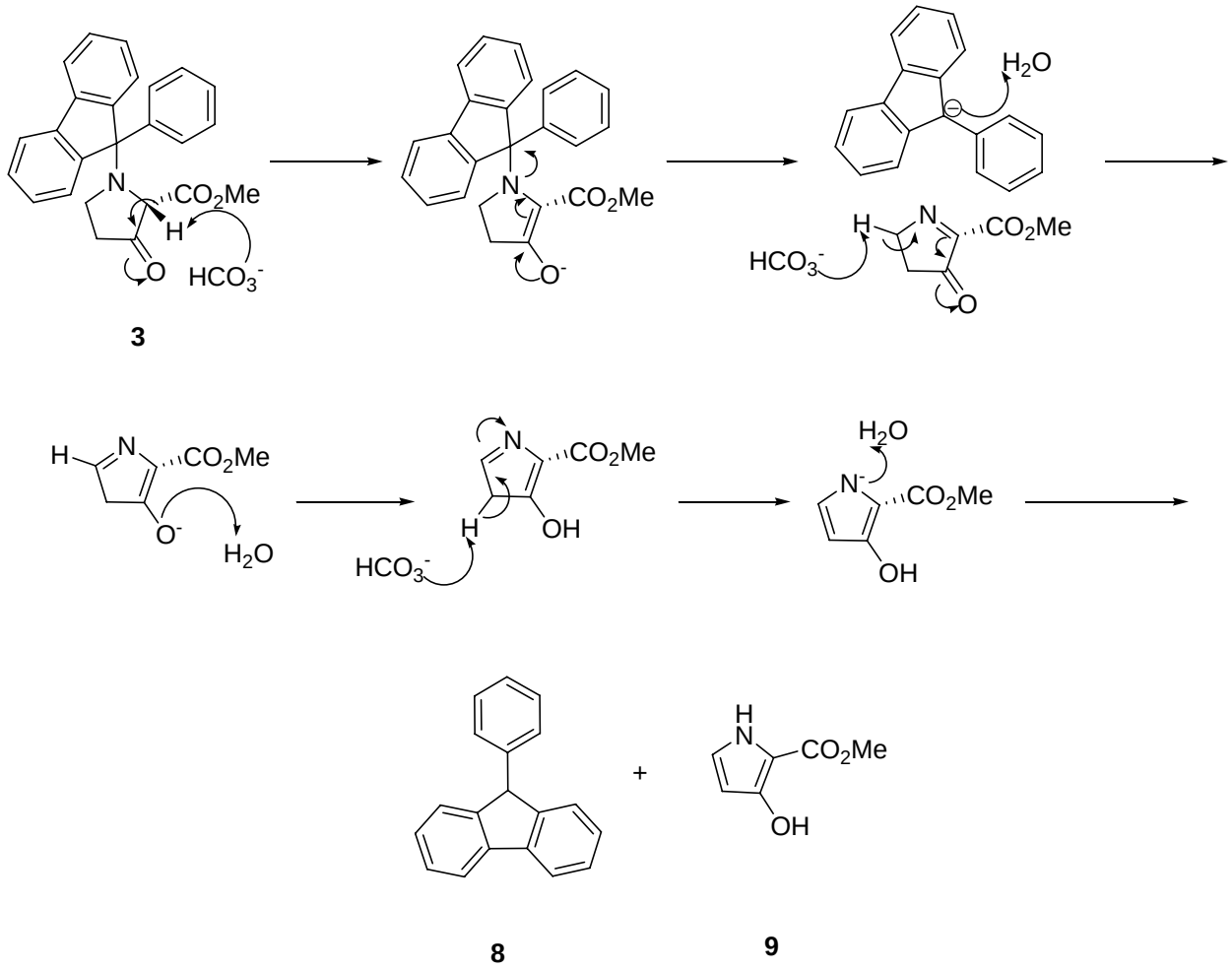

Figure 7. Pyrrole Formation Mechanism from PhF Pyrrolidine

hexamethyldisilazide) resulting in attack on the ketone by the trichloromethyl anion (71.0% overall yield). The trichloromethyl anion was observed to favor addition from the *si* face of the ketone over the *re* face (Figure 8) in a 15:1 ratio as determined by HPLC analysis of the quenched reaction mixture. The preference for formation of **11a** over **11b** was due to the

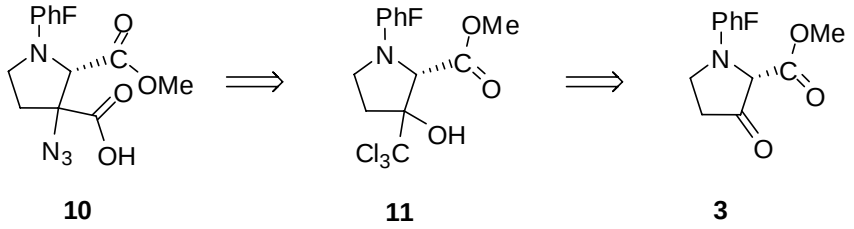

Scheme 3. Retrosynthesis via the Modified Corey-Link Reaction

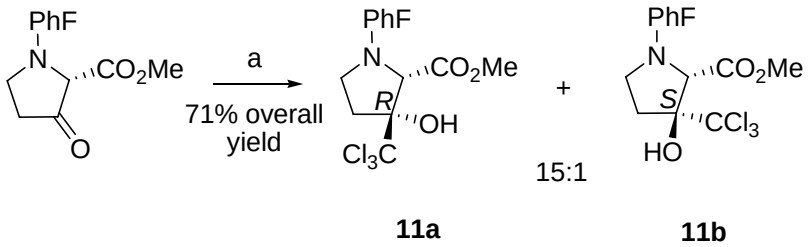

a.) LHMDS, $CHCl_3$, THF, -78°C

Figure 8. Diastereomeric Preference of the Trichloromethyl Anion Addition

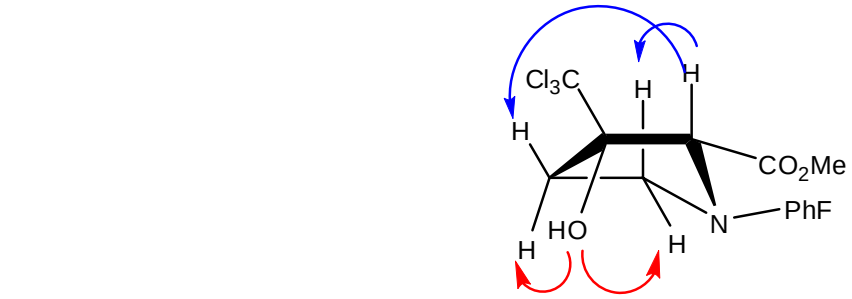

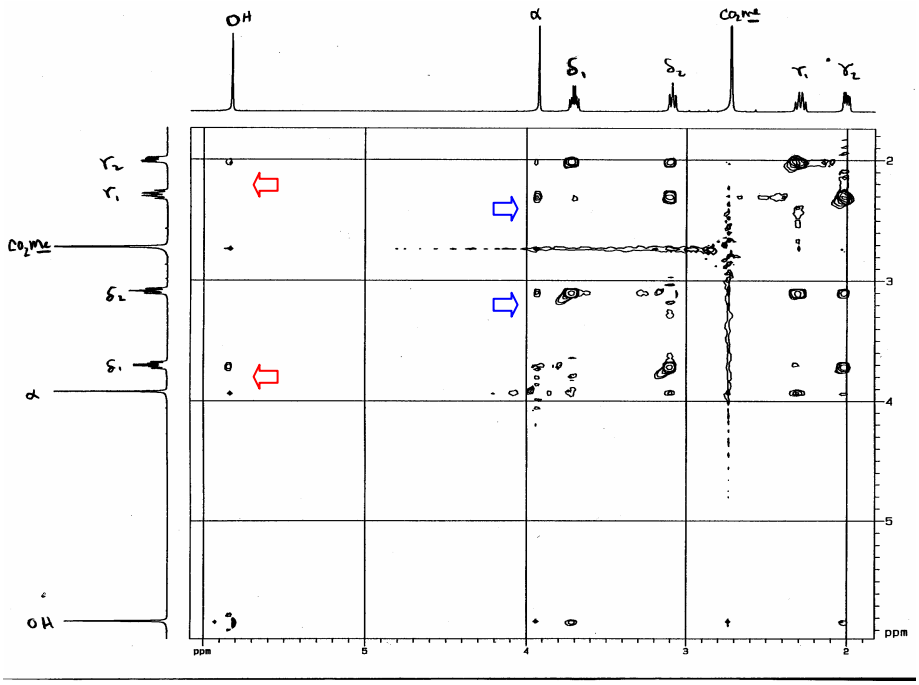

Arrows indicate major cross peaks of note.

Figure 9. 500 MHz ROESy Spectrum of Major Diastereomer of Trichlorocarbinol 11a

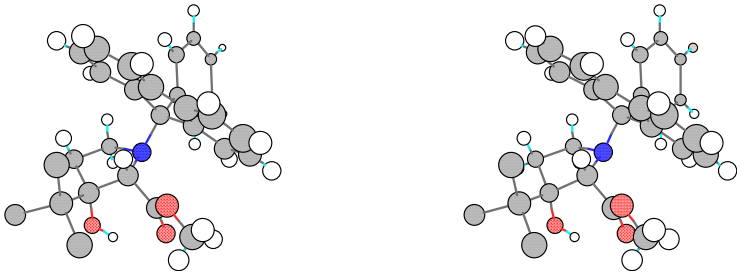

Figure 10. Stereoview of X-ray Diffraction Crystal Structure of 11a

presence of the methyl ester at C2. Compound **11a** was purified by column chromatography followed by crystallization from ethyl acetate and hexanes.

Assignment of the stereochemistry at the C3 center of the major trichlorocarbinol product was initially performed using ROESY NMR spectroscopy in deuterated chloroform. In the ROESY spectrum (Figure 9), strong correlations were observed between the alcohol proton and one of each of the geminal hydrogen atoms on the γ- and δ-carbons of the pyrrolidine ring, while the C2 hydrogen atom displayed strong correlations in the spectrum with the opposite geminal hydrogen atom on each of these carbon atoms. This evidence led to our conclusion that the alcohol and the C2 hydrogen atom were on opposite faces of the pyrrolidine ring in the major diastereomer. This stereochemical relationship was confirmed by the X-ray diffraction crystal structure obtained from the major diastereomer (Figure 10).

The formation of the dimethyl ester **12** from trichlorocarbinol **11a** was accomplished using sodium methoxide in methanol solvent (83 % yield), while conversion of **11a** to the α-azidoacid **13** (yield 95%) was performed with sodium hydroxide in 3:2 dioxane: water (Scheme 4).

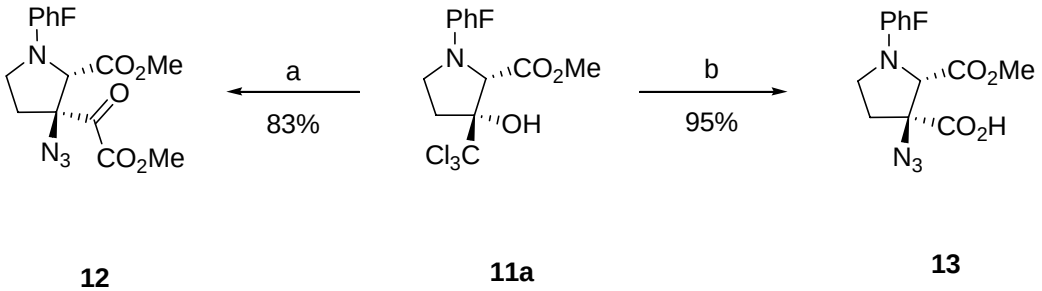

12 **11a** **13**

a.) NaOMe, NaN_3, MeOH, RT b.) NaOH, NaN_3, 18-crown-6, dioxane, water, RT

Scheme 4. Conversion of the Trichlorocarbinol to α-Azido Carbonyl Compounds

The mechanism proposed for conversion of the trichlorocarbinol **11a** into **12** and **13** was put forth by Corey and Link[17,18] (Figure 11). Initiation of the reaction was accomplished by deprotonation of the C3 alcohol with either sodium methoxide or sodium hydroxide. The C3 alkoxide performed an S_N2 attack on the trichloromethyl group to form a dichloroepoxide intermediate. Opening of the dichloroepoxide at C3 of the pyrrolidine ring with azide ion resulted in the formation of an acid chloride. The resultant acid chloride further reacted with either methanol or water solvent to yield either **12** (83.7 % yield) or **13** (95.2% yield) respectively.

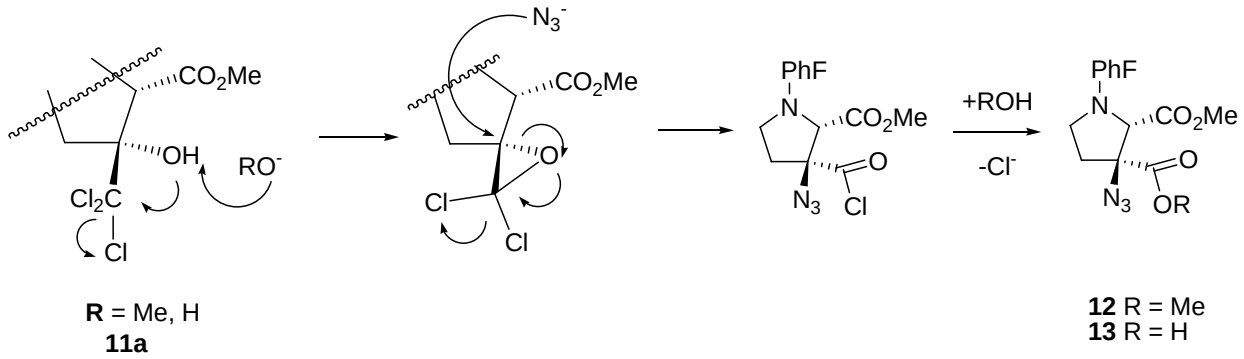

Figure 11. Corey-Link Reaction Mechanism

2.4 DETERMINATION OF THE PURITY OF THE MONOMER

The stereochemical purity of acid **13** was determined by formation of an amide bond to samples of both (*R*)- and (*S*)-phenylethylamine using HATU (*O*-(7-azabenzotriazol-1-yl)-*N*,*N*,*N*',*N*'-tetramethyluronium hexafluorophosphate) in 20% dichloromethane (DCM) in DMF (N,N-dimethylformamide). The reaction provided diastereomeric derivatives of **13** that could be differentiated using reverse phase HPLC (Figure 12). In the chromatogram, trace R refers to **13** reacted with (*R*)-phenylethylamine, trace S refers to the product of the reaction with the (*S*) enantiomer of the amine, and trace R+S is a mixture of samples from the (*S*)- and (*R*)-phenylethylamine products. The products of both the (R) and (S) enantiomers yielded expected *m/z* ($[M+H]^+$) = 558 by LCMS. The results reveal that the product **13** of the Corey-Link reaction can be isolated as a single stereoisomer with greater than 99% purity.

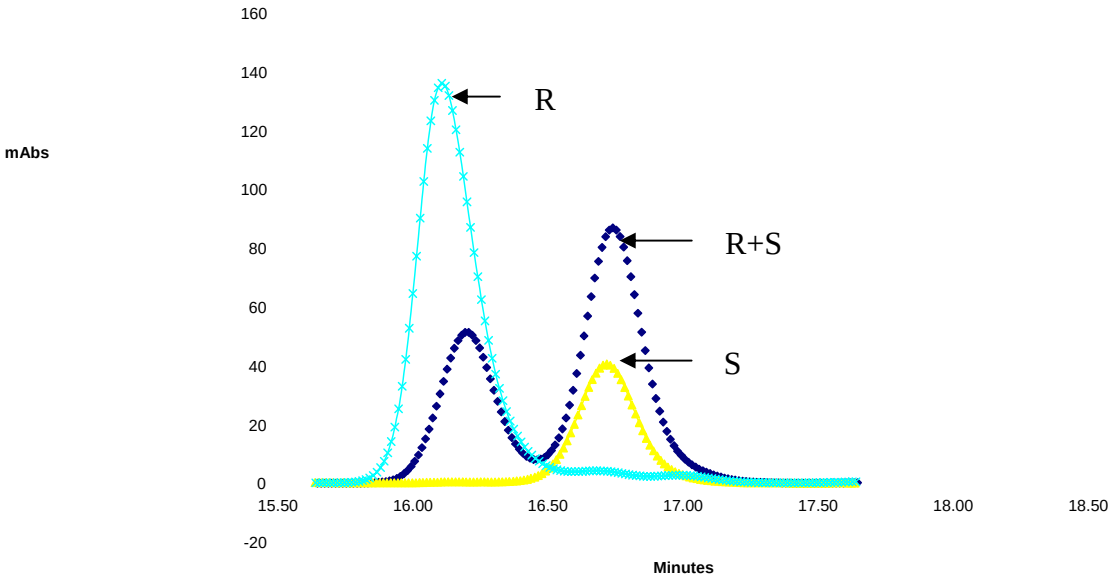

HPLC traces of **13** coupled to either *(R)*- or *(S)*-phenylethylamine and a mixture of both products. Each sample (5μL) was introduced to the C_{18} column in methanol at room temperature. The solvent was run at a gradient of 50% to 80% over 30 minutes of acetonitrile in H_2O with 0.1% TFA added. The milliabsorbance of the solution was measured at 274 nm

Figure 12. HPLC Trace of Products of (R) and (S)-Phenylethylamine Coupling

2.5 SOLUTION PHASE COUPLING OF MONOMERS

Solid phase peptide synthesis techniques were employed in an attempt to form a short oligomer containing two monomers of **13.** The formation of the sequence Tyr-**13**-**13**-Ala (Scheme 5) was attempted on a resin with an MBHA (methylbenzhydrylamine) linker and another resin with a hydrazine linker. The resins were treated to cleave the sequence from the linkers, and the resulting products were analyzed by LC/MS. The mass spectrum of each cleavage solution contained a component consistent with amide bond formation between tyrosine

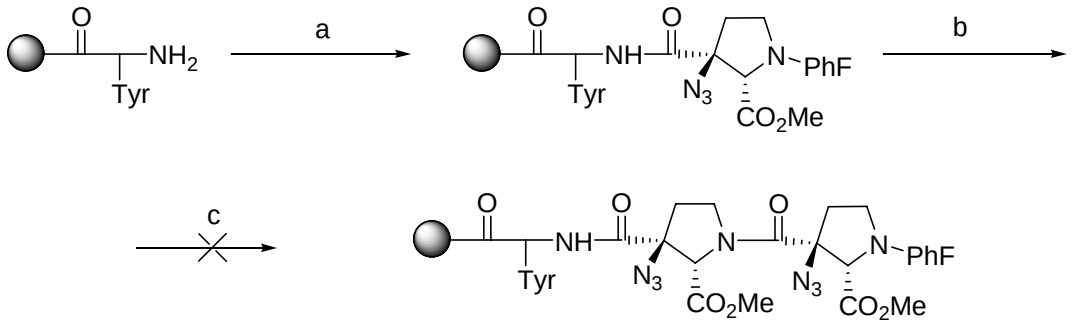

A.) **13** (2 eq.), HATU (2eq.), DIPEA, 20% DMF in DCM. B.) 1:1 DMC:TFA (trifluoroacetic acid) C.) **13** (2 eq.), HATU (2eq.), DIPEA, 20% DMF in DCM. Reactions were performed on both MBHA and Hydrazino likers on a polystyrene bead.

Scheme 5. Attempt to Form a Tyr-13-13-Ala Sequence on Solid Phase

and **13**, however the mass spectrometry data showed no compound with a mass corresponding to the incorporation of a second monomer of **13**.

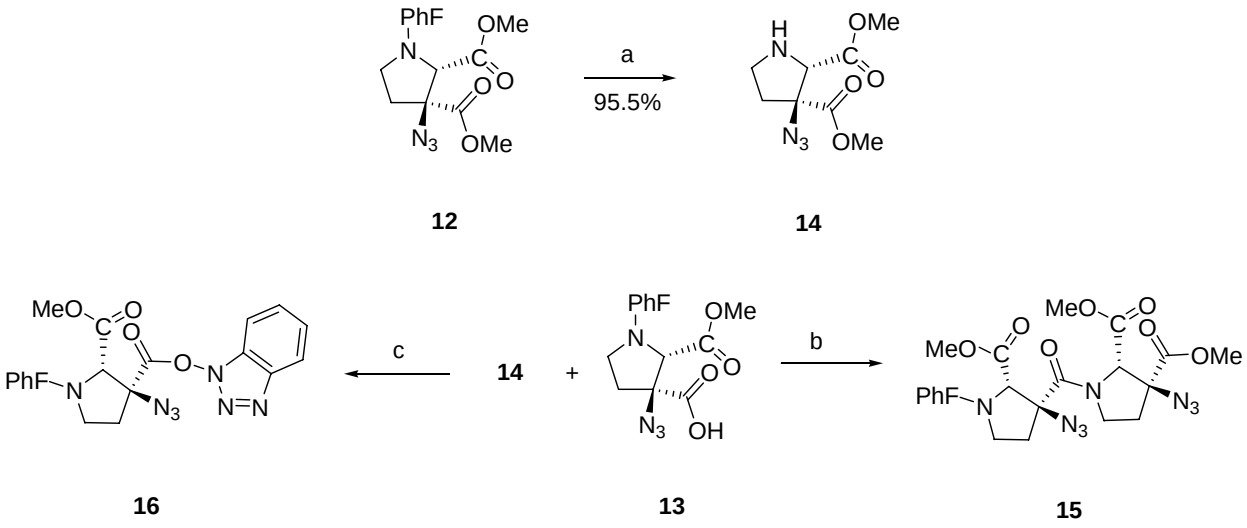

a.) 2.5% TFA, 3 eq. MeOH, DCM, 30 min RT. b.) see Table 1. c.) HOBt, DCC, THF, DCM

Scheme 6. Dimer Formation with the Secondary Amine in Solution Phase

We next attempted the solution phase formation of an amide bond between the acid in **13** and the pyrrolidine nitrogen atom of another monomer, **14** (Scheme 6). The pyrrolidine nitrogen atom in dimethyl ester **12** was deprotected using 2.5% TFA (trifluoroacetic acid) in DCM to yield **14** in 95% yield. The coupling of **14** and **13** was attempted using HOBt (hydroxyl

benztriazole) and DCC (dicyclohexylcarbodiimide) in 4:1 THF (tetrahydrofuran):DCM (Scheme 6). From this reaction **13** and its hydroxyl benztriazole (OBt) ester **16** were isolated after purification by silica gel chromatography. The isolation of the **16** suggested that the coupling had failed due to steric crowding at the C3 acid of **13** as the OBt esters are considered to be highly electrophilic esters. Compound **16** partially hydrolyzed over two days back into the acid **13** upon exposure to ambient conditions.

Solution phase formation of dimer **15** with coupling agents TFFH (tetrafluoroformamidinium hexalfluorophosphate), PyBrop (Bromo-tris-pyrrolidino-phosphonium hexafluorophosphate) or HATU demonstrated some amide bond formation between **13** and **14**, but yields of **15** were low (Table 1). The best yield of **15** (yield 36.4%) occurred using HATU in 20% DCM in DMF incubated at room temperature for 24 hours. The isolated product **15** was characterized by high-resolution mass spectrometry, but attempts to obtain a ^{1}H NMR spectrum free from rotational isomers were unsuccessful at temperatures up to and including 360 K.

Table 1. Conditions and Yields of Coupling Reactions to Form 15

Coupling Reagent	Equivalents of **13**	Equivalents of **14**	Solvent	Reaction Time (hour)	Yield of **15**
HATU	1.0	1.0	20% DMF in DCM	24	34%
PyBroP	1.25	1.0	DCM	24	27%
HATU	1.5	1.0	DMF	24	9%
TFFH	1.26	1.0	DCM	24	0%
HOBt, DCC	1.26	1.0	4:1 THF:DCM	18	0%

2.6 SYNTHESIS OF THE MONOMER WITH A CARBOXYLIC ACID AT C2

Due to the low yields of amide bond formation with the C3 acid in **13**, the synthesis of the *pro3* class of monomers was modified to allow the installation of a carboxylic acid at C2 of the pyrrolidine ring (Scheme 7) and conversion of the C3 acid to a methyl ester. The sequence utilized a Corey-Link reaction to install the C3 masked α-amino acid functional group. Starting from (2*S*,3*S*)-3-hydroxy-proline **5**, Fischer esterification formed the allyl ester **17** in quantitative yield. Protection of the amine of **17** with 9-bromo-9-phenyl-fluorene yielded **18** (75% yield), which was converted to the β-ketoester **19** by Swern oxidation (80% yield). The formation of **20** (61% yield) was accomplished at -78°C by allowing ketone **19** to react with an excess of

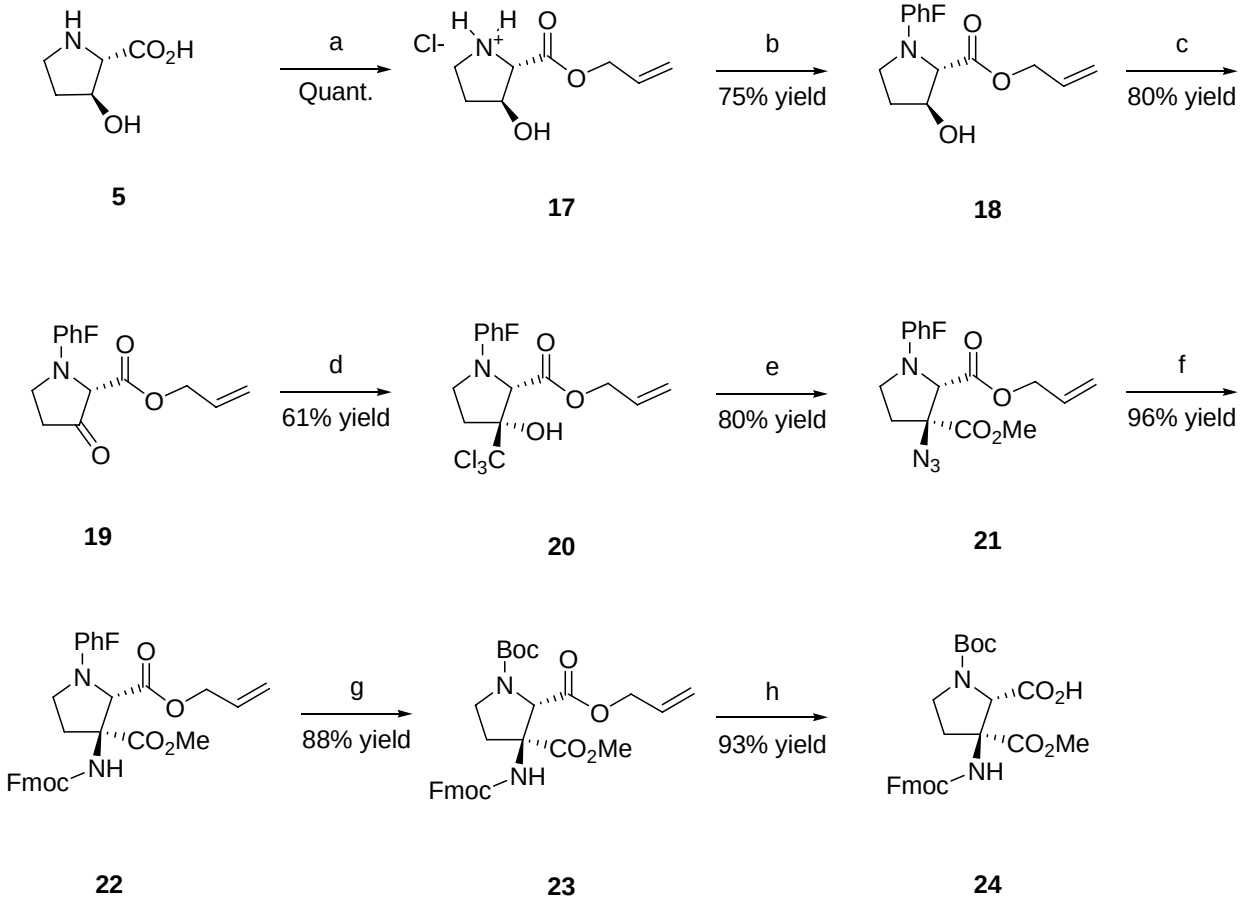

a.) HCl (g), allyl alcohol b.) i) 2 eq. TMSCl, DIPEA, DCM ii.) 0.9 eq MeOH iii.) PhFBr, $Pb(NO_3)_2$, DIPEA iv.) 10% citric acid in MeOH c.) i.) DMSO, $SOCl_2$, DCM, -78°C. (5 min). ii.) TEA (-78°C to 25°C.) d.) Chloroform, LHMDS, THF, -78°C e.) NaN_3, DBU, 18-crown-6, MeOH f.) i.) Zn, HOAc, THF ii.) FmocCl, DIPEA, DCM g.) i.) TFA, MeOH, DCM ii.) Boc_2O, DIPEA, DCM h.) $Pd(PPh_3)_4$, morpholine, THF

Scheme 7. Synthesis of the Monomer 24

chloroform and one equivalent of LHMDS (lithium hexamethyldisilazide). Addition of the trichloromethyl carbanion hypothesized to occur from less hindered face of ketone **19,** and the stereochemistry of **20** was inferred from the major trichlorocarbinol diastereomer **11a**. No amount of the trichlorocarbinol diastereomer corresponding to addition to the opposite face of **19** could be observed by NMR in either the crude reaction mixture or the purified product.

The conversion of the trichlorocarbinol **20** into the α-azido ester **21** was accomplished using DBU (1,8-diazabicyclo[5.4.0]undec7-ene), sodium azide and 18-crown-6 (80% yield) in methanol[15]. The reduction of the azide **21** to the amine using Zn/acetic acid followed by Fmoc ((9*H*-fluoren-9-yl) methyl carbamate) protection gave **22** in 96% yield over two steps. The removal of the PhF protecting group with TFA, was followed by Boc protection with di-*t*-butyl carbonate of the amine to give **23** (93% yield). Deprotection of the allyl ester of **23** was accomplished using $Pd(PPh_3)_4$ and morpholine to provide the orthogonally protected bis-amino acid **24** (93% yield) in an overall yield of 24% from **5.**

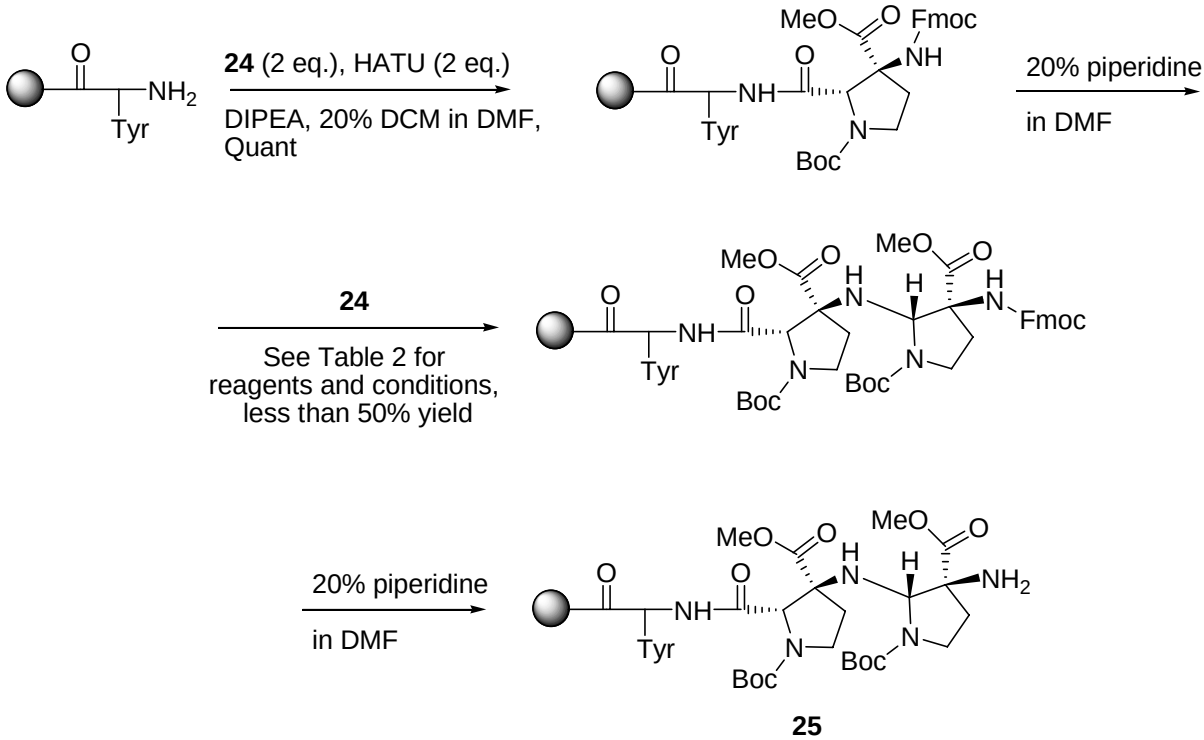

Scheme 8. Solid Phase Formation of Tyr-24-24 Sequence

Compound **24** was used in an attempt to form the sequence Tyr-**24**-**24** by solid phase peptide synthesis (Scheme 8). The formations of an amide bond between **24** and resin bound tyrosine using HATU preactivation occurred in quantitative yield. We subsequently encountered difficulty incorporating a second residue of **24** into the resin bound sequence to form **25** (Scheme 8)**.** Our attempts to form this amide bond included the use of HATU, PyBrop, and TFFH activating reagents, but all reagents provided yields of **25** below 60% as measured by Fmoc release from the resin (Table 2). The quantity of Fmoc released from the resin was calculated from the absorbance of the piperidine-fulvene adduct in the 20% DMF in DCM deprotection solution as measured at λ = 301 nm.

Table 2. Conditions and Yields of Solid Phase Formation of Tyr-24-24 Sequence

Coupling Reagent	Time of Reaction	Number of Coupling Reaction Repeats	Yield of **25**
2 eq. HATU	2 hours	2	42%
2 eq. TFFH	2 hours	2	31%
2 eq. PyBroP	2 hours	2	28%
2 eq. HATU	2 hours	1	15%
2 eq. HATU	4 hours	2	55%

These unexpectedly low yields lead us to probe the effect of reaction time on the formation of **25**. Reaction time was varied using 2 equivalents of HATU preactivated monomer **24** and the yields of **25** are shown in Table 2. A reaction time of 4 hours gave the best yield (55%), but only a 13% improvement in yield of **25** over the normal 2 hour coupling time. Since only a modest increase in yield was noted upon extended reaction time further increases in reaction time were not investigated.

The formation of a Tyr-**24**-*pro4*(2S4S) sequence was attempted to determine if quantitative amide bond formation was possible with other bis-amino acids. We encountered difficulty in the formation of the amide bond between resin bound **24** and the *pro4*(2S4S) monomer to form **26** (Scheme 9). The formation of **26** was attempted with coupling agents

HATU, TFFH and PyBrop preactivation with HATU providing the best yield. The yields of **26** for the various reagents are shown in Table 3, but no reagent was able to yield more than 60% of **26**.

Table 3 Conditions and Yields of Solid Phase Formation of Tyr-24-*pro4*(2S4S) Sequence

Coupling Reagent	Time of Reaction	Number of Coupling Reaction Repeats	Yield of **26**
HATU	2 hours	2	60%
TFFH	2 hours	2	20%
PyBroP	2 hours	2	35%

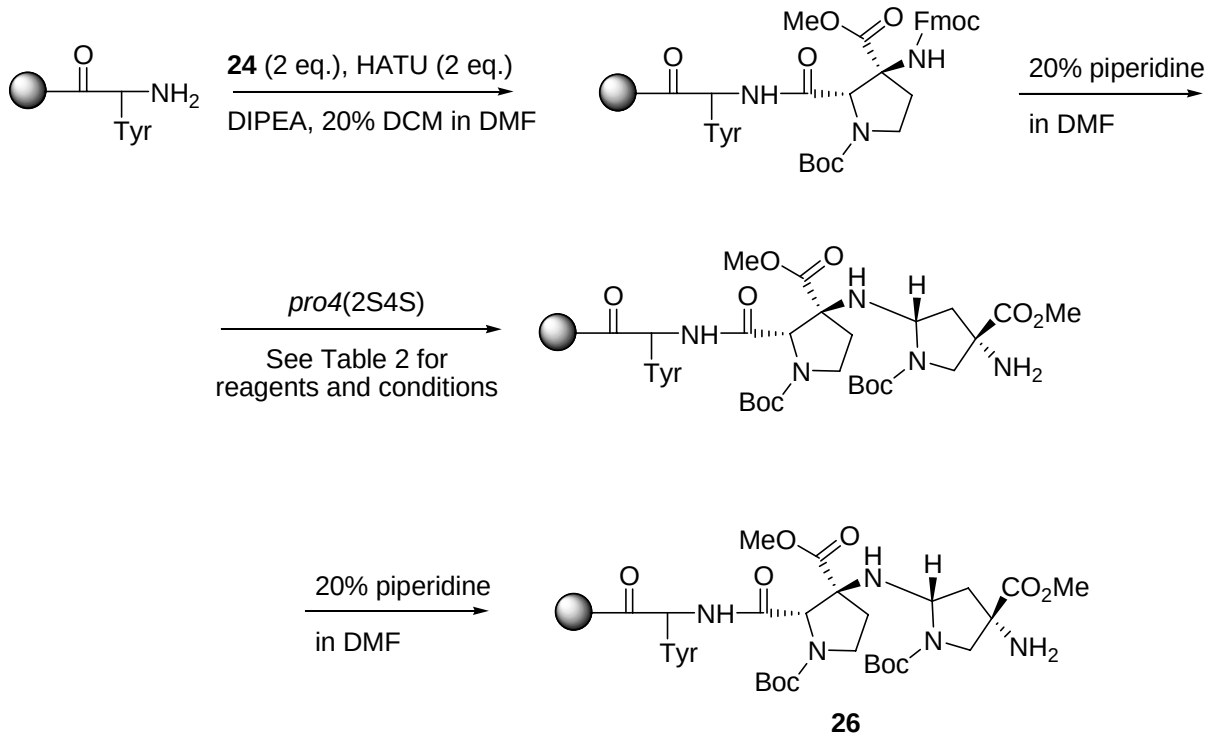

26

Scheme 9. Solid Phase Formation of Tyr-24-*pro4*(2S4S) Sequence

2.7 EPIMERIZATION OF THE PRO3(2S,3S) MONOMER WITHIN A BIS-PEPTIDE

While studying the coupling yields of **24**, the diketopiperazine linked sequence Tyr-**24**-*pro4*-**24**-Gly, **27** (Figure 13) was formed by SPPS albeit in low yields. An attempt to determine the solution phase NMR structure of **27** at pH 3.5 in water/10% D_2O ammonium acetate-d_7/acetic acid-d_4 buffer was undertaken.

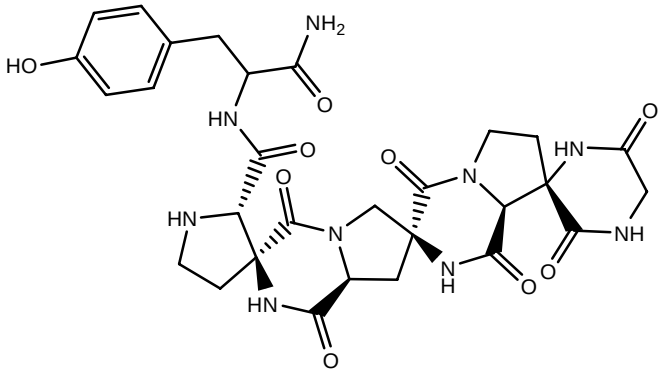

27

Figure 13. Structure of the Tyr-24-*pro4*-24-Gly Diketopiperazine Linked Oligomer

A one-dimensional ^1H NMR spectrum was taken prior to further two-dimensional NMR spectroscopic experiments. These two-dimensional NMR experiments covered a 48 hour time period. After 48 hours a second one-dimensional ^1H NMR spectrum was taken. The sample was noted to have multiple new resonances present in the second one-dimensional ^1H NMR spectrum.

Prior to initiation of the NMR experiments, a C_{18} reverse phase chromatogram of the NMR sample was obtained. This sample showed only one compound with an elution time of 17.1 minutes during a 30 minute runtime (0-25% gradient of acetonitrile in water with 0.1% TFA added) as detected at both 220 nm and 274 nm wavelengths by UV/Vis absorbance. After the 48 hours of NMR experimentation, the NMR sample was reinjected to obtain a second C_{18} reverse phase chromatogram. The later injection was found to contain two compounds: one eluting at 17.1 minutes and another eluting at 17.8 minutes (30 minute runtime, 0-25% gradient of acetonitrile in water with 0.1% TFA added).

A.)

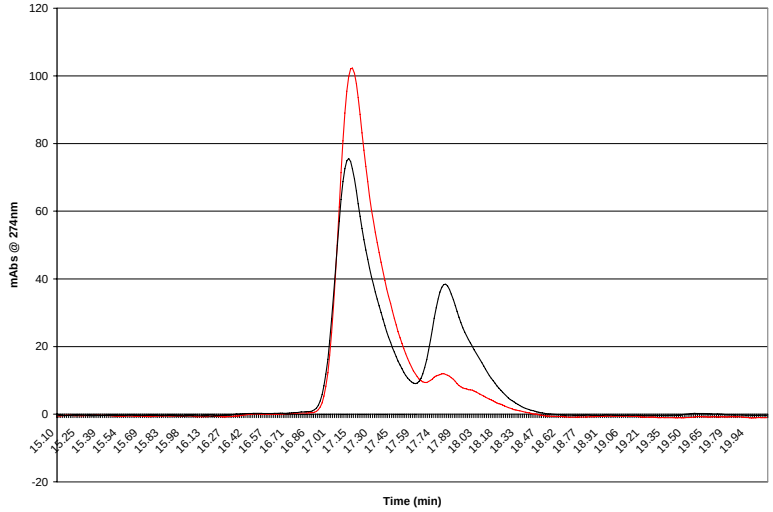

B.)

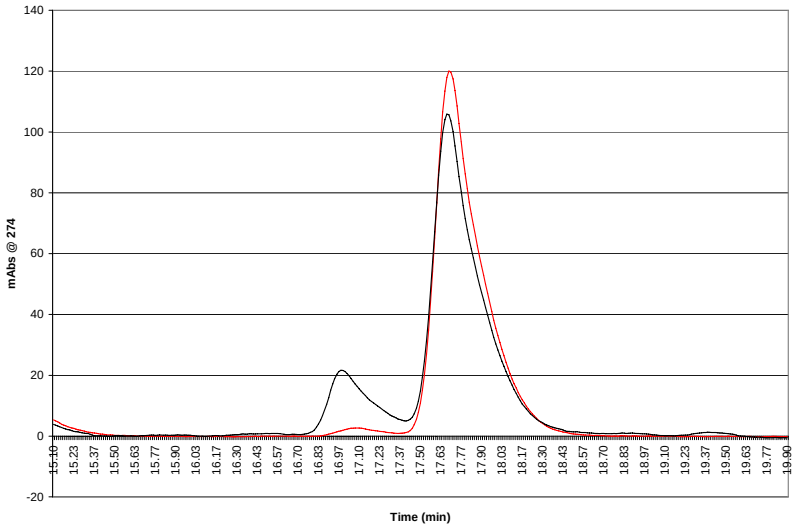

Graph A shows the HPLC traces at 1 day (red trace) and 4 days (black trace) of a sample of **27** incubated in D_2O at pD 3.5. Graph B shows epi-27 under the same conditions at 1 day (red trace) and 4 days (black trace). Each run was detected at λ=220nm and λ=274 nm by UV/Vis absorbance during a 30 minute runtime with a gradient of 0-25% acetonitrile in water with 0.1% TFA added.

Figure 14. RP-HPLC Chromatograms of the Epimerization of 27

Each of the compounds in the NMR sample had an *m/z* [(M+H)] = 652, which corresponded to the molecular mass of **27 + H**. This suggested that **27** was epimerizing to form at least one new compound with a different retention time: **27** eluting at 17.1 minutes and Compound A eluting at 17.8 minutes.

A new sample of **27** was synthesized, purified and allowed to incubate in pH 3.5 acetate buffered water, and monitored by HPLC for one week. After one week two compounds corresponding in retention time to **27** and Compound A of the NMR sample mentioned above were contained in the sample. The compounds were separated by RP-HPLC and each was placed in D_2O (pD 3.5 acetate-d_3 buffer). A sample of each compound dissolved in the acetate buffered D_2O was injected separately into an analytical C_{18} reverse phase liquid chromatography column and eluted on a 30 minute gradient of 0-25% acetonitrile in water with 0.1% TFA added. Repeated injections were performed at 24 hour intervals up to 96 hours after the samples were placed in the acetate buffer.

In Figure 14a, the C_{18} reverse phase chromatogram of the sample containing **27** in acetate buffered D_2O after 24 hours is shown in black, and the chromatogram shown in red was performed on the same solution at 96 hours. The 96 hour chromatogram shows an increase in the amount of Compound A, and the mass spectrum of Compound A shows an increase in molecular mass of one Dalton over **27**. This increase in molecular mass is consistent with the incorporation of deuterium into Compound A upon conversion from **27**.

Figure 14b shows the C_{18} reverse phase chromatogram at 24 hours (red trace) and 96 hours (black trace) of the acetate buffered sample which originally contained Compound A. The formation **27** can be noted in the 96 hour sample. In this sample, the mass spectrum of **27** showed a one Dalton increase in molecular mass over Compound a, which again was consistent with incorporation of deuterium. The chromatograms in Figure 14 were evidence of the epimerization of **27,** with Compound B representing an epimeric form of **27**.

Sequences involving *pro4* monomers and tyrosine had previously been formed and studied at similar pH levels and did not epimerize. We therefore concluded that at least one of the *pro3* monomers within **27** was the site for the epimerization. The most likely position for the epimerization was at C2 of the pyrrolidine ring, but exactly which pro3 monomer was epimerizing is not known.

The proximity of the two amino acid functional groups in **24** may account for its decreased stereochemical stability as compared to *pro4* monomers. In **24**, the two amino acids are in a 1,2 relationship, whereas in the *pro4* monomers the two amino acids are in a 1,3 relationship. The proximity of the electron withdrawing groups may lower the pKa of the C2 hydrogen atom of the pyrrolidine ring allowing deprotonation at this position and subsequent epimerization..

2.8 CONCLUSIONS

Two *pro3* class monomers, **13** and **24**, with differing protecting group configurations were successfully synthesized. In both **13** and **24** the amino acid functional groups are attached to adjacent carbon atoms. We believe this placement of the amino acid groups has lead to poor performance of monomers **13** and **24** in bis-peptide synthesis**.**

Neither **13** nor **24** were capable of producing quantitative amide bond formation with other bis-amino acids**.** We believe the low yield of amide bond formation can be attributed to steric hindrance due to the proximity of the two amino acid functional groups. Amide bond formation with sterically hindered amino acids is known to be difficult, as both the amine and acid can suffer reduced reactivity[19,20].

The incorporation of **24** into a diketopiperazine linked oligomer led to the discovery that the monomer was prone to epimerization in aqueous acidic solution. Epimerization has not been seen in other diketopiperazine linked oligomers formed by our group, but no other monomer contains amino acids on adjacent carbon atoms. We believe the proximity of the electron withdrawing amino acid groups causes the *pro3* class of monomers to be prone to epimerization.

The goals for the bis-amino acid linked oligomer project included the formation, in high yield, of stereochemically stable oligomers. The *pro3* class monomers formed did not satisfy either of these conditions. We therefore chose not to proceed with further studies on the *pro3* monomer class.

2.9 GENERAL EXPERIMENTAL METHODS

THF was distilled from Na/benzophenone under N_2. CH_2Cl_2 was distilled from CaH_2. All other reagents were used as received unless otherwise noted. All reactions were carried out in flame-dried or oven-dried glassware under N_2 atmosphere unless otherwise noted. Column chromatography was performed either manually using ICN Silitech 32-63 D (60A) grade silica gel or using Redisep normal phase flash chromatography silica columns on Combiflash Companion Purification System from ISCO Inc. NMR spectroscopy was performed on Bruker Avance 300 MHz, Bruker Avance DRX 500 MHz, or Bruker Avance DRX 600 MHz spectrometers. Chemical shifts (δ) are reported relative to $CDCl_3$, or DMSO-d_6 residual solvents peaks, unless otherwise noted. Optical rotation values were obtained on a Perkin-Elmer 241 polarimeter at 25°C. High resolution ESI-MS was performed on Hewlett-Packard Series 1050 instrument with diode array detector, using a Varian Chrompack Microsorb 100 C_{18} column (5 μm packing, 2.6 mm x250 mm). HPLC-MS analysis was performed on a Hewlett-Packard Series 1100 instrument with a diode array detector, HP 1100 MS detector (ESI), using Waters Xterra MS C_{18} column (8 mm packing; 21.5 mm x 50 mm). Analysis of 2D NMR data was performed using Sparky software.

(2S,3S)-3-Oxo-1-(9-phenyl-9*H*-fluoren-9-yl)-pyrrolidine-2-carboxylic acid methyl ester (3).

9-Phenylfluorenyl protected 3-Hydroxy-proline methyl ester (**4**) (1.84 g, 4.8 mmol) was dissolved in dry dichloromethane. Previously dried 4-Methylmorpholine N-oxide (NMO) (0.94 g, 8.0 mmol) and 2.6 g of activated 4A molecular sieves were added to the solution and then the flask was placed in an ice bath. Tetrapropylammoniun perruthenate (TPAP) was immediately added in one portion and the flask was sealed under N_2 atomsphere and stirred at 0°C for 10 minutes and room temperature for 30 minutes more. The reaction solution was filtered, and the filtrate was run through a silica pad with 2:1 ethyl acetate: hexanes. The eluent was concentrated by rotary evaporation to an off-white solid. Two sequential recrystallizations (recrystallization, dissolution in ethyl acetate followed by a second recrystallization) from neat ethyl acetate yielded 1.67 g (90.5%) of short, off-white crystalline solid. Mp = 122°C ORD $[\alpha]_D$ +73.4° (*c*.020, $CHCl_3$); IR (neat): 3059, 2950, 1765, 1736, 1450, 1266, 1145, 741, 704 cm^{-1}; ^1H NMR (300 MHz, $CDCl_3$): δ 7.79-7.14 (m, 13H, Ar), 3.65 (ddd, 1H, *J* = 18.2, 8.6, 3.7 Hz, -C_5H_α), 3.34

(s, 1H, -C_2H), 3.30 (s, 3H, - OCH_3), 3.17 (ddd, 1H, J = 18.2, 9.1, 7.3 Hz, -C_5H_β), 2.65 (ddd, 1H, J = 17.7, 9.1, 8.6 Hz, -C_4H_β), 2.38 (ddd, 1H, J = 17.7, 7.3, 3.7 Hz, -C_4H_α); ^{13}C NMR (75 MHz, CDCl3): δ 208, 169, 146, 144, 141, 141, 139, 129, 128.7, 128.5, 127.6, 127.4 127.3, 127.2, 127.1, 126, 120., 119, 76, 68, 51, 44, 37; HR MS (EI) calcd for $C_{25}H_{21}NO_3$ (M+) 383.1521, found 383.1539.

(2S,3S)-3-Hydroxy-2-Methoxycarbonyl pyrrolidine hydrochloride (6).

(2S,3S)-3-Hydroxy-pyrrolidine-2-carboxylic acid (**5)** (2.04 g, 15.6 mmol) was dissolved in16 mL of methanol and HCl gas was bubbled through the methanol for five minutes after the last of the starting material became soluble. The flask was sealed with a rubber stopper and let stir at room temperature for 2 hours. The solvent was removed by rotary evaporation until a clear thick oil remained, which upon standing crystallized. ^{1}H NMR (300 MHz, D_2O): δ 4.57 (br s, 1H, -OH), 4.14 (br s, 1H, -C_5H), 3.66 (s, 3H, -OCH_3), 3.38 (t, 2H, -C_5H_2), 3.13 (s, 1H, -C_2H), 2.02 (m, 1H, -C_4H_β), 1.91 (m, 1H, -C_4H_α); ^{13}C NMR (75 MHz, D_2O): 168, 73, 54, 44, 31.

(2S,3S)-3-Hydroxy-1-(9-phenyl-9*H*-fluoren-9-yl)-pyrrolidine-2-carboxylic acid methyl ester (4).

(2S,3S)-3-Hydroxy-2-methoxycarbonyl pyrrolidine hydrochloride (**7**) (2.00 g, 11.0 mmol) was dissolved in 30 mL of dichloromethane followed by addition of chlorotrimethylsilane (2.8 mL, 22.0 mmol). The flask was then cooled on an ice bath and diisopropylethylamine (6.7 mL, 38.6 mmol) was added. The flask was left at 0^{o}C for five minutes then fitted with a reflux adapter and refluxed for 1.5 hours in an oil bath under N_2. The flask was cooled to 0^{o}C and methanol (402 μL, 9.9 mmol) in 3 mL of dichloromethane was added with stirring under N_2. The mixture was removed from the ice bath after five minutes and allowed to stir at room temperature for 1 hour. 9-Bromo-9-phenyl-9*H*-fluorene (5.25 g, 16.3 mmol), diisopropylethylamine (1.9 mL, 11.0 mmol), and lead (II) nitrate (3.33 g, 10.0 mmol) were added. The flask was again flushed with N_2, and the solution was stirred under N_2. The reaction mixture was allowed to stir for 18 hours and was filtered and concentrated by rotary evaporation. The resultant brown oil was diluted with 40 mL of methanol into which 4.2 g of citric acid were added and stirred at room temperature for 1 hour after which time the mixture was again filtered and concentrated. The brown oil was brought up in 100 mL ethyl acetate and washed with 5% w/v citric acid in water (2 x 50 mL), saturated aqueous $NaHCO_3$ (2 x 50 mL), then brine (1 x 50 mL), dried with $MgSO_4$ and concentrated by rotary evaporation. The product was purified by

column chromatography with 1:3 ethyl acetate: hexanes over silica gel to yield 2.81 g (7.5 mmol, 68.5%) of the light yellow solid title compound. Analytical specimen was obtained by crystallization from ethyl acetate and hexanes. Mp = 135.6°C ORD $[\alpha]_D$ +210.5° (*c* 0.022, $CHCl_3$); IR (neat): 3443, 3057, 2946, 1729, 1450, 1207,1155, 741, 703 cm^{-1}; ^1H NMR (300MHz, $CDCl_3$): δ 7.76-7.14 (m, 13H, Ar), 4.12 (ddd, 1H, *J* = 12.0, 4.8, 1.9 Hz, -C_3H), 3.37 (ddd, 1H, *J* = 9.2, 7.2, 2.4 Hz, -C_5H_α), 3.35 (s, 3H, -OCH_3), 3.18 (ddd, 1H, *J* = 9.8, 9.2, 5.5 Hz, -C_5H_β), 2.89 (d, 1H, *J* = 1.9 Hz, -C_2H), 2.12 (dddd, 1H, *J* = 11.0, 9.8, 7.2, 4.8 Hz, -C_4H_β), 1.72 (dddd, 1H, *J* = 12.0, 11.0, 5.5, 2.4 Hz, -C_4H_α); ^{13}C NMR (75 MHz, CDCl3): δ 174.6, 148.0, 146.8, 145.8, 142.3, 141.6, 139.3, 128.6,128.2, 128.0, 127.7, 127.3, 127.1, 126.8, 126.3, 125.5, 125.3, 120.0, 119.9, 69.7, 51.4, 46.7, 33.5; HR MS (EI) calcd for $C_{25}H_{23}NO_3$ (M+) 385.1678, found 385.1681.

9-Phenyl-9*H*-fluorene (8).

Isolated as a byproduct of the Bucherer-Bergs reaction with PhF protected pyrrolidine nitrogen and the Corey-Link reaction. ^1H NMR (300 MHz, $CDCl_3$): δ 7.81, (d, 2H), 7.41-7.23 (m, 9H), 7.10 (d, 2H), 5.06 (s, 1H).

3-Hydroxy-1*H*-pyrrole-2-carboxylic acid methyl ester (9).

Isolated as a byproduct of the Corey-Link and Bucherer-Bergs reactions. ^1H NMR (300 MHz, $CDCl_3$): δ 8.13 (br s, 1H), 6.23 (br s, 1H), 5.89 (t, 1H), 3.89 (s, 3H).

(2S,3R)-3-Hydroxy-1-(9-phenyl-9*H*-fluoren-9-yl)-3-trichloromethyl-pyrrolidine-2-carboxylic acid methyl ester (11a).

Compound **3** (1.63 g, 4.3 mmol) was dissolved in 90 mL tetrahydrofuran under an atmosphere of N_2, and cooled to -78°C. Chloroform (1 mL, 12.9 mmol) was added. After five minutes 8.6 mL of 1 M lithium hexamethyldisilazane (LHMDS) was added. The mixture was stirred at -78°C for 3 hours. The solution was allowed to warm to -25°C before it was quenched with saturated aqueous ammonium chloride, removed from the bath, and allowed to reach room temperature. The reaction was diluted with 100 mL water and extracted twice with 50 mL diethyl ether. The organic layers were combined and washed with two portions of 50 mL water, 50 mL of brine, and dried with $MgSO_4$. The solvent was removed under rotary evaporation to yield dark brown oil. Purification of the material was possible with flash chromatography on silica gel eluted with 1:8 ethyl acetate hexanes. Removal of solvent yielded 1.43 g (65.4%) of light yellow solid. Analytical sample was recrystallized from ethyl acetate and hexanes. Mp =

126.7°C ORD $[\alpha]_D$ +59.2° (*c*.016, $CHCl_3$); IR (neat):3407, 3060, 2950, 2108, 1715, 1488, 1450, 1209, 1177, 910, 791, 739, 703 cm^{-1}; ^1H NMR (300 MHz, $CDCl_3$): δ 7.80-7.09 (m, 13H, Ar) , 5.29 (s, 1H, -O*H*), 3.76 (ddd, 1H, *J* = 12.5, 11.0, 6.2 Hz, $-C_5H_\alpha$), 3.73 (s, 1H, $-C_2H$), 3.37 (ddd, 1H, *J* = 12.5, 9.5, 7.1 Hz, $-C_5H_\beta$), 3.08 (s, 3H, $-OCH_3$), 2.44 (ddd, 1H, *J* = 12.2, 11.0, 9.5 Hz, $-C_4H_\beta$), 2.07 (ddd, 1H, *J* = 12.2, 7.1, 6.2 Hz, $-C_4H_\alpha$); ^{13}C NMR ($CDCl_3$, 75 MHz): δ 175.6, 147.3, 146.1, 143.1, 141.8, 139.6, 129.0,128.4, 128.1, 127.4, 127.0, 126.8, 125.60, 120.10, 103.8, 91.7, 63.2, 52.3, 49.1, 36.3; HR MS (EI) calcd for $C_{26}H_{22}Cl_3NO_3$ (M+) 501.0665 found 501.0655. The stereochemistry of this molecule was assigned first by ROESy NMR spectroscopy and was subsequently confirmed by x-ray diffraction crystallography.

(2S,3S)-3-Hydroxy-1-(9-phenyl-9*H*-fluoren-9-yl)-3-trichloromethyl-pyrrolidine-2-carboxylic acid methyl ester (11b).

Isolated as minor diastereomer of (**11a**).^1H NMR (300 MHz, $CDCl_3$): δ 7.97 (m,13H, Ar), 3.56 (ddd, 1H, *J* = 10.7, 9.4, 2.8 Hz, $-C_5H_\alpha$), 3.52 (s, 1H, $-C_\alpha H$), 3.45 (s, 1H, -O*H*), 3.29 (ddd, 1H, *J* = 10.7, 8.8, 6.4 Hz, $-C_5H_\beta$), 3.27 (s, 3H, $-OCH_3$), 2.44 (ddd, 1H, *J* = 12.0, 9.4, 8.8 Hz, $-C_4H_\beta$), 2.36 (ddd, 1H, *J* = 12.0, 6.4, 2.8 Hz, $-C_4H_\alpha$); ^{13}C NMR (75 MHz, $CDCl_3$): δ 170.67, 146.76, 145.56, 141.29, 140.79, 140.08, 129.04, 128.70, 128.60, 128.17, 127.70, 127.52, 127.02, 126.46, 120.86, 120.22, 120.07, 75.08, 74.37, 68.97, 51.31, 44.92, 38.10.

(2S,3S)-3-Azido-1-(9-phenyl-9*H*-fluoren-9-yl)-pyrrolidine-2,3-dicarcoxylic acid dimethyl ester (12).

Trichlorocarbinol (**11a**) (1.68 g, 3.3 mmol) was dissolved in 30 mL of dry methanol at room temperature. To this solution was added sodium azide (1.12 g, 17.2 mmol), followed by 1.8 mL of sodium methoxide 30% (w/v) in methanol. The solution was allowed to stir at room temperature for 18 hours. The reaction was diluted with 30 mL of 1 M HCl and extracted with diethyl ether (2 x 15mL). The organic layers were washed with water (2 x 15 mL), and then brine (1 x 15 mL), followed by drying with $MgSO_4$. The ether was removed with rotary evaporation. Flash chromatography over silica gel with 99:1 $CHCl_3$:MeOH yielded 1.27 g (83.7%) of white solid title compound. Crystalization was preformed using ethyl acetate and hexanes. Mp = 98°C (decomp.) ORD $[\alpha]_D$ +160.8°(*c* 0.0195, $CHCl_3$); IR (neat): 2108, 1744, 1450, 1435, 1264, 1197, 1160 cm^{-1}; ^1H NMR (300 MHz, $CDCl_3$):δ 7.75-7.07 (m, 13H, Ar), 3.63 (s, 3H, $-OCH_3$), 3.53 (dd, *J* = 11.6, 7.5 Hz, 1H, $-C_5H_\alpha$), 3.29 (s, 3H, $-OCH_3$), 3.26 (ddd, 1H, *J* = 11.6, 10.5, 5.7

Hz, -C_5H_β), 3.22 (s, 1H, -$C_\alpha H$), 2.62 (ddd, 1H, *J* = 12.9, 10.5, 7.5 Hz, -C_4H_β), 1.82 (dd, 1H, *J* = 12.9, 5.7 Hz, -C_4H_α); ^{13}C NMR (75 MHz, $CDCl_3$): δ 172.1, 169.0, 147.8, 145.3, 141.8, 141.5, 139.5, 129.1, 128.5, 128.4, 127.9, 127.6, 127.2, 126.7, 120.3, 120.1, 75.6, 74.4, 67.3, 52.9, 51.8, 46.6, 33.2; HR MS (EI) calcd for $C_{27}H_{24}N_4O_4$ (M+) 468.1798, found 468.1794.

(2S,3S)-3-Azido-1-(9-phenyl-9*H*-fluoren-9-yl)-pyrrolidine-2,3-dicarboxylic acid 2-methyl ester (13).

The trichlorocarbinol (**11a**) (811.5 mg, 1.6 mmol) was dissolved in dioxane (8 mL) and diluted with 5 mL of water. Sodium hydroxide (303.4 mg, 7.6 mmol) was added to the solution followed quickly by sodium azide (234.2 mg, 3.6 mmol). The reaction was stirred at room temperature for 1 hour. The reaction was diluted with 10 mL of 1 M HCl and 10 mL of diethyl ether and the aqueous and organic layer were separated. The aqueous layer was extracted 2 times with ether (10 mL each). The ether was washed twice with saturated aqueous sodium bicarbonate (10 mL each), then washed once with 10 mL of brine. The organic layer was dried with $MgSO_4$ and concentrated under rotary evaporation to give the title compound as clear oil (692.8 mg, 95.2% yield). ORD $[\alpha]_D$ +124.5^o (*c* = 0.0157, $CHCl_3$); IR (neat): 3059, 2951, 2109, 1742, 1450, 1250, 1162, 740, 703 cm^{-1}; ^{1}H NMR (300 MHz, $CDCl_3$): 7.94-7.11 (m, 13H, Ar), 3.50 (ddd, *J* = 13.3, 8.0, 1.2 Hz, 1H, -$C_\delta H_\alpha$), 3.27 (ddd, *J* = 13.3, 10.2, 5.6 Hz, 1H, -$C_\delta H_\beta$), 3.23 (s, 3H, -OCH_3), 3.22 (s, 1H, -$C_\alpha H$), 2.57 (ddd, J = 12.9, 10.2, 8.0 Hz, 1H, -$C_\gamma H_\beta$), 1.83 (ddd, *J* = 12.9, 5.6, 1.2 Hz, 1H, -$C_\gamma H_\alpha$); ^{13}C NMR (75 MHz, $CDCl_3$): 173.4, 172.1, 147.4, 144.9, 141.5, 141.3, 139.2, 129.0, 128.4, 128.3, 127.7, 127.4, 127.1, 126.5, 126.5, 120.1, 119.9, 75.5, 73.9, 66.8, 51.8, 46.6, 32.8; HR MS (EI) calcd for $C_{25}H_{21}N_4O_2$

(2S,3S)-3-Azido-pyrrolidine-2,3-dicarboxylic acid dimethyl ester (14).

Phenyl-fluorenyl protected azido dimethyl ester (**12**) (76.1 mg, 0.16 mmol) was dissolved in dichloromethane, and methanol (20 μL, 0.48 mmol) was added. To this solution was added 50 μL of trifluoroacetic acid with stirring for 2 hours. The reaction mixture was concentrated by rotary evaporation to yellow oil. The oil was introduced to a 5 mL silica pad and run with chloroform to remove the aromatic residue. Next, the pad was washed with 1 % (v/v) triethylamine in chloroform to neutralize the pyrrolidine salt and move it off the silica. Rotary evaporation of those fractions containing the pyrrolidine provided the title compound as yellow oil (34.8 mg, 95.5% yield). ORD $[\alpha]_D$ +5.17 (*c* 0.0358, $CHCl_3$); IR (thin film): 3323, 3155, 2955, 2115, 1749, 1450, 1437, 724 cm^{-1}; ^{1}H NMR (300 MHz, $CDCl_3$): δ 3.86 (s, 1H, -C_2H), 3.78

(s, 3H, -OCH_3), 3.73 (s, 3H, -OCH_3), 3.31 (ddd, 1H, J = 11.4, 8.0, 3.5 Hz,-C_5H_α), 3.06 (ddd, 1H, J = 11.4, 8.4, 7.1 Hz, -C_5H_β), 2.32 (ddd, 1H, J = 13.3, 8.4, 7.1 Hz, -C_4H_β), 2.06 (ddd, 1H, J = 13.3, 7.1, 3.5 Hz, -C_5H_α); ^{13}C NMR (75 MHz, $CDCl_3$): 170.8, 170.3, 74.8, 70.8, 53.0, 52.5, 45.9, 38.1.

(2S,3S,2'S,3'S)-3'-Azido-1[3-azdio-2methoxycarbonyl-1-(9-phenyl-9*H*-fluoren-9-yl)-pyrrolidine-3-carbonyl]-pyrrolidine-2',3'-dicarboxylic acid dimethyl ester (15).

HATU coupling method in 20% dimethylformamide/dichloromethane: The phenyl-fluorenyl protected 3-carboxylic acid pyrrolidine (**13**) (53.8 mg, 0.12 mmol) was dissolved in dichloromethane (960 μL) and dimethylformamide (240 μL), and HATU (51.4 mg, 0.14 mmol) was added to the mixture. Diisopropylethylamine amine was added and the solution was stirred for 2 minutes after which the 1*H*-pyrrolidine (**14**) (27.0 mg, 0.12 mmol) was added. The reaction was stirred under N_2 for 24 hours and was diluted with 1 mL 1 M HCl. The reaction mixture was transferred to a separation funnel and extracted with dichloromethane (3 x 5 mL). The organic layer was dried with sodium sulfate and concentrated. Flash chromatography with 1:3 ethyl acetate: hexanes gave a mixture of the product and the starting acid. This mixture was separated using a 5 mL silica pad eluted with neat chloroform to provide pure title compound as clear oil (27.6 mg, 34.6% yield). ORD +32.2^o (*c* 0.038, $CHCl_3$); IR (neat): 2953, 2107, 1749, 1650, 1450, 1435, 1264, 1174, 735 cm^{-1}; ^{1}H NMR (300 MHz, $CDCl_3$)(rotational isomers unresolved at 360 K in d_6-DMSO): δ 7.72-7.22 (m, 13 H), 4.08 (m, 1H), 3.84 (m, 1H), 3.80 (s, 3H), 3.68-3.65 (m, 3H), 3.55-3.50 (m, 2H), 3.32-3.30 (m, 1H), 3.29-3.28 (m, 3H), 3.04 (m, 1H), 2.57 (m, 1H), 2.22 (m, 2H), 1.96 (m, 1H); HR MS (EI) calcd for $C_{34}H_{32}N_5O_7$ ([M-N_3]$^+$) 622.2296 found 622.2278.

HOBt/DCC coupling method: The 1*H*-pyrrolidine (**13**) (20.2 mg, 0.09 mmol) was dissolved in 2 mL of 1:4 tetrahydrofuran: dichloromethane and the 3-carboxylic acid pyrrolidine (**14**) (51.7 mg, 0.11 mmol) was added, followed by addition of dicyclohexyl carbodiimide (26.9 mg, 0.13 mmol) and HOBt (1-hydroxybenzotriaxzole) (16.5 mg, 0.12 mmol). The reaction was stirred at 0^{o}C for three hours and allowed to warm to room temperature, with stirring, for an additional 18 hours. Concentration under rotary evaporation of the reaction mixture resulted in a yellow residue that was brought up in 10 mL ethyl acetate, washed with 1 M HCl (2 x 10 mL), saturated aqueous sodium bicarbonate (2 x 10 mL), and brine (1 x 10 mL). The organic layer was dried with $MgSO_4$ and concentrated. The residue was purified by flash chromatography (1:6

ethyl acetate hexanes), yielding what appeared, by ^{1}H NMR to be the OBt ester (**16**) of the acid starting material along with the acid starting material. ^{1}H NMR (300 MHz, $CDCl_3$): δ 7.83-7.16 (m, 17H, Ar), 3.54 (ddd, 1H, *J* = 10.0, 9.8, 2.1 Hz, -C_5H_α), 3.34 (s, 3H, -OCH_3), 3.15 (ddd, 1H, *J* = 10.0, 7.5, 4.0 Hz, -C_5H_β), 3.12 (s, 1H, -C_2H), 2.42 (ddd, 1H, *J* = 12.1, 9.8, 7.5 Hz, -C_4H_β), 2.03 (ddd, 1H, *J* = 12.1, 4.0, 2.1 Hz, -C_4H_α).

PyBroP coupling method: The free amine (**14**) (51.3 mg, 0.22 mmol) was dissolved in dichloromethane. The 3-carboxylic acid (**13**) (125.9 mg, 0.27 mmol) was added to the solution along with PyBroP (bromotripyrrolidinophosphonium hexafluorophosphate) (154.8 mg, 0.33 mmol) and diisopropylethylamine (77 μL, 0.44 mmol). The reaction was stirred under N_2 for 24 hours, after which the solvent was removed and the residue was taken up in ethyl acetate (10 mL). The organic layer was washed three times with 5% $KHSO_4$ (10 ml), then 10 mL brine, three 10 ml portions of saturated aqueous sodium bicarbonate, and finally with one portion of 10 mL brine. The organic layer was dried with Na_2SO_4, and concentrated under rotary evaporation. Flash chromatography with 1:3 hexanes provided the dimeric product in 27.1% yield (38.8 mg).

HATU coupling method in neat dimethylformamide: The 3-carboxylic acid (**13)** (91.7 mg, 0.20 mmol) was dissolved in dimethylformamide (1 mL), and HATU (83.0 mg, 0.22 mmol) was added along with diisopropylethylamine amine (45 μL, 0.26mmol). The mixture was stirred for two minutes after which the free amine (**14**) (30.3 mg, 0.13 mmol) was introduced. The reaction was stirred under N_2 for 24 hours, after which it was diluted with 30 ml ethyl acetate. The solution was washed with 1 M HCl (2 x 10mL), water (1 x 10 mL), saturated aqueous sodium bicarbonate (2 x 10 mL), and 10 mL of brine, and dried with $MgSO_4$. Rotary evaporation yielded yellow oil that was introduced to a silica gel column for flash chromatography with 1:3 ethyl acetate hexanes to yield the dimer in 8.6% yield (11.4 mg).

(2S,3S)-allyl 3-Hydroxypyrrolidine-2-carboxylate Hydrochloride (17)

(2*S*,3*S*)-3-hydroxyproline (5.14 g, 38.1 mmol) was suspended in allyl alcohol (50 mL) and HCl gas was bubbled through until a homogenous solution resulted. The solution was sealed and stirred for 2 hours. The solution was evaporated by rotary evaporation and allowed to sit until solidification occurred to a light brown crystalline solid. Yield 7.89g, 100%. ^{1}H NMR (300 MHz, DMSO) δ 9.81 (br s, 1H), 5.94 (m, 1H), 5.37 (ddd, J = 17.4, 3.3, 1.8 Hz, 1H), 5.26 (ddd, J = 10.5, 3.0, 1.5 Hz, 1H) 4.69 (m, 2H), 4.36 (m, 1H) 4.16 (d, J = 3.0 Hz, 1H) 3.33 (m, 2H), 1.94 (m, 2H).

(2S,3S)-allyl 3-hydroxy-1-(9-phenyl-9H-fluoren-9-yl)pyrrolidine-2-carboxylate (18)

Compound **17** (8.78 g, 42.4 mmol) was suspended in 100 ml DCM. Trimethylsilylchloride (12.1 mL, 95.4 mmol) was added followed by DIPEA (24.2 mL, 148.4 mmol). This solution was refluxed under N_2 for 1 hour then cooled to 0^oC. 1.5 ml of methanol in 10.6 ml DCM was added and the solution was stirred for 1 hour at 0^oC. Phenylfluorenyl-bromide (20.56g, 69.0 mmol), lead II nitrate (13.59g, 41.0 mmol), and DIPEA (6.9 mL, 42.4 mmol) were added and the solution was stirred under N_2 overnight. The solution was evaporated and the residue was brought up in a solution of 10% w/v citric acid in methanol (50 mL) and stirred for 1 hour. The methanol was evaporated and the residue was brought up in ethyl acetate (300 mL). This solution was washed with water (100 mL) three times and brine once dried and evaporated. A column of 1:3 EtOAc:hexanes was run. The resulting product was evaporated and recrystallized from EtOAc and hexanes to yield off-white crystals (13.14g, 75.3%). Mp = 152.5^oC ORD $[\alpha]_D$ $+184.6^o$(*c* 0.0412, $CHCl_3$); IR (neat): 3447, 3058, 3019, 2940, 2873, 1733, 1450, 1154, 986, 742, 703 cm^{-1}; ^1H NMR (300 MHz, $CDCl_3$) δ 7.83-7.11 (m, Ar, 13H), 5.71 (ddd, J = 6.0, 5.6, 5.3 Hz, 1H), 5.19 (dd, J = 5.3, 1.2 Hz, 1H), 5.14 (d, J = 1.2 Hz, 1H), 4.29 (dd, J = 13.2, 6.0 Hz, 1H), 4.14 (dd, J = 13.2, 5.6 Hz, 1H), 3.37 (ddd, J = 15.9, 7.7, 2.4 Hz, 1H), 3.19 (ddd, J = 15.9, 10.1, 5.8 Hz, 1H), 2.93 (dd, J = 3.6, 2.1 Hz, 1H) 2.11 (m, J = 15.5, 5.8, 2.4, 2.1, 1H), 2.06 (d, J = 3.6, 1H) 1.73 (ddd, J = 15.5, 10.1, 7.7 Hz, 1H); ^{13}C NMR (125 Mz, $CDCl_3$) 173.7, 148.0, 145.9, 142.3, 141.5, 139.3, 131.9, 128.5, 128.3, 127.7, 127.4, 127.2, 127.1, 126.8, 126.3, 120.0, 119.7, 118.1, 76.0, 75.9, 69.7, 65.0, 46.7, 33.4; HR MS (EI) calcd for $C_{27}H_{25}N_1O_3$ (M+) 411.1834, found 411.1823.

(S)-allyl 3-oxo-1-(9-phenyl-9H-fluoren-9-yl)pyrrolidine-2-carboxylate (19)

Into 30 ml of DCM, 1.2 ml (13.5 mmol) of oxalyl chloride was added under N_2 and stirred. The solution was cooled to -78^oC and 1.9 mL (26.8 mmol) of DMSO was added and stirred for 2 min. 5.04 g (12.2 mmol) of **18** was dissolved in 24 mL of1:1 DCM:DMSO and added to the above solution. After 5 minutes 8.1 mL (61.0 mmol) of TEA was added. The reaction was allowed to warm to room temperature over two hours when 50 ml of H_2O was added. Extraction with DCM x2 of the aqueous layer and combination of the organic layers followed. The organic layers were washed with 1M HCl x2, sat aq $NaHCO_3$ x2, then brine. The solution was dried with $MgSO_4$ and concentrated. A silica column eluted with 1:6 EtOAc:hexanes yielded the title compound as a yellow oil (3.9976 g, 80.0% yield). ORD $[\alpha]_D$

+43.0°(*c* 0.0217, $CHCl_3$); IR (neat): 3439, 3060, 3021, 2945, 2871, 1765, 1736, 1450, 1143, 741, 703 cm^{-1}; ^1H NMR (300 MHz, $CDCl_3$) δ 8.02-7.25 (m, Ar, 13H), 5.69 (ddd, J = 11.25, 5.7, 5.5 Hz, 1H), 5.20 (ddd, J = 11.25, 1.5, 1.4 Hz, 1H), 5.16 (ddd, J = 2.8, 2.7, 1.4 Hz, 1H), 4.20 (m, J = 13.3, 5.7, 2.7, 1.4 Hz, 1H), 4.08 (dddd, J = 13.3, 5.5, 2.8, 1.5 Hz, 1H), 3.67 (ddd, J = 18.3, 8.5, 3.9 Hz, 1H), 3.38 (s, 1H) 3.17 (ddd, J = 18.3, 8.9, 7.3 Hz, 1H), 2.64 (ddd, J = 17.4, 8.9, 8.5 Hz, 1H) 2.40 (ddd, J = 17.4, 7.3, 3.9 Hz, 1H); ^{13}C NMR (75 Mz, $CDCl_3$); 208.6, 168.5, 146.3 144.0, 141.4, 140.9, 139.7, 131.4, 128.9, 128.6, 128.4, 128.1, 127.5, 127.5, 127.2, 127.1, 126.4, 120.2, 119.8, 117.9, 76.5, 76.0, 68.4, 65.4, 44.3, 37.4; HR MS (EI) calcd for $C_{27}H_{23}N_1O_3$ (M+) 409.1678, found 409.1671.

(2S,3R)-allyl 3-(trichloromethyl)-3-hydroxy-1-(9-phenyl-9H-fluoren-9-yl)pyrrolidine-2-carboxylate (20)

In 150 mL of THF, 3.9976g (9.8 mmol) of **19** was dissolved and the solution cooled to -78°C. Chloroform (7.8 mL, 98 mmol) was added followed by 10.8 ml (10.8 mmol) of 1 M LHMDS in THF. The reaction was stirred under N_2 for 4 hours at -78°C. The reaction was allowed to warm to RT and 50 mL saturated aqueous ammonium chloride was added along with 50mL of ether. The organic layer was washed x3 with H_2O then brine x1, dried and concentrated. Silica flash column eluted with 1:2 EtOAc:hexanes and recyrstallization from chloroform/hexanes yielded the title product as white crystals (3.3021 g, 61.2% yield). Mp = 112.1°C ORD $[\alpha]_D$ +86.3°(*c* 0.0179, $CHCl_3$); IR (neat): 3409, 3059,3020, 2888, 1713, 1450, 1191, 791, 741, 726, 702 cm^{-1}; ^1H NMR (300 MHz, $CDCl_3$) δ 7.89-7.25 (m, Ar, 13H), 5.53 (m, 1H), 5.13 (m, 2H), 5.08 (dd, J = 9.0, 1.4 Hz, 1H), 4.15 (ddd, J = 12.9, 6.9, 1.4 Hz, 1H), 3.79 (s, 1H), 3.71 (m, 2H), 3.36 (ddd, J = 10.8, 9.0, 1.4 1H), 2.50 (ddd, J = 20.1, 9.0, 1.4 Hz, 1H) 2.11 (ddd, J = 20.1, 10.8, 1.4 Hz, 1H); ^{13}C NMR (75 Mz, $CDCl_3$); 174.5, 147.1, 146.1, 143.0, 141.5, 139.7, 130.8, 128.9, 128.5, 128.4, 128.0, 127.4, 127.4, 126.9, 126.8, 125.6, 120.1, 120.0, 119.0, 103.9, 91.7, 77.3, 77.2, 66.4,63.7,48.9,36.4; HR MS (EI) calcd for $C_{28}H_{24}NO_3Cl_3$ (M+) 527.0822, found 527.0816.

(2S,3S)-2-allyl 3-methyl 3-azido-1-(9-phenyl-9H-fluoren-9-yl)pyrrolidine-2,3-dicarboxylate (21)

In dry methanol (50 mL), **20** (2.97 g, 5.6mmol) was dissolved and sodium azide (1.81 g, 27.8 mmol), 18-crown-6 (88.6 mg, 6.0 mole%) and DBU (4.2 ml, 28 mmol) were added. The flask was sealed and stirred under N_2 overnight. Saturated ammonium chloride solution (50 ml)

was added to the reaction along with 50 ml of ether. The ether layer was washed with 1M HCl x2 then brine x1. The organic layer was dried and concentrated. The product was recovered as white crystals from crystallization with chloroform/hexanes (2.22g, 80.3 % yield). Mp = 92.5°C (decomp.) ORD $[\alpha]_D$ +119.4°(*c* 0.0388, $CHCl_3$); IR (neat): 3409, 3059,3020, 2888, 2109, 1741, 1646, 1450, 1263, 1157, 742, 726, 704 cm^{-1}; ^1H NMR (300 MHz, $CDCl_3$) δ 8.0-7.13 (m, Ar, 13H), 5.69 (m, 1H), 5.20 (m, 1H), 5.15 (m, 1H), 4.21 (dddd, J = 22.5, 10.5, 1.4, 1.2 Hz, 1H), 4.17 (dddd, J = 22.5, 10.5, 1.4, 1.2, 1H), 3.62 (s, 3H), 3.55 (ddd, J = 10.8, 9.5, 1.4 1H), 3.31 (ddd, 10.8, 7.8, 6.0) 3.25 (s, 1H) 2.64 (ddd, J = 12.9, 9.5, 7.8 Hz, 1H) 1.84 (ddd, J = 12.9, 6.0,1.4 Hz, 1H); ^{13}C NMR (75 Mz, $CDCl_3$) 171.1, 168.9, 147.7, 145.6, 141.9, 141.4, 139.6, 131.9, 129.1, 128.5, 128.4, 127.8, 127.6, 127.5, 127.3, 126.8, 126.7, 124.8, 120.2, 118.4, 75.7, 74.4, 67.5, 65.7, 52.7, 46.6, 33.0; HR MS (EI) calcd for $C_{29}H_{26}N_4O_4$ (M+) 494.1954, found 494.1935.

(9H-fluoren-9-yl)methyl (2S,3S)-2-((allyloxy)carbonyl)-3-(methoxycarbonyl)-1-(9-phenyl-9H-fluoren-9-yl)pyrrolidin-3-ylcarbamate (22)

In 40 ml of 1:1 acetic acid:THF were dissolved 3.30 g of **21**. Added to the flask was 4.42 g of Zn dust. The reaction was allowed to stir vigorously for 1 hour at which time the Zn dust was filtered off and the filtrate was diluted with 100 ml of EtOAc. The filtrate solution was washed with saturated aqueous $NaHCO_3$ x3, H2O x2, then brine x1, dried and concentrated. No further purification was done on the clear oil/white foam product. The product (2.44 g, 5.2 mmol) was dissolved in 30 ml of DCM and 1.73 g (6.7 mmol) of Fmoc-Cl was added along with 1.0 mL (6.2 mmol) DIPEA. The reaction was stirred under N_2 for 2 hours at which time the reaction was complete and the solution was concentrated. The residue was brought up in 1:3 EtOAc:hexanes and a flash column was run over silica eluting with the same solution. This yielded 3.47 g (96.7 %) of the title product as a white foamy solid. ORD $[\alpha]_D$ +237.5°(*c* 0.0336, $CHCl_3$); IR (neat): 3417, 3019, 2950, 2878, 1751, 1727, 1497, 1449, 1295, 1239, 1158, 741, 704, 637 cm^{-1}; ^1H NMR (300 MHz, $CDCl_3$) δ 7.95-7.15 (m, 22H) 5.75 (m, 1H), 5.32-5.19 (m, 2H) 4.39 (dd, J = 17.1, 9.6 Hz, 1H), 4.26 (dd, J = 7.2, 6.6 Hz, 1H) 4.22-4.05 (m, 3H), 3.72 (s, 1H), 3.53 (s, 3H), 3.48 (ddd, J = 10.5, 5.1, 1.2 Hz, 1H), 3.27 (ddd, J = 10.5, 8.1, 1.5 Hz, 1H) 2.56 (ddd, J = 11.7, 8.1, 1.2 Hz, 1H), 2.26 (ddd, J = 11.7, 5.1, 1.5 Hz, 1H); ^{13}C NMR (75 Mz, $CDCl_3$);170.8, 170.2, 154.8, 146.5, 143.8, 143.6, 142.4, 140.7, 139.9, 129.5, 132.4, 128.2, 127.7, 127.3, 127.1, 126.9, 126.6, 125.8, 125.3, 125.1, 120.1, 117.8, 74.5, 67.0, 66.3, 65.6, 64.4, 52.1, 46.5, 44.9, 42.8, 33.3; HR MS (EI) calcd for $C_{44}H_{38}N_2O_6$ (M+) 690.2730, found 690.2719.

(9H-fluoren-9-yl)methyl (2S,3S)-2-((allyloxy)carbonyl)-1-(tert-butoxycarbonyl)-3-(methoxycarbonyl)pyrrolidin-3-ylcarbamate (23)

Compound **22** (3.37 g, 4.9 mmol) was dissolved in 40 ml DCM, 10 ml TFA and 600 μl of methanol were added. The reaction was allowed to stir for 1 hour. Upon completion the solution was washed with water x2. The aqueous layers were combined and made basic with $NaHCO_3$. The basic aqueous solution was extracted x2 with DCM. All organic layers were combined and washed with saturated $NaHCO_3$ x2 and brine x1. The organic layer was dried and concentrated. The resulting reddish oil was taken up in 50 ml of DCM into which were added 880 ml (5.4 mmol) of DIPEA and 1.60 g (5.4 mmol) of Boc_2O. The reaction was stirred under N_2 for two hours. Upon completion the solution was concentrated and a flash column of 1:3 EtOAc:hexanes was performed to purify material. Yield of product was 2.38 g (88.1%) of clear oil. ORD $[\alpha]_D$ +49.7^o(*c* 0.0201, $CHCl_3$); IR (neat): 3318, 3020, 2997, 2897, 1755, 1681, 1525, 1410, 1247, 1182, 758, 666 cm^{-1}; ^{1}H NMR (300 MHz, DMSO, 350K) δ 8.03 (s, 1H), 7.85 (d, J = 7.2, 2H), 7.68 (d, J = 7.2, 2H), 7.40 (m, 4H), 5.87 (m, 1H), 5.38 (d, J = 12.4 Hz, 1H), 5.29 (d, J = 10.8 Hz, 1H), 4.58-4.40 (br m, 5H), 4.22 (t, J = 7.2, 1H), 3.60-3.54 (m, 4H), 3.34 (br s, 1H), 2.50-2.44 (br m, 2H), 1.36 (br s, 9H) ; ^{13}C NMR (75 Mz, DMSO 350 K) 168.8, 168.4, 154.9, 152.3, 143.4, 143.3, 140.5, 131.5, 127.2, 126.6, 124.7, 119.6, 118.2, 79.1, 78.7, 67.4, 66.5, 65.4, 65.2, 52.0, 46.5, 43.4, 27.6; HR MS (ES) calcd for $C_{30}H_{34}N_2O_8Na$ (M+) 573.2237, found 573.2225.

(9H-fluoren-9-yl)methyl (2S,3S)-2-(carbomethoxy)-1-(tert-butoxycarbonyl)-3-(methoxycarbonyl)pyrrolidin-3-ylcarbamate (24)

Compound **23** (2.34 g, 3.8 mmol) was dissolved in 40 mL of THF, $Pd(PPh_3)_4$ (277.7 mg, 0.24 mmol) and morpholine (365 μL, 4.2 mmol) were added. The reaction was sealed and stirred under N_2 for 1.5 hours. After completion the reaction solution was washed with 1M HCl three times and once with brine. The organic layer was dried, concentrated and purifed by automated flash chromatography (gradient 0-10% MeOH in $CHCl_3$). Product isolated in 93.4 % yield as off-white foam. %). ORD $[\alpha]_D$ +43.8^o(*c* 0.0459, $CHCl_3$); IR (neat): 3307, 3011, 2978, 1755, 1710, 1683, 1527, 1450, 1412, 1251, 1162, 758, 666 cm^{-1}; ^{1}H NMR (300 MHz, DMSO, 345K rotational isomers not fully resolved) δ 8.01 (s, 1H), 7.84 (d, J = 7.2, 2H), 7.68 (d, J = 7.2, 2H), 7.40 (m, 4H), 4.40 (br m, 3H), 4.22 (t, J = 7.2, 1H), 3.62-3.51 (m, 4H), 3.32 (br s, 1H), 2.50 (br m, 1H), 2.30 (br m, 1H), 1.38 (br s, 9H) ; ^{13}C NMR (75 Mz, DMSO 350 K) 169.9, 169.0,

155.0, 152.7, 143.5, 143.4, 140.5, 127.2, 126.6, 124.7, 124.7, 119.6, 78.8, 67.5, 65.7, 65.2, 51.9, 46.6, 43.4, 30.4 %). HR MS (ES) calcd for $C_{30}H_{34}N_2O_8Na$ (M+) 573.2237, found 573.2225.

3.0 SYNTHESIS OF *PIP4(2S4R)* AND *PIP4(2S4S)* MONOMERS

3.1 OVERVIEW OF PIP MONOMER CLASS

Our ability to design molecules which place functional groups in close proximity to each other is dependent upon the formation of curved oligomeric sequences. The formation of a greater number of curved oligomeric sequences requires the development of new bis-amino acid monomers. We therefore have continued the expansion of our bis-amino acid monomer library. To further expand our library we have taken a side product formed in the synthesis of the *pip5*(2S5S) bis-amino acid monomer[5] and created a new class of monomer, the *pip4* class (Figure 15).

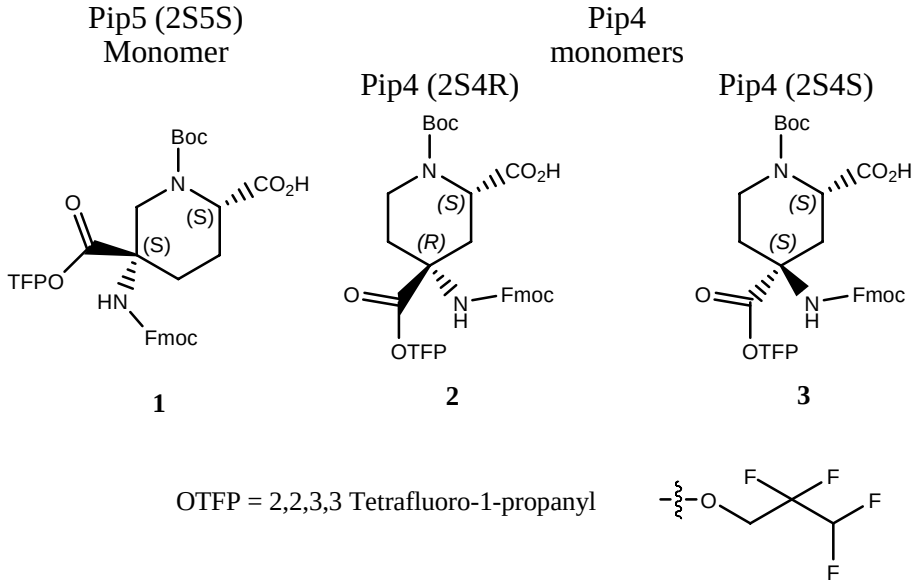

Figure 15. Currently Developed Pip Class Monomers

Gupta, Das and Schafmeister reported the synthesis of the *pip5*(2S5S) monomer[5], **1** (Figure 15). During the synthesis of this monomer, a ring expansion homologation reaction was performed which produced the regio-isomeric ketones **8** and **9** (Scheme 10). Ketone **8** was used in the synthesis of **1,** while ketone **9** was not used and was set aside for later development into *pip4* monomers. In this chapter, I describe the transformation of ketone **9** into the *pip4*(2S4R) monomer **2** and *pip4*(2S4S) monomer **3** (Figure 15).

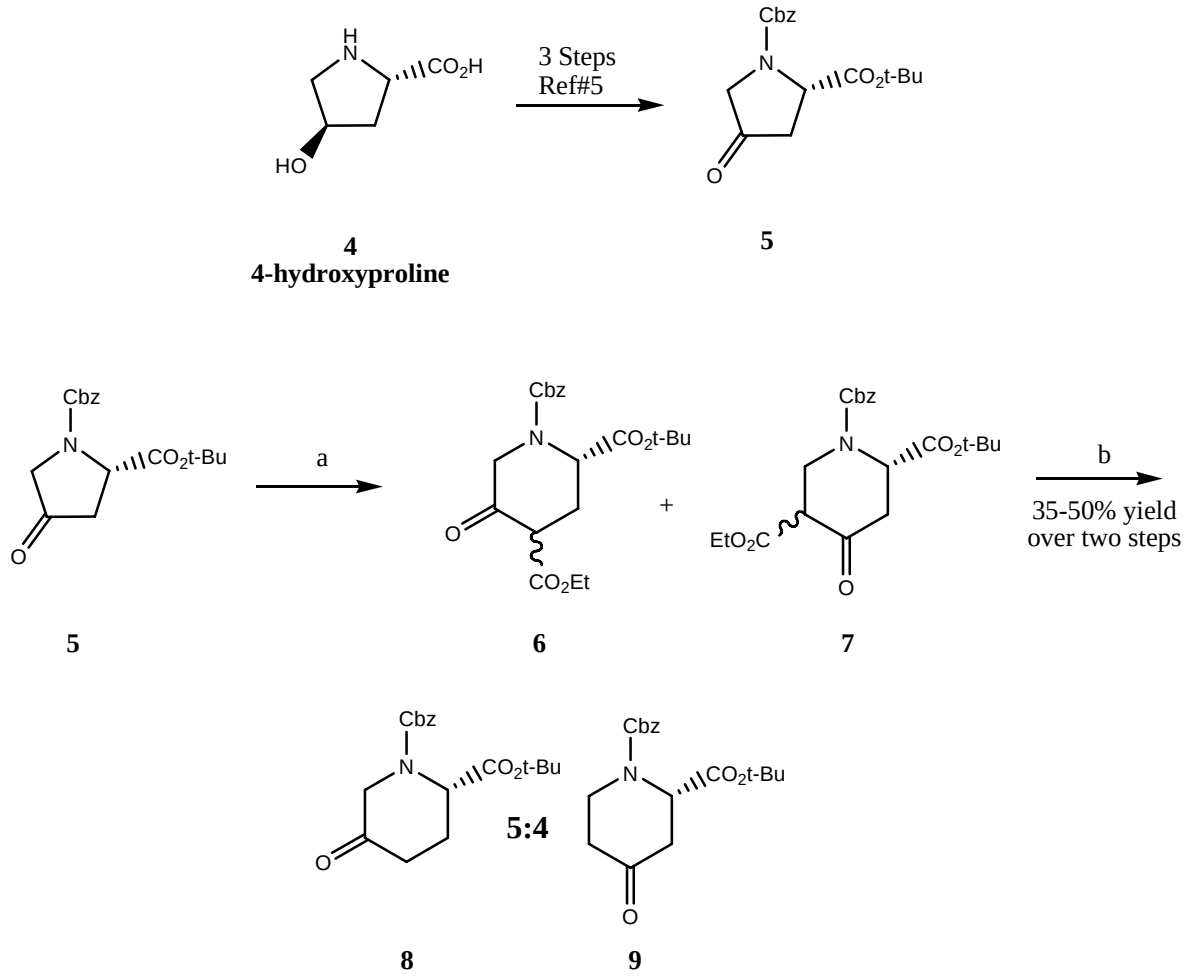

a.) ethyldiazoacetate, BF_3·etherate b.) Krapcho decarboxylation

Scheme 10. Formation of 4-oxo and 5-oxo-Pipecolic Acid Derivatives Using Ethyldiazoacetate

3.2 SYNTHESIS OF 4-OXO AND 5-OXO-PIPECOLIC ACID DERIVATIVES

Scheme 10 shows the homologation reaction of ketone **5** as developed by Pellicciari[21] and coworkers and used by Gupta and coworkers[5,21] to form pipecolic acid derived ketones **8** and **9.** This reaction yielded a 5:4 mixture of **8** and **9** respectively in a variable yield (35-50%) over two steps. The method utilized the addition of ethyl diazoacetate to ketone **5**, with ring homologation resulting upon loss of N_2 to form intermediates **6** and **7**. β-Keto-esters **6** and **7** were subjected to Krapcho decarboxylation conditions to yield ketones **8** and **9**.

I set out to develop a higher yielding homologation reaction. This reaction utilized borontrifluoride catalyzed addition of trimethylsilyldiazomethane into ketone **5** (Scheme 11)[22], followed by subsequent ring expansion with loss of N_2 to form intermediates **10** and **11**. Removal of the trimethylsilyl group with K_2CO_3 in methanol resulted in the formation of **8** and **9** in a 4:5 ratio and overall yield of 36%. The isomeric ratio was determined by ^{1}H NMR spectroscopy of the crude reaction mixture.

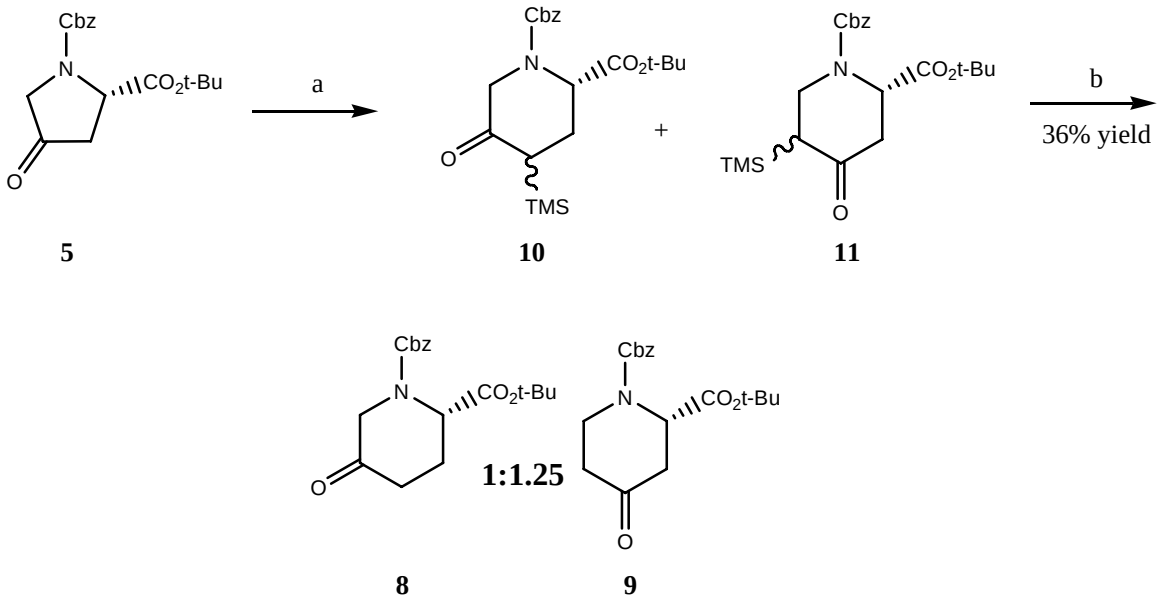

5 **10** **11**

8 **9**

a.) TMS-CH=N_2, BF_3·etherate, -78°C to RT b.) K_2CO_3, methanol.

Scheme 11. Formation of 4-oxo and 5-oxo-Pipecolic Acid Derivatives Using Trimethylsilyldiazoemthane

As the yields of the two homologation methods were comparable, our choice to use a particular homologation method would be driven by the monomer class to be synthesized. The *pip5* monomer utilized ketone **8** in its formation and would benefit from the use of the conditions

developed by Pellicciari, which produced ketone **8** in greater proportion. Our development of the *pip4* monomer was based on the use of ketone **9.** Ketone **9** was the major product of the trimethylsilyldiazomethane homologation reaction and would indicate the further use of this method in the development of the *pip4* monomer class. Both routes have similar yield and further work needs to be done to improve one or both of these routes.

3.3 STEREOCHEMISTRY OF THE BUCHERER BERGS REACTION PRODUCTS

Samples of ketone **9** were produced through both homologation methods and were combined prior to use in a Bucherer-Bergs reaction[11,12]. The Bucherer-Bergs reaction was used to convert the ketone at C4 of **9** into diastereomeric hydantoins **12** and **13**. These compounds were utilized as precursors to the formation of the α-amino acid at C4 of the *pip4* monomers **2** and **3**.

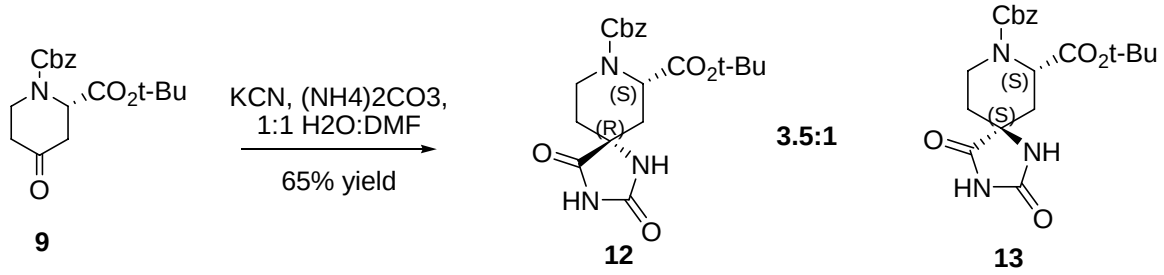

Scheme 12. Products of the Bucherer-Bergs Reaction

The Bucherer-Bergs reaction formed a mixture of spiro-hydantoin diastereomers **12** and **13** in a 7:2 ratio, as measured by ^{1}H NMR spectroscopy, in 65% overall yield (Scheme 12). The separation of **12** and **13** was performed by silica gel column chromatography (chromatography was performed on an ISCO chromatography system with a gradient: 1:8 to 1:2 ethyl acetate in hexanes).

We attempted to determine the stereochemistry of **12** using a NOESY NMR experiment, but the NOESY spectrum of **12** was ambiguous in terms of the assignment of the C4 stereochemistry. I rationalized that the Cbz group would be forcing the adjacent *t*-butyl ester into a pseudo-axial orientation, and forcing the six-membered ring to adopt the chair

conformation shown in Figure 16. I further rationalized that if I removed the Cbz group, the six membered ring could flip into the other chair conformation giving rise to a new set of NOESY correlations that might be easier to interpret. The Cbz group was removed from **12** by hydrogenolysis to produce **14** (Figure 16). A NOESY spectrum of **14** was obtained. In the spectrum a correlation was observed between the C2 hydrogen atom and one of the geminal C6 hydrogen atoms suggesting a 1,3 diaxial arrangement for these hydrogens (Figure 16). One geminal hydrogen atom on C3 of the piperidine ring and one geminal hydrogen atom on C5 also displayed a correlation in the NOESY spectrum, but no correlations were observed between either of the C3 hydrogen atoms and either C6 hydrogen atom. Nor was a correlation observed between the C2 hydrogen atom and either C5 hydrogen atom. This arrangement of NOESY correlations is consistent with the chair conformation of **14** shown in Figure 16, where the axial C3 hydrogen atom and the axial C5 hydrogen atom are on the opposite face of the piperidine ring from the C2 hydrogen atom. The stereochemistry at C4 of the pyrrolidine ring was assigned by the presence of a NOESY correlation between the hydantoin amide proton with both of the C3 and C5 axial protons as shown in Figure 16. The stereochemistry of the C4 center on **13** could not confirmed by NOE spectroscopy due to resonance overlap, but was inferred to be opposite the stereochemistry of the C4 center on **12**.

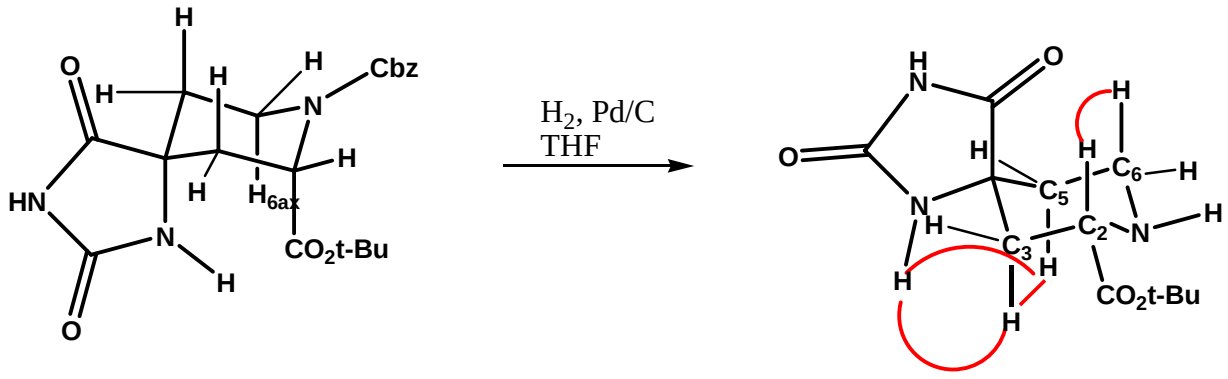

12 **14**

Correlations seen in the NOESY spectrum of **14** that helped to determine the stereochemistry at the C4 center are shown as red curves.

Figure 16. NOESY Interactions seen in Major Hydantoin Diastereomer

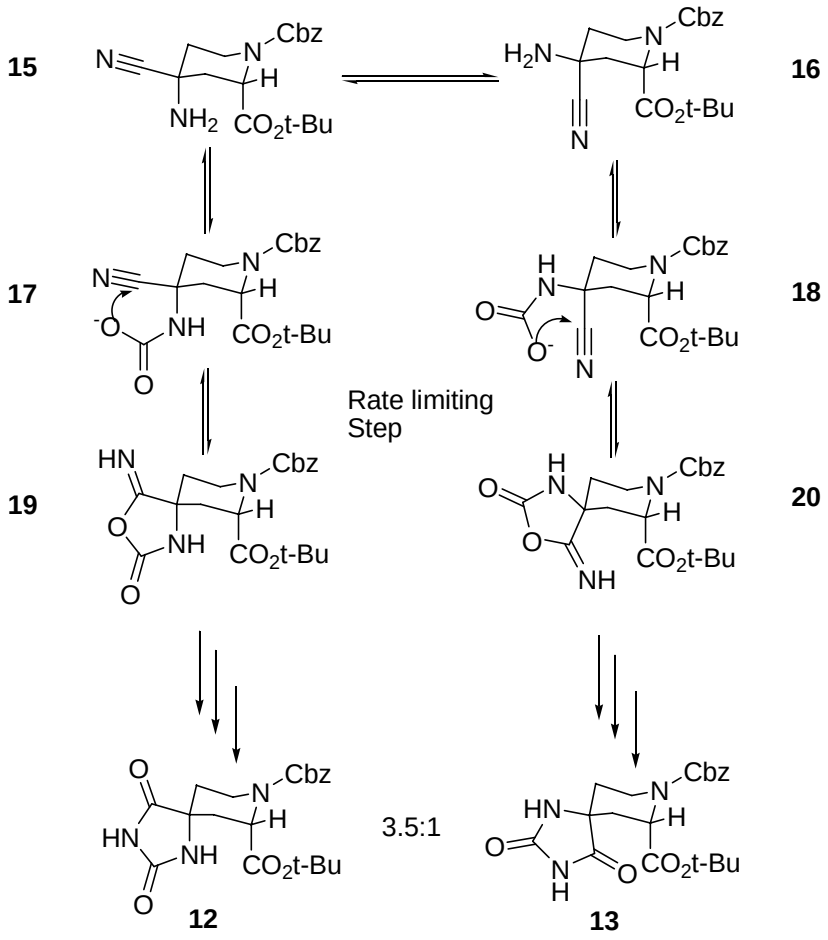

Figure 17. Mechanism of the Bucherer-Bergs Reaction

3.4 DIASTEREOSELECTIVITY OF THE BUCHERER-BERGS REACTION

In a study of the Bucherer-Bergs reaction mechanism performed by Edward and Jitrangsri[23] on 4-*tert*-butyl cyclohexanone, it was found that the rate limiting step of the hydantoin formation involved intermediates similar to **17** and **18** (Figure 17). The rate limiting step was determined to be the attack of the carboxylate oxygen into the nitrile carbon attached to C4 of these two intermediates. In **18**, this attack forced the nitrile nitrogen atom to approach the axial C2 ester and axial C6 hydrogen atom in the transition state. In **17**, the attack of the carboxylate does not produce as great a steric interaction with groups on the pyrrolidine ring in

the transition state. The production of spirohydantoin **12** as the major diastereomer of the Bucherer-Bergs reaction is consistent with the proposed mechanism.

3.5 COMPLETION OF THE SYNTHESIS OF 3

The hydrolysis of hydantoins such as **12** generally occurs under harsh conditions, NaOH or $Ba(OH)_2$, H_2O, 100^oC, which would destroy the Cbz and t-butyl protecting groups of **13**. We reacted spirohydantoin **12** with di-*tert*-butyl carbonate (Boc_2O), and 4-dimethylaminopyridine (DMAP) in THF[24]. This reaction placed Boc groups on the amide and imide nitrogen atoms of the hydantoin to form the more hydrolysable bis-Boc-hydantoin derivative **21** in 74% yield (Scheme 13)**.** The hydrolysis of **21** to form the C4 amino acid was performed in a biphasic reaction with 2M KOH and THF at room temperature for 30 minutes. The free amino acid product of the hydrolysis was isolated by precipitation and used without further purification in a Schotten-Bauman reaction with *N*-(9-fluorenylmethoxycarbonyl)-succinamide (Fmoc-OSu) in 1:1 dioxane:water to yield **22** in 78% yield over two steps.

The esterification of the C4 acid with dicyclohexylcarbodiimide (DCC), 4-dimethylaminopyridine (DMAP) and 2,2,3,3-tetrafluoro-1-propanol in dichloromethane (DCM) provided **23** in 72% yield. The synthesis of the 2,2,3,3-tetrafluoro-1-propanyl ester was indicated from the incorporation of the *pip5*(2S5S) monomer **1** into bis-peptide oligomeric other bis-amino aicds through the C5 carbonyl was facilitated by the use of the 2,2,3,3-tetrafluoro-propanylester[25].

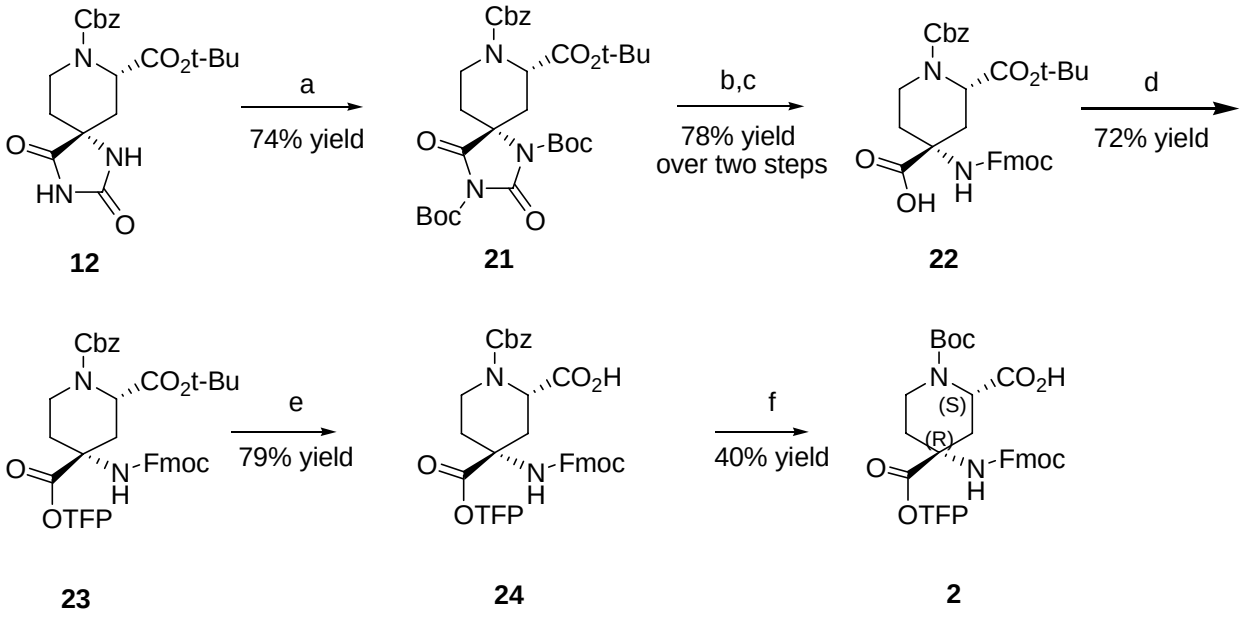

a) Boc_2O, DMAP, THF b.) 2M KOH, dioxane c.) Fmoc-Osu, K_2CO_3 d.) DCC, DMAP, 2,2,3,3 tetrafluoro-1-propanol (TFPOH) e.) 1:1 TFA:DCM f.) i) H_2, Pd/C, THF ii.) Boc_2O, DIPEA, DCM

Scheme 13. Synthesis of the *Pip4 (2S4R)* Bis Amino Acid

After the esterification at C4 to form **22** was complete, the *tert*-butyl ester at C2 of **23** was converted to the carboxylic acid with 1:1 TFA in DCM to form **24** (79% yield). Hydrogenolysis of the Cbz group followed by Boc protection with Boc_2O provided the final monomer **2** in an overall yield of 13.5% (unoptimized) from hydantoin **12**.

3.6 COMPLETION OF THE SYNTHESIS OF 4

Monomer **3** was developed from the minor hydantoin diastereomer **13**. The conversion of **13** into **3** followed the same route as the formation of **2** from **12** (Scheme 14). The overall yield of **3** was 21.8% (unoptimized) from hydantoin **13**.

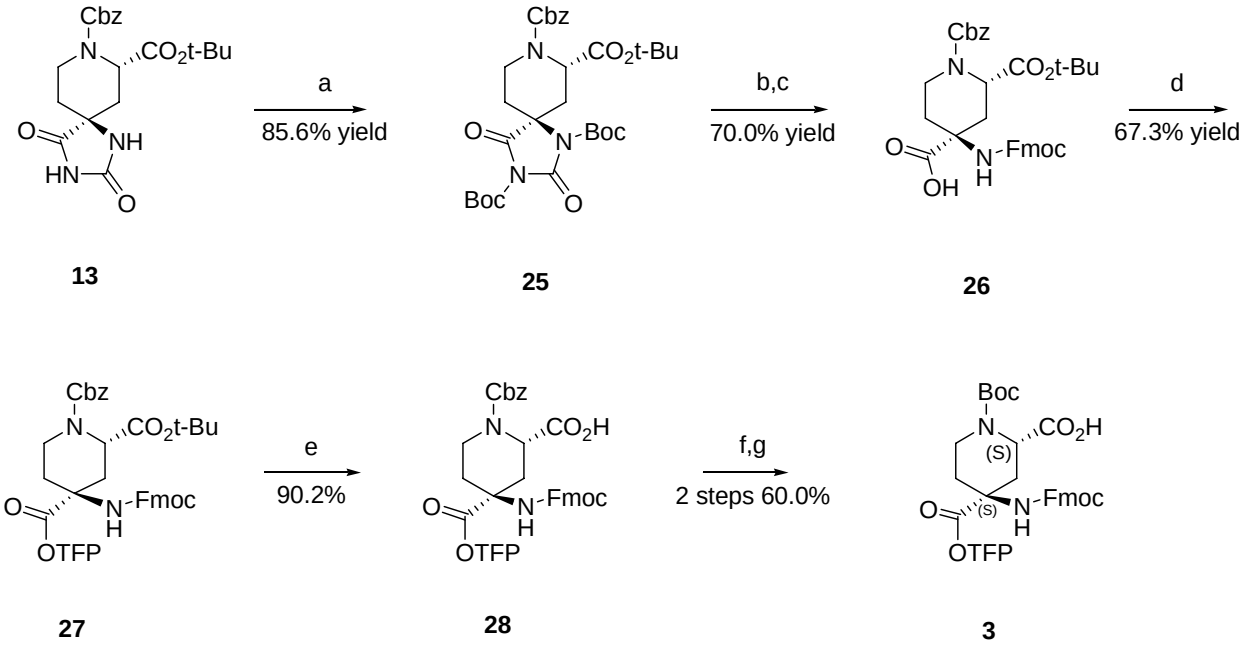

a.) Boc_2O, DMAP, THF b.) 2M KOH, dioxane c.) Fmoc-*O*-succinamide, K_2CO_3 d.) DCC, DMAP, 2,2,3,3 tetrafluoro-1-propanol (TFPOH) e.) 1:1 TFA:DCM f.) H_2, Pd/C, THF g.)Boc_2O, DIPEA, DCM

Scheme 14. Synthesis of 4

3.7 CONCLUSIONS

I applied a homologation reaction involving the use of trimethylsilyldiazomethane in the synthesis of ketones **8** and **9**. While the yield of the trimethylsilyldiazomethane reaction was comparable to the method previously employed by Gupta and coworkers, the trimethylsilyldiazomethane reaction showed reversed selectivity forming ketone **9** in slight excess. This pattern of yield was reversed from the previously applied homologation method.

I was able to complete the synthesis of the *pip4*(2S4R*)* monomer **2** in 13.5% from hydantoin **12**. I also accomplished synthesis of *pip4*(2S4S) in 21.8% overall yield from **13**. The **2** and **3** have been characterized and were observed to be stable upon storage for at least one month.

3.8 EXPERIMENTAL METHODS

(2S)-4-oxopiperidine-1,2-dicarboxylic acid 1-benzyl ester 2-tert-butyl ester (9)

Compound **5** (17.25 g, 54.0 mmol) was dissolved in 500 mL of DCM and cooled to -78^{o}C. Borontrifluoride etherate (13 mL, 51.3 mmol) was added and the solution stirred for ten minutes at which time trimethylsilyl diazomethane was added. The reaction was stirred at -78^{o}C under N2 for 4 hours, allowed to warm to room temperature and saturated aqueous sodium bicarbonate was added. The aqueous layer was washed twice with DCM and the organic layers were combined, washed with water twice, dried and concentrated. The residue was brought up in 500 mL methanol and 22.45 g (3.1 mmol) of K_2CO_3 were added. The reaction was stirred for 2 hours, then diluted with 800 mL of water. The solution was extracted with ethyl acetate twice. The ethyl acetate layers were combined, washed twice with 1M HCl, then water and once with brine, dried and concentrated. An automated flash chromatography column was performed (gradient 1:4 to 1:2 ethyl aceteate:hexanes) to clean and separate products. The compounds **8** and **9** were isolated in 36% overall yield. After separation compound **8** was isolated as yellow oil. 1H NMR (300 MHz, 345 K, DMSO) δ 7.42 (m, 5H), 5.19 (s, 2H), 4.88 (dd, J = 7.5, 3.9 Hz, 1H), 4.08 (ddd, J = 14.2, 7.2, 6.9Hz, 1H), 3.69 (ddd, J = 13.3, 8.4, 5.1, 1H), 2.98 (dd, J = 15.9, 7.5 Hz, 1H), 2.64 (dd, J = 15.9, 3.9 Hz, 1H) 2.55-2.41 (br m, 2H), 1.41 (s, 9H); 13C NMR (75 MHz, DMSO, 345 K) 204.9, 169.6, 154.4, 136.1, 127.8, 127.3, 127.0, 81.2, 66.3, 54.7, 38.6, 38.5, 27.1; HR MS (EI) calcd for $C_{13}H_{14}N_1O_3$ 232.0974 found 232.0967.

(5S,9R)-2,4-dioxo-1,3,8,triazaspiro[4.5]decane-8,9-dicarboxylic acid 8-benzyl ester 9-*tert*-butyl ester (12)

Compound **9** (10.45 g, 31.3 mmol) was placed in a reaction vessel along with 3.34 g (51.2 mmol) potassium cyanide and 16.11 g (167.7 mmol) ammonium carbonate. Water and DMF were added to the reaction vessel (80 ml each) and the vessel was sealed, stirred and heated to 70^{o}C for 4 hours. The vessel was cooled and the reaction mixture diluted with 150 ml water and extracted with ethyl acetate (2x 50 ml). The organic layer was washed with aqueous LiCl (1/2 saturated concentration) (2x 25mL) and brine, dried with $MgSO_4$ and concentrated. A flash chromatography column was run on an ISCO automated chromatography system (gradient 1:8 to 1:2 ethyl acetate in hexanes) to purify and separate the title product and its diastereomer at C_4. The title compound was crystallized from ethyl acetate/hexanes to yield white needle-like

crystals, 6.34g 50.2% yield. Mp = 105°C (decomp.) ORD $[\alpha]_D$ -24.1°(*c* 0.0359, $CHCl_3$); IR (neat): 2980, 2935, 1791, 1785, 1741,1345, 1320, 1252, 1142, 841, 752, 697 cm^{-1}; ^1H NMR (300 MHz, DMSO, 345K rotational isomers not fully resolved) δ 10.6 (s, 1H), 7.33 (m, 5H), 7.15 (s, 1H), 5.15 (d, J = 12.6, 1H), 5.08 (d, J = 12.6, 1H), 4.75 (br s, 1H), 4.00 (d, J = 13.8, 1H), 3.41 (dd, J = 12.0, 10.5 Hz, 1H) 2.11 (br m, 2H), 1.85 (ddd, J = 13.2, 13.3, 4.8 Hz, 1H) 1.65 (br m, 1H) 1.41 (s, 9H ; ^{13}C NMR (75 Mz, DMSO, 345 K) 177.0, 169.8, 156.2, 155.0, 136.3, 127.9, 127.4, 127.0, 81.3, 66.3, 59.0, 51.8, 36.8, 33.2, 30.9, 27.2; HR MS (EI) calcd for $C_{20}H_{26}N_3O_6$ (M+) 404.1822, found 404.1835.

(5S,9S)-2,4-dioxo-1,3,8,triazaspiro[4.5]decane-8,9-dicarboxylic acid 8-benzyl ester 9-*tert*-butyl ester (13)

Minor diastereomer of **12** isolated as white glassy solid 1.81 g, 14.3% yield**.** ORD $[\alpha]_D$ -13.1°(*c* 0.0151, $CHCl_3$); IR (neat): 3243, 3066, 2978, 2935, 1779, 1731, 1408, 1341, 1269, 1239, 1215, 1155, 841, 754, 697 cm^{-1}; ^1H NMR (300 MHz, DMSO, 345K) δ 10.4 (br s, 1H), 7.82 (d, J = 6.0 Hz, 1H), 7.43 (m, 5H), 5.18 (d, J = 12.6, 1H), 5.14 (d, J = 12.6, 1H), 4.63 (dd, J = 7.2, 4.5 Hz, 1H), 3.88 (ddd, J = 9.5, 9.0, 4.5 Hz, 1H) 3.56 (ddd, J = 11.1, 9.5, 3.3 Hz, 1H) 2.30 (dd, J = 13.8, 4.2 Hz, 1H) 1.93 (m, 2H), 1.67 (ddd, J = 13.2, 11.1, 5.4 Hz, 1H) 1.36 (s, 9H) ; ^{13}C NMR (75 Mz, DMSO, 345 K) 176.8, 168.0, 155.4, 154.9, 136.3, 127.9, 127.3, 127.0, 80.5, 78.4, 66.1, 57.4, 52.7, 37.5, 32.6, 32.0, 27.2; HR MS (EI) calcd for $C_{20}H_{26}N_3O_6Na$ (M+Na) 426.1641, found 426.1618.

(5S,9R)-2,4-dioxo-1,3,8,triazaspiro[4.5]decane-1,3,8,9-tetracarboxylic acid 8-benzyl ester 1,3,9-tri-*tert*-butyl ester (21)

Compound **12** (1.79 g, 4.9 mmol), ditert-butyl dicarbonate (2.31 g, 10.6 mmol) and 4-dimethyl-amino pyridine (36.1 mg, 6.0 mole%) were dissolved in 50 mL of DCM and the flask was sealed and stirred under N_2 overnight. The reaction mixture was concentrated and a flash chromatography column with a gradient of 1:4 to 1:1 EtOAc:hexanes was performed on an ISCO automated chromatography system. Title compound was isolated as a white foam (2.19g, 74.0% yield). ORD $[\alpha]_D$ -11.7°(*c* 0.0239, $CHCl_3$); IR (neat): 2981, 2935, 1826, 1781, 1744, 1456, 1420, 1370, 1338, 1306, 1252, 1144, 844, 756, 698 cm^{-1}; ^1H NMR (300 MHz, DMSO, 345K) δ 7.41 (m, 5H), 5.22 (d, J = 12.6, 1H), 5.12 (d, J = 12.6, 1H), 4.44 (dd, J = 12.3, 5.7 Hz, 1H), 3.88 (ddd, J = 9.3, 9.0, 4.5 Hz, 1H) 3.56 (m, 1H) 2.72 (dd, J = 13.8, 12.3 Hz, 1H) 2.50 (dd, J = 14.1 , 5.7 Hz, 1H), 2.24 (m, 2H) 1.58 (s, 18H), 1.41 (s, 9H) ; ^{13}C NMR (75 Mz, DMSO, 345 K) 174.2,

169.6, 169.4, 154.2, 147.5, 145.8, 144.4, 136.2, 127.8, 127.2, 126.8, 85.2, 83.9, 80.6, 78.6, 66.1, 60.2, 57.4, 52.7, 38.2, 30.4, 27.3, 27.1, 27.0, 23.2; HR MS (EI) calcd for $C_{25}H_{32}N_3O_8$ (M^+-$C_5H_9O_2$) 502.2189, found 502.2172.

(2S,4R)-4-(9H-Fluoren-9-ylcarbonylamino)-piperidine-1,2,4-tricarboxylic acid-1-benzyl ester 2-*tert*-butyl ester (22)

Compound **21** (5.55 g, 9.2 mmol) was dissolved in THF (36 mL). Potassium hydroxide solution (36 mL, 2M) was added and the biphasic solution was stirred vigorously for 2 hours. The reaction solution was diluted with 36 ml of ether and the organic and aqueous layers were separated. The ether layer was washed twice with 1% KCl (2x 36 mL). The aqueous layers were combined and cooled to 0^{o}C and 2M HCl was added slowly until precipitate formed. The precipitate was collected by filtration, washed with cold water and dried under vacuum to a white powder (3.20 g, 91.9% yield). Material was used without further purification in the next reaction. The material from the previous reaction (2.52 g, 6.6 mmol) was suspended in 60 mL of 1:1 H_2O:Dioxane to which 11.6 mmol (1.56 g) of potassium carbonate and 2.74 g (8.1 mmol) of Fmoc-*O*-succinate were added. The biphasic solution became homogenous and was allowed to react for 12 hours, after which the reaction solution was diluted with 30 mL of ether. The organic layer was separated and washed twice with 50 mL each of 1 M HCl. The aqueous layers were combined and backwashed with ether 2 x 25 ml. The combined organic layers were washed with brine, dried and concentrated. Flash chromatography with 3% Methanol in DCM with 0.1% HOAc added yielded the title compound, which was crystallized from EtOAc:hexanes to give white needles (3.09 g, 78.0% yield). Mp = 118.4^{o}C ORD $[\alpha]_D$ -14.4^o(*c* 0.0127, $CHCl_3$); IR (neat): 3324, 2977, 2935,1713, 1449, 1423,1368, 1341, 1268, 1155, 1065, 758, 741, 698 cm^{-1}; ^{1}H NMR (300 MHz, DMSO, 345K) δ 12.20 (br s, 1H) 7.86-7.31 (m, 13H), 7.15 (s, 1H), 5.22 (br s, 2H), 4.58 (dd, J = 6.9, 1.5 Hz, 1H) 4.38 (dd, J = 7.6, 5.7 Hz, 1H), 3.13 (dd, J = 7.6, 6.9 Hz, 1H) 3.98 (dd, J = 17.4, 15.2 Hz, 1H), 3.83 (br m, 1H) 3.33 (br m, 1H), 2.91 (d, J = 11.4 Hz, 1H), 2.22 (dd, J = 14.7, 7.2 Hz, 1H) 2.00 (br m, 1H), 1.68 (ddd, J = 13.4, 13.2, 5.1 Hz, 1H) 1.30 (s, 9H) ; ^{13}C NMR (75 Mz, DMSO, 345 K) 175.2, 170.4, 156.3, 155.9, 144.5, 144.3, 144.3, 141.3, 141.2, 137.3, 128.8, 128.2, 128.1, 127.9, 127.6, 127.5, 125.9, 125.6, 125.6, 120.5, 81.4, 56.5, 52.6, 47.5, 47.3, 37.2, 34.8, 32.5, 30.4, 28.0; HR MS (EI) calcd for $C_{34}H_{36}N_2O_8Na$ (M^++Na) 623.2369, found 623.2371.

(2S,4R)-4-(9H-Fluoren-9-ylcarbonylamino)-piperidine-1,2,4-tricarboxylic acid-4-(2',2',3',3')-tetrapropyl ester 1-benzyl ester 2-*tert*-butyl ester (23)

Compound **22** (3.09 g, 5.1 mmol), dicyclohexyl carbodiimide (1.69 g, 8.2 mmol), and 4-dimethylamino pyridine (80 mg, 0.65 mmol) were dissolved in DCM. To this solution was added 916 μL (10.2 mmol) of 2,2,3,3 tetrafluoro-1-propanol. The reaction was stirred overnight under N_2. The solution was filtered and concentrated. A flash chromatography column was performed with 1:3 ethyl acetate: hexanes and the title compound was produced in 72.1% yield (2.63 g) as white foam. ORD $[\alpha]_D$ -15.9^o(*c* 0.0377, $CHCl_3$); IR (neat): 3323, 2976, 2935,1708, 1517, 1450, 1419, 1368, 1271, 1220, 1156, 1107, 1078, 758, 741, 698 cm^{-1}; ^{1}H NMR (300 MHz, DMSO, 345K) δ 12.20 (br s, 1H) 7.86-7.31 (m, 14H), 6.43 (ddd, J = 52.2 Hz, 5.1, 5.1 Hz, 1H) 5.22 (br m, 2H), 4.64-4.54 (m, 5H) 4.14 (m, 2H), 3.88 (br m, 1H), 3.36 (br m, 1H), 2.93 (d, J = 11.4 Hz, 1H), 2.25 (dd, J = 14.4, 6.9 Hz, 1H) 2.00 (br m, 1H), 1.68 (ddd, J = 13.4, 12.9, 4.8 Hz, 1H) 1.30 (s, 9H) ; ^{13}C NMR (75 Mz, DMSO, 345 K) 172.7, 170.1, 156.4, 155.9, 144.3, 144.2, 144.1, 141.3, 141.2, 137.3, 128.7, 128.4, 128.2, 128.1, 127.9, 127.7, 127.5, 127.4, 125.7, 125.5, 125.4, 120.5, 109.7, 81.5, 67.0, 66.6, 60.7, 57.1, 52.5, 47.4, 47.3, 37.0, 32.3, 30.3, 28.1; HR MS (EI) calcd for $C_{37}H_{38}F_4N_2O_8Na$ (M^++Na) 737.2462, found 737.2393.

(2S,4R)-4-(9H-Fluoren-9-ylcarbonylamino)-piperidine-1,2,4-tricarboxylic acid-4-(2',2',3',3')-tetrapropyl ester 1-benzyl ester (24)

Compound **23** (2.06 g, 2.9 mmol) was dissolved in DCM (15 ml), and 15 mL of TFA were added to the solution. The reaction was sealed and stirred under N_2 for 6 hours. The reaction solution was concentrated and the residue brought up in 75 mL ether. The ether solution was washed with 1 M HCl (2x 75 mL), and brine, dried and concentrated. An automated flash chromatography column was run with a gradient of 0-5 %methanol in DCM with 0.1% HOAc added. This yielded the title compound as white foam in 79.5% yield (1.52 g). ORD $[\alpha]_D$ +27.7^o(*c* 0.0173, $CHCl_3$); IR (neat): 3271, 3017, 2957, 2935,1760, 1723, 1450, 1414, 1340, 1270, 1220, 1164, 1108, 1077, 743, 697 cm^{-1}; ^{1}H NMR (300 MHz, DMSO, 345K rotational isomers not fully resolved) δ 12.20 (br s, 1H) 7.86-7.31 (m, 14H), 6.47 (ddd, J = 52.2 Hz, 5.1, 5.1 Hz, 1H) 5.18 (br s, 2H), 4.77-4.23 (m, 6H) 3.96 (br m, 1H), 3.52 (br m, 1H), 3.05 (d, J = 11.4 Hz, 1H), 2.27 (dd, J = 14.4, 6.9 Hz, 1H) 2.06 (br m, 1H), 1.77 (ddd, J = 13.4, 12.9, 4.8 Hz, 1H); ^{13}C NMR (75 Mz, DMSO, 345 K) 171.7, 155.2, 155.0, 143.7, 143.3, 140.4, 140.3, 136.5, 134.7,

127.9, 127.3, 127.2, 126.9, 126.6, 124.9, 124.8, 119.5, 109.3, 66.1, 65.9, 59.7, 56.1, 50.9, 46.5, 36.1, 31.4, 29.6; HR MS (EI) calcd for $C_{33}H_{30}F_4N_2O_8$ (M^+) 681.1836, found 681.1824.

(2S,4R)-4-(9H-Fluoren-9-ylcarbonylamino)-piperidine-1,2,4-tricarboxylic acid-4-(2',2',3',3')-tetrapropyl ester 1-*tert*-butyl ester (2)

Compound **24** was dissolved in 20 mL of THF and 150 mg of Pd/C was added the vessel was sealed and flushed three times with H_2. The reaction was stirred at balloon pressure under H2 for 12 hours. The Pd/C was removed by filtration through Celite, and the filtrate was concentrated. The residue was brought up in 20 mL of THF and 679.1 mg (3.1 mmol) of di-tert-butyl dicarbonate was added along with 360 μL of DIPEA. The reaction was sealed and stirred for 4 hours. When complete the reaction was concentrated brought up in ether and washed with 1M HCl twice and once with brine. After drying and concentration the compound was purified by automated flash chromatography (0-5% MeOH in DCM with 0.1% HOAc). Compound 3.8 was isolated as white foam in 40.9% yield (500.9 mg). ORD $[\alpha]_D$ +42.7^o(*c* 0.0217, $CHCl_3$); IR (neat): 3271, 3017, 2957, 2935,1760, 1723, 1450, 1414, 1340, 1270, 1220, 1164, 1108, 1077, 743, 697 cm^{-1}; ^1H NMR (300 MHz, DMSO, 345K) δ 12.15 (br s, 1H) 7.87-7.31 (m, 9H), 6.41 (ddd, J = 52.2, 5.1, 5.1 Hz, 1H) 4.62-4.43 (m, 3H) 4.27-4.18 (m, 3H), 3.75 (br m, 1H), 3.36 (br m, 1H), 2.90 (d, J = 11.4 Hz, 1H), 2.20 (dd, J = 14.4, 6.9 Hz, 1H) 1.98 (br m, 1H), 1.67 (ddd, J = 13.4, 12.9, 4.8 Hz, 1H) 1.42 (s, 9H) ; ^{13}C NMR (75 Mz, DMSO, 345 K) 172.8, 156.0, 155.2, 144.5, 144.2, 141.3, 128.1, 127.2, 127.5, 125.7, 120.4, 109.7, 79.8, 66.7, 60.6, 57.0, 51.6, 47.4, 36.7, 32.4, 30.6, 28.5; HR MS (EI) calcd for $C_{30}H_{32}F_4N_2O_8Na$ (M^++Na) 647.1992, found 647.2020.

(5S,9S)-2,4-dioxo-1,3,8,triazaspiro[4.5]decane-1,3,8,9-tetracarboxylic acid 8-benzyl ester 1,3,9-tri-*tert*-butyl ester (25)

Compound **13** (0.51 g, 0.1 mmol), ditert-butyl dicarbonate (0.43 g, 0.2 mmol) and 4-dimethyl-amino pyridine (5.2 mg, 4.8 mole%) were dissolved in 50 mL of DCM and the flask was sealed and stirred under N_2 overnight. The reaction mixture was concentrated and a flash chromatography column with a gradient of 1:4 to 1:1 EtOAc:hexanes was performed on an ISCO automated chromatography system. Crystallization of **25** from ethyl acetate/hexanes was possible to yield white needles. Yield 85.6%. Mp = 155.9^{o}C ORD $[\alpha]_D$ -2.49^o(*c* 0.0117, $CHCl_3$); IR (neat): 2981, 2935, 1880, 1781, 1744, 1456, 1420, 1370, 1338, 1252, 1144, 756, 698 cm^{-1}; ^1H NMR (300 MHz, DMSO, 345K) 7.34 (br s, 5H), 5.14 (br m, 2H) 4.84 (d, J = 7.5 Hz, 1H), 4.0

(dd, J = 14.1, 3.0 Hz, 1H), 3.48 (br m, 1H), 2.77 (br m, 1H), 2.53-2.42 (br m, 2H) 2.04 (br m, 1H), 1.51 (s, 9H), 1.48 (s, 9H), 1.38 (s, 9H) ; ^{13}C NMR (75 Mz, $CDCl_3$) 168.7, 168.6, 167.9, 167.6, 155.7, 155.5, 148.3, 147.0, 144.9, 136.3, 128.4, 128.3, 127.9, 127.9, 127.8, 86.7, 85.2, 82.2, 67.6, 61.1, 52.8, 52.5, 37.2, 28.7, 27.8, 27.6; HR MS (EI) calcd for $C_{30}H_{41}N_3O_{10}Na$ (M^++Na) 626.2690, found 626.2683.

(2S,4S)-4-(9H-Fluoren-9-ylcarbonylamino)-piperidine-1,2,4-tricarboxylic acid-4-(2',2',3',3')-tetrapropyl ester 1-benzyl ester 2-*tert*-butyl ester (26)

Compound **25** (3.25 g, 5.2 mmol) was dissolved in THF (25 mL). Potassium hydroxide solution (25 mL, 2M) was added and the biphasic solution was stirred vigorously for 2 hours. The reaction solution was diluted with 36 ml of ether and the organic and aqueous layers were separated. The ether layer was washed twice with 1% KCl (2x 36 mL). The aqueous layers were combined and cooled to 0^{o}C and 2M HCl was added slowly until precipitate formed. The precipitate was collected by filtration, washed with cold water and dried under vacuum to a white powder. Material was used without further purification in the next reaction. The material from the previous reaction (1.49 g, 4.4 mmol) was suspended in 30 mL of 1:1 H_2O:Dioxane to which 5.6 mmol (0.78 g) of potassium carbonate and 1.37g (4.6 mmol) of Fmoc-*O*-succinate were added. The biphasic solution became homogenous and was allowed to react for 12 hours, after which the reaction solution was diluted with 30 mL of ether. The organic layer was separated and washed twice with 50 mL each of 1 M HCl. The aqueous layers were combined and backwashed with ether 2 x 25 ml. The combined organic layers were washed with brine, dried and concentrated. Flash chromatography with 3% Methanol in DCM with 0.1% HOAc added yielded the title compound as a clear oil (2.48g,Yield 67%). ORD $[\alpha]_D$ -11.8^o(*c* 0.0122, $CHCl_3$); IR (neat): 3323, 2977, 2935, 1759, 1705, 1525, 1450, 1420, 1368, 1268, 1218, 1155, 1107, 845, 758, 741, 698 cm^{-1}; ^{1}H NMR (300 MHz, DMSO, 345K rotational isomers not fully resolved) δ 7.86-7.30 (m, 14H), 6.39 (ddd, J = 52.2 Hz, 5.1, 5.1 Hz, 1H) 5.10 (br m, 2H), 4.49-4.32 (m, 7H) 4.20 (br m, 1H), 3.75 (br m, 1H), 3.27 (br m, 1H), 2.56 (br m, 1H), 2.20-2.15 (br m, 2H) 1.67 (br m, 1H), 1.36 (s, 9H) ; ^{13}C NMR (75 Mz, DMSO, 345 K) 170.9, 169.1, 154.9, 154.7, 143.3, 140.4, 136.3, 127.8, 127.3, 127.1, 127.0, 126.5, 124.5, 119.5, 108.7, 80.7, 66.1, 65.4, 59.7, 55.4, 52.6, 37.6, 31.9, 31.0, 27.2; HR MS (EI) calcd for $C_{37}H_{38}F_4N_2O_8Na$ (M^++Na) 737.2462, found 737.2437.

(2S,4R)-4-(9H-Fluoren-9-ylcarbonylamino)-piperidine-1,2,4-tricarboxylic acid-4-(2',2',3',3')-tetrapropyl ester 1-benzyl ester (27)

Compound **26** (1.54 g, 2.5 mmol), dicyclohexyl carbodiimide (0.85 g, 4.1 mmol), and 4-dimethylamino pyridine (40 mg, 0.32 mmol) were dissolved in DCM. To this solution was added 916 μL (10.2 mmol) of 2,2,3,3-tetrafluoro-1-propanol. The reaction was stirred overnight under N_2. The solution was filtered and concentrated. A flash chromatography column was performed with 1:3 ethyl acetate:hexane and the title compound was produced in as white foam (1.54 g, yield 90.2%). ORD $[\alpha]_D$ +12.6^o(*c* 0.0165, $CHCl_3$); IR (neat): 3308, 3034, 2940, 1758, 1716, 1450, 1425, 1359, 1268, 1218, 1187, 1108, 1077, 758, 743, 698 cm^{-1}; ^{1}H NMR (300 MHz, DMSO, 345K rotational isomers not fully resolved) δ 12.20 (br s, 1H) 7.86-7.33 (m, 14H), 6.38 (ddd, J = 52.2 Hz, 5.1, 5.1 Hz, 1H) 5.14 (br s, 2H), 4.58-4.19 (Br m, 6H) 3.82 (br m, 1H), 3.33 (br m, 1H), 2.55 (Brm, 1H), 2.26-2.05 (Br m, 1H) 1.97-.174 (br m, 3H), 1.25 (Br m, 1H); ^{13}C NMR (75 Mz, DMSO, 345 K) 171.2, 170.8, 154.9, 154.8, 143.4, 143.3, 140.4, 136.4, 127.9, 127.3, 127.1, 126.9, 126.6, 124.6, 119.6, 108.8, 66.1, 65.4, 59.5, 55.4, 51.8, 47.3, 46.5, 37.7, 32.9, 31.4; HR MS (EI) calcd for $C_{33}H_{30}F_4N_2O_8$ (M^+) 681.1836, found 681.1840.

(2S,4S)-4-(9H-Fluoren-9-ylcarbonylamino)-piperidine-1,2,4-tricarboxylic acid-4-(2',2',3',3')-tetrapropyl ester 1-*tert*-butyl ester (3)

Compound **27** (1.03 g, 1.8 mmol) was dissolved in DCM (7 ml), and 7 mL of TFA were added to the solution. The reaction was sealed and stirred under N_2 for 6 hours. The reaction solution was concentrated and the residue brought up in 40 mL ether. The ether solution was washed with 1 M HCl (2x 40 mL), and brine, dried and concentrated. An automated flash chromatography column was run with a gradient of 0-5 %methanol in DCM with 0.1% HOAc added. This yielded the title compound as white foam Yield over 2 steps 60.0% (0.68 g). ORD $[\alpha]_D$ -4.8^o(*c* 0.0121, $CHCl_3$); IR (neat): 3324, 3017, 2932, 2856, 1755, 1704, 1525, 1450, 1415, 1367, 1253, 1178, 1108, 758, 742, 698 cm^{-1}; ^{1}H NMR (300 MHz, DMSO, 345K, rotational isomers not fully resolved) δ 12.15 (br s, 1H) 7.87-7.31 (m, 14H), 6.39 (m, 1H) 4.62-4.18 (m, 6H), 3.65 (br m, 1H), 3.09 (br m, 1H), 2.10 (br m, 1H), 1.65 (br m, 1H) 1.98 (br m, 1H), 1.38 (br s, 9H), 1.20 (βρ μ, 2H) ; ^{13}C NMR (75 Mz, DMSO, 345 K) 171.1, 155.0, 143.3, 140.4, 128.4, 127.8, 127.1, 126.8, 126.5, 124.5, 119.5, 109.7, 66.1, 59.7, 47.2, 46.4, 32.9, 27.5, 28.5.

4.0 APPLICATION OF RESIDUAL DIPOLAR COUPLINGS TO THE DETERMINATION OF BIS-PEPTIDE OLIGOMER SOLUTION STRUCTURE

4.1 INTRODUCTION

In the bis-peptide approach (Chapter 1) to macromolecular synthesis all monomers are linked covalently through pairs of amide bonds to create spiroladder oligomers[4-8]. The shape of the oligomer is dependent upon the monomers included in the sequence, the stereochemistry and conformation of the monomers, and the order in which the monomers occur in the sequence[7]. Due to the covalently bonded, poly-cyclic nature of the oligomers, the conformations available to bis-peptide oligomers are limited when compared to polypeptides and other more flexible macromolecules.

In order to develop applications for bis-peptides, it is valuable to be able to determine the solution structures of bis-peptide oligomers. Our research in this area has made use of ROESY NMR spectroscopy[4,5,7,8,26,27], double electron-electron resonance (DEER) experiments[28] and fluorescence energy transfer experiments (FRET)[6] to obtain information about the structure and flexibility of bis-peptides.

ROESY NMR spectroscopy has taught us[4-8] the preferred conformations of individual rings from NOE correlations of ^{1}H atoms. For each monomer within an oligomer there are typically only a small number of ROESY correlations, generally between zero and three. Often potential correlations are obscured by overlap with other signals and overlap with the solvent peak further reducing the data available to determine solution structure; thus ROESY spectroscopy alone provides few constraints for structure determination.

The use of ROESY spectroscopy and residual dipolar couplings (RDCs) in structure determination is complementary, and the use of both techniques can provide a greater number of

constraints to the possible conformations of a molecule than either one alone. With a greater number of constraints, we can feel more confident in our identification of the solution structure of a bis-peptide.

ROESY spectroscopy provides distance information concerning the hydrogen atoms within a molecule. A correlation between hydrogen atoms indicates that the atoms are in close proximity to each other, generally within 4 Angstroms. The intensity of the observed correlations can be used to filter a set of reasonable conformational models by constraining the distance between pairs of hydrogen atoms. The possibility of small errors in the intensity measurement of the NOE signals could place the correlated atoms at improper distances from each other. The cumulative effect of the errors in distance may lead to the interpretation of an improper conformation. The distance information provided by ROESY spectroscopy can be supplemented by the measurement of RDCs, which provide information on the orientation of an internuclear vector with respect to the magnetic field of a nuclear magnetic resonance (NMR) spectrometer. Residual dipolar coupling values arise from the interaction of two dipolar nuclei within a molecule if molecular rotation is partially impeded in an ordered fashion within the magnetic field of a nuclear magnetic resonance (NMR) spectrometer.

Organic chemists have begun to utilize RDC's for structural determination only within the last five years[29-34]. A delay from its use in structural biology[35] ensued largely due to the lack of suitable NMR alignment media that were soluble in organic solvents. Most studies to date have been performed to distinguish between diastereotopic geminal protons[31-34] in molecules with little conformational flexibility. However, Bush and coworkers[36,37] have reported the use of residual dipolar couplings and ROESY spectroscopy as constraints to filter libraries of conformational models to determine the solution conformation of short oligosaccharides.

In the past our group has used ROESY spectroscopy alone[4-8] to filter a set of candidate structures to determine the solution structure of bis-peptides. In the first portion of this chapter, I report the first use of residual dipolar coupling supported by ROESY spectroscopy to filter a set of DFT refined conformations to determine the solution phase structure of bis-peptide **1** (Figure 18). We determined that we can measure the RDC values for the C-H bonds in the cyclic backbone of **1**, and that the RDC values can be used to identify a single, model of **1** that fits best to the collected RDC data. Our modeling of **1** was independent of constraints derived from NMR spectroscopy data.

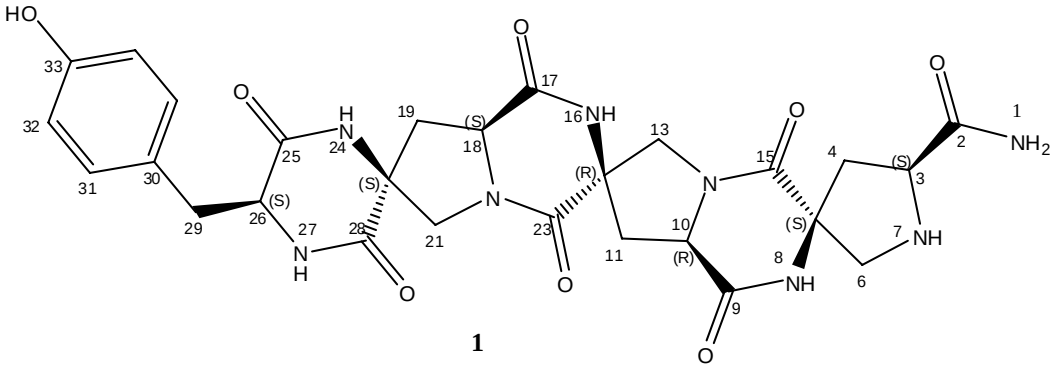

1

Figure 18. Structure of *pro4(2S4S)-pro4(2R4R)-pro4(2S4s)*-Tyr

The second portion of the chapter details the solution structure determination of a second bis-peptide oligomer by ROESY spectroscopy alone.

4.2 RESIDUAL DIPOLAR COUPLING STUDIES OF BIS-PEPTIDE OLIGOMER *PRO4*(2S4S)-*PRO4*(2R4R)-*PRO4*(2S4S)-TYR

Residual dipolar couplings (RDCs) are of most value when the molecule maintains a single conformation in solution, as each conformation present in a dynamic ensemble will give rise to different a different set of RDC values for each set of interacting dipolar nuclei. The observed value of the RDCs will be a weighted average dependent upon the populations of the conformations in the ensemble. The interpretation of such a set of RDCs becomes more difficult with the number of different conformations present in the ensemble.

My study involved the measurement of RDCs between naturally abundant ^{1}H and ^{13}C atoms bonded to one another. In the context of ^{1}H-^{13}C bonds, RDC values contain information on the orientation, with respect to the NMR magnetic field B_o, of the ^{1}H-^{13}C bonds for which RDCs have been determined. By constraining the orientations of the C-H bonds within a molecule to a single frame of reference, RDCs also constrain the orientation of the bonds to one another even if the bonds are remote in covalent structure and distance. The constraints on bond orientation provided by RDCs provide a powerful tool to determine the solution phase structure

of a molecule, as the orientations of the bonds within a molecule are altered with respect to one another between conformations.

The measurement of residual dipolar coupling requires molecular rotation to be partially impeded. The impediment to rotation, called an alignment medium, must have a single orientation with respect to B_o. Common alignment media are solutions of liquid crystals in aqueous samples[38,39] or strained gels in the case of molecules soluble in organic solvents[40]. The alignment medium ensures that the molecule tumbles in an anisotropic manner, which means all of the orientations of the molecule with respect to the spectrometer magnetic field B_o are not equally likely. Alignment media must be chosen to weakly align the small molecule so as to create dipolar coupling values that would be about 1/10,000 of the solid state values[41]. The alignment medium used in my study was a 10mg/ml solution of Pf1 phage in D_2O[39]. The aligned phage particles interact with the molecule to impede its tumbling, and do not contribute to the NMR spectrum because they do not tumble. The phage NMR signals are broadened into the baseline due to extremely fast T_2 relaxation.

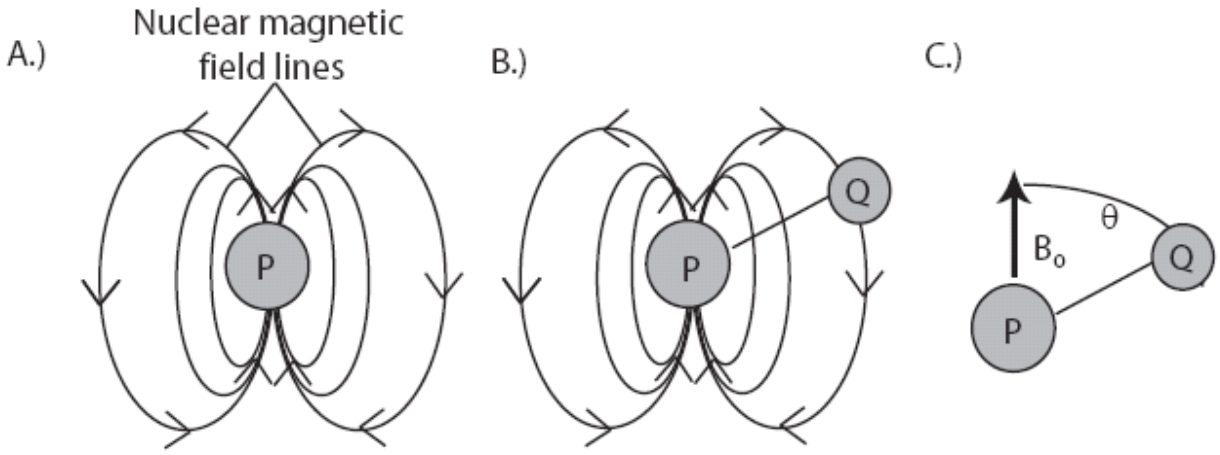

A.) The magnetic field generated by a dipolar, magnetically active nucleus P. B.) The P nuclear magnetic field can have a shielding or deshielding effect on a nearby nucleus Q with respect to the applied magnetic field B_o. C.) The effect of the nuclear magnetic field on a nearby magnetically active nuclei is dependent upon the angle θ between the internuclear vector PQ or QP and the applied field; this type of coupling is called dipolar coupling.

Figure 19

A dipolar nucleus, P, generates a local magnetic field (Figure 19). If P is placed in a strong magnetic field B_o, such as in an NMR spectrometer, its magnetic field aligns with the external field. The magnetic field experienced by another nearby, dipolar nucleus Q is the sum of the P nuclear field at Q and the external field B_o; this is termed dipolar coupling. The magnitude of dipolar coupling is related to the inverse cube of the distance between the nuclei and the angle the internuclear vector makes with B_o; when P and Q atoms are bonded to each other the internuclear vector is the bond between the atoms. If a crystalline solid was placed in an NMR spectrometer, the orientation of the PQ bond would be held constant with respect to the external field and the magnitude of dipolar coupling would be described by Equation 1.

Equation 1 $D^{PQ} = D^{PQ}_{max} (3\cos^2\theta-1)/2$

Where θ is the angle between the internuclear vector and B_o, and D^{PQ}max is:

Equation 2 $D^{PQ}_{max} = -\mu_o (h/2\pi) \gamma_P\gamma_Q / (4\pi^2 r^3_{PQ})$.

The term μ_o is the permittivity of vacuum, h is Planck's constant γ_P and γ_Q are the magnetogyric ratios of P and Q respectively an r_{PQ} is the distance between the nuclei. The value of the dipolar coupling in the case of a ^1H-^{13}C bond in a solid can be on the order of 60 KHz.

When dissolved in solution the molecule tumbles, and the orientation of the PQ bond with respect to B_o is not constant but varies with time and from molecule to molecule. The value of the dipolar coupling can be described in this case by Equation 3.

Equation 3 $D^{PQ} = D^{PQ}_{max} \langle(3\cos^2\theta-1)/2\rangle$

The brackets <> in Equation 3 indicate the average of the term $(3\cos^2\theta-1/2)$ over time. In the case of isotropic tumbling, the $\langle(3\cos^2\theta-1/2)\rangle$ term averages to zero, and the dipolar coupling is not observed in the NMR spectrum. If a molecule is partially aligned it no longer tumbles isotropically and it becomes "partially aligned". In a partially aligned situation, some orientations of the molecule with respect to B_o become more probable than others and a portion

of the dipolar coupling, called residual dipolar coupling can be observed. A set of residual dipolar couplings for a molecule can be calculated in terms of Equation 4:

$$\textbf{Equation 4}\ D_{ij} = D_{\max} / r_{ij}^3 \sum_{k,l} S_{kl} \cos(\theta_k) \cos(\theta_l)$$

Here S_{kl} contains information about the partial alignment of the molecular coordinate axes with respect to B_o, and the cosine terms relate the internuclear vectors of the bonds to the molecular coordinate axes. The value of an RDC is determined from a pair of NMR spectra, and the directional cosines are obtained from the conformational model leaving the partial alignment of the molecule be calculated. A complete description of the partial alignment of the molecule is called the alignment tensor, **S**. The calculation of the alignment tensor requires a set of at least 5 measured, non-degenerate residual dipolar couplings and the coordinates of the interacting nuclei from a conformational model.

In this study, the calculation of alignment tensors was performed using the REDCAT program developed by Prestegard and coworkers[42]. The input for REDCAT is the set of at least 5 experimentally determined RDC values, an error range for each RDC value, ε_{ij}, and the coordinates of the interacting nuclei. The model structure is used to determine the internuclear distance for each bond and to create a matrix, **A**, of direction cosines which relate the individual internuclear vectors to the molecular coordinate system.

A set of RDCs, b can be calculated from the matrix **A** and an alignment tensor **S** using matrix multiplication (Equation 5)

Equation 5 b = AS.

REDCAT uses singular value decomposition to determine the left pseudo-inverse of **A**, $\mathbf{A^{-1}}$ as a real matrix. If both sides of Equation 5 are multiplied by $\mathbf{A^{-1}}$, **S** can be calculated.

Equation 6 $\mathbf{S = A^{-1}b}$

The alignment tensor **S** is converted into a 3x3 matrix that can be diagonalized resulting in a set of three eigenvalues and eigenvectors. The eigenvalues are sorted and assigned the terms

Axx, Ayy, and Azz such that Azz has greatest magnitude and Axx has the lowest magnitude. The diagonalization also produces three eigenvectors which are the x, y, and z axes of a new coordinate system called the principle axis system (PAS) of the molecule. The values of Axx, Ayy, Azz are the probability that the PAS x, y, z axes of the molecule will align with the direction of the external field B_0.

Once an alignment tensor, **S**, is calculated by REDCAT it can be used to determine a predicted set of RDC values, $b_{predicted}$, from the structure matrix **A** (Equation 7). The fit between $b_{predicted}$ and the measured RDC values, b is calculated as the root mean square difference (RMSD) between the values.

Equation 7 $\mathbf{b_{predicted} = AS}$

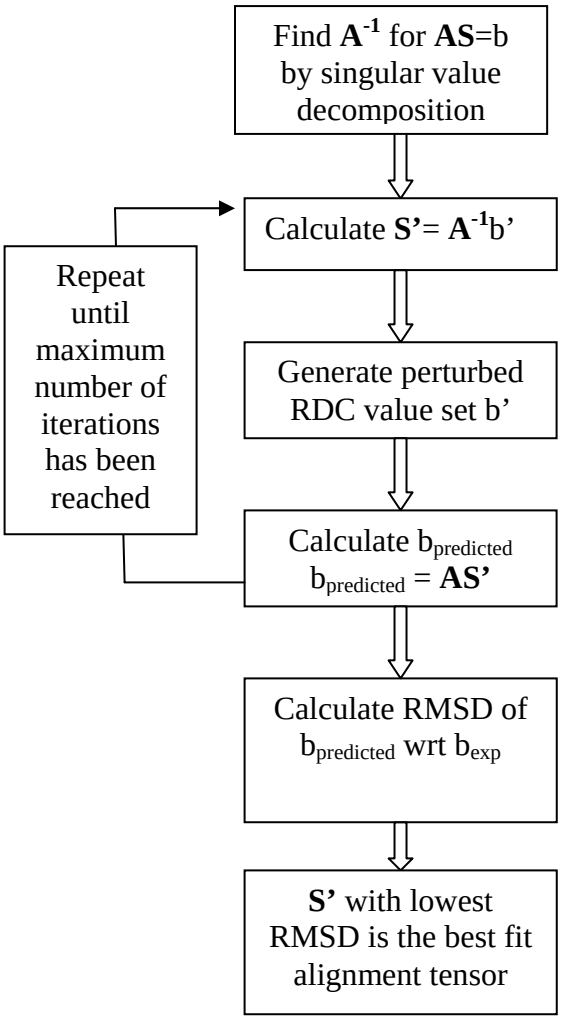

Figure 20. Flowchart of the REDCAT Process for the Calculation of Best Fit Alignment Tensor

Due to uncertainty in the measured RDC values, multiple alignment tensors **S'**, are calculated iteratively from perturbed sets of RDC values, b' (Equation 8)

Equation 8 $\mathbf{S' = A^{-1}b'}$

The sets of perturbed RDC values are obtained by random variation of each input RDC within the error range $\pm\varepsilon_{ij}$, which is given to REDCAT as user defined input (

Figure 20). All alignment tensors calculated are evaluated for their ability to predict the input set of RDCs (Equation 9)

Equation 9 $\mathbf{b_{predicted}' = AS'}$

The best fit alignment tensor for the input RDCs will be the alignment tensor which has the lowest RMSD between $b_{predicted}$' and the measured RDC values, b. The best fit alignment tensor for the conformational model and the input RDCs is reported by REDCAT. REDCAT can also report the values of the predicted RDCs from the best fit alignment tensor and the conformational model. We assess the fit of a conformational model to the measured RDC data

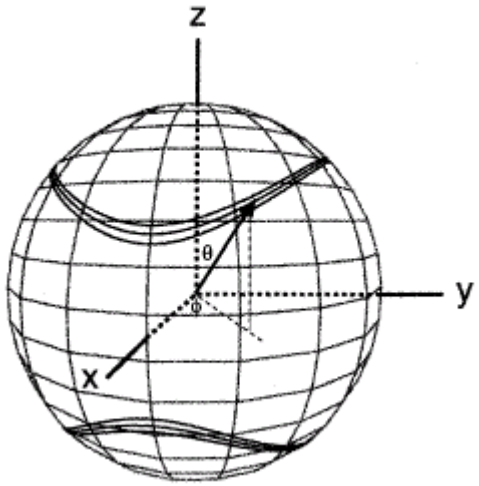

The conical regions of space where the internuclear vector PQ , or its inverse QP could lie. Note the appearance of the cone is not circular, but ovoid. Copied from ref [41]

Figure 21. Conical Region of Space Containing Internuclear Vectors

by comparing the RMSD fit between the RDCs predicted by the best fit alignment tensor and the measured RDCs. A model which does not correctly predict the bond orientations within the solution phase structure will predict RDCs that do not match the measured RDCs.

If the coordinates of the internuclear vectors are given in polar coordinates with respect to the PAS, equation 4 can be rewritten as Equation 10 which can be used to predict the value of a residual dipolar coupling.

Equation 10 $$D^{PQ} = 3/4 D_{\max}^{PQ}\left[\left(3\cos^2\theta\right)A_{ZZ} + \sin^2\theta\cos 2\phi\left(A_{xx} - A_{yy}\right)\right]$$

This equation predicts that a residual dipolar coupling value may arise from the orientation of the PQ bond anywhere on a conical section of space. The internuclear vectors PQ and QP produce the same value for a residual dipolar coupling so the region of space where the bond could lie is described by two conic sections. Additionally, these conic sections of space are not circular, but are distorted due to the higher probability of molecular alignment along the molecular y axis over the molecular x axis (Figure 21). Equation 10 tells us that a single RDC value only constrains a bond vector to lie somewhere on these two conical sections of space but it does not constrain it within the conical section of space. This is a fundamental limit on the structural information provided by a single RDC value with regards to the orientation of a single bond.

The REDCAT program has the ability to use summed RDC values of methylenes in its analysis; this feature became important to us because we obtained the least error in our measurements when we measured RDC values in the carbon (F1) dimension of the HSQC spectrum. In the case of a methylene unit, a carbon with two attached hydrogens Ha and Hb the value in Hertz obtained from the resonance splitting in the unaligned HSQC spectrum is the sum $^1J_{CHa} + ^1J_{CHb}$ and the value in Hertz obtained from the resonance splitting in the aligned HSQC spectrum is the sum $^1J_{CHa} + ^1D_{CHa} + ^1J_{CHb} + ^1D_{CHb}$. The difference between these two splittings is the sum of the two RDCs $^1D_{CHa} + ^1D_{CHb}$. This is a fundamental limitation in our ability to measure RDCs that arises because we are measuring the splittings in the carbon (F1) dimension. The consequence of this limitation is that we have fewer RDCs available for refinement and we had to learn how to deal with the added complexity of summed values of RDCs. For instance, we

were not able to figure out how to configure the commonly used residual dipolar coupling software PALES[43] to deal with summed values of RDCs. However, we did learn how to deal with these values using REDCAT. This problem only arises for us because we are measuring RDC values between carbon and hydrogen and most of our carbons are methylenes; this is not a problem for methines and we don't have methyl groups (and we would ignore them if we did). In NMR structure determination of biomolecules this problem does not arise; RDCs are commonly measured between ^{15}N atoms and their attached ^{1}H atoms of amide bonds, and alpha carbons and their attached hydrogen atoms (methines). The structure refinement program XPLOR does support summed RDC values.

4.3 DATA COLLECTION

Our approach to structure determination was to compare measured RDC values to the residual dipolar couplings predicted through the use of REDCAT of a small collection of chemically reasonable models of **1**. The chemically reasonable models of **1** were generated in a stochastic search[44] utilizing the AMBER 94[10] force field in the molecular modeling program MOE[9] and further refined by DFT calculations (Becke3LYP/6-31g* level of theory). The goal was to determine if there was a single conformation that fit the RDC data well. We were also interested in determining if the lowest energy model corresponded to the model that gave the best fit of predicted and experimental RDC's.

Prior to the measurement of RDC's the assignment of all proton and carbon resonances was performed based on TOCSY, HMBC and ROESY spectral data (spectra are available in the Appendix, see experimental data for sample preparation) including the assignment of individual diastereotopic geminal protons.

The measurement of the RDC values was accomplished by comparing the differences of the resonance splitting seen in two ^{1}H-^{13}C coupled HSQC (Heteronuclear Single Quantum Coherence) spectra: one spectrum collected on a sample of **1** without phage added and one collected from a sample of **1** with 10mg/ml Pf1 phage solution added (Pf1 phage solution was obtained from Asla Biotech and suspended in pH 7.5, 50 mM phosphate buffered D_2O). The

phage free sample was used to measure the $^{1}J_{CH}$ (one bond J coupling between ^{13}C and ^{1}H atoms) values for the C-H bonds in the cyclic backbone, C3-C26, of **1**, and the phage containing sample was used to measure the $^{1}J_{CH}$ + $^{1}D_{CH}$ (the sum of the J coupling and the one bond dipolar coupling between ^{13}C and ^{1}H atoms) values for the same C-H bonds (spectra are available in the Appendix, see experimental data for sample preparation). The difference in Hertz between the $^{1}J_{CH}$ coupling and the $^{1}J_{CH}$+$^{1}D_{CH}$ coupling was the value of the residual dipolar coupling.

The measurement of RDC's in organic molecules has often been performed by measuring the CH coupling in the more densely sampled F2 (^{1}H) dimension[30-34]. In this method of HSQC experimentation $^{1}J_{CH}$ and $^{1}D_{CH}$ coupling is allowed to build during the signal acquisition by turning off the decoupling pulses (Figure 22). Unfortunately our experience was that the alignment medium caused severe line broadening in the ^{1}H (F2) dimension (Figure 23) preventing the accurate measurement of the RDC values.

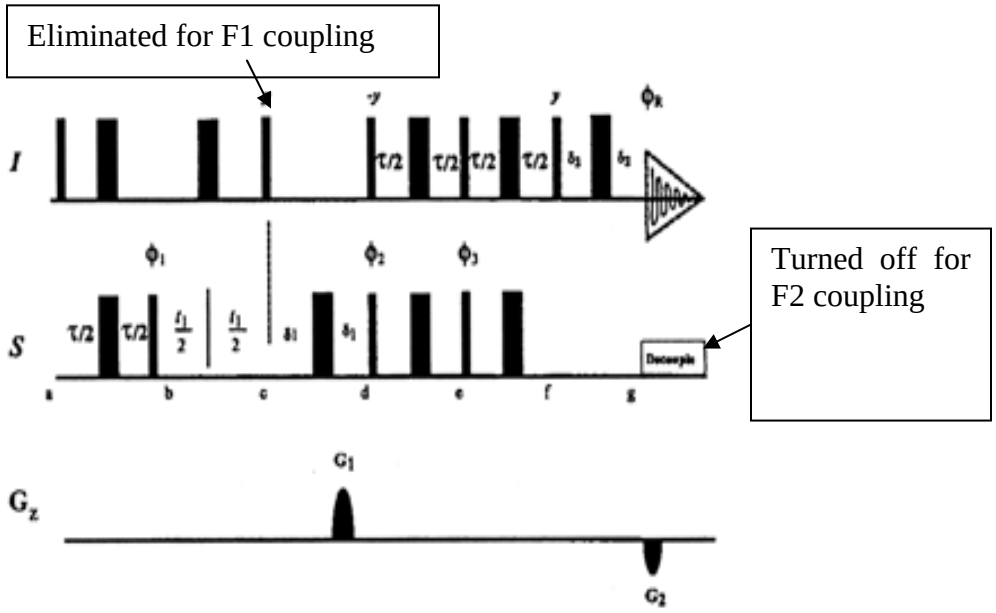

Figure 22 Pulse Sequence of the HSQC NMR Experiments

As can be seen in the spectra in Figure 23c, the line broadening of the aligned sample caused the loss of all proton-proton J-coupling from the resonance and resulted in a broad peak. This hampered our ability to obtain accurate RDC values (less than estimated 1Hz error) from the spectrum (Table 4).

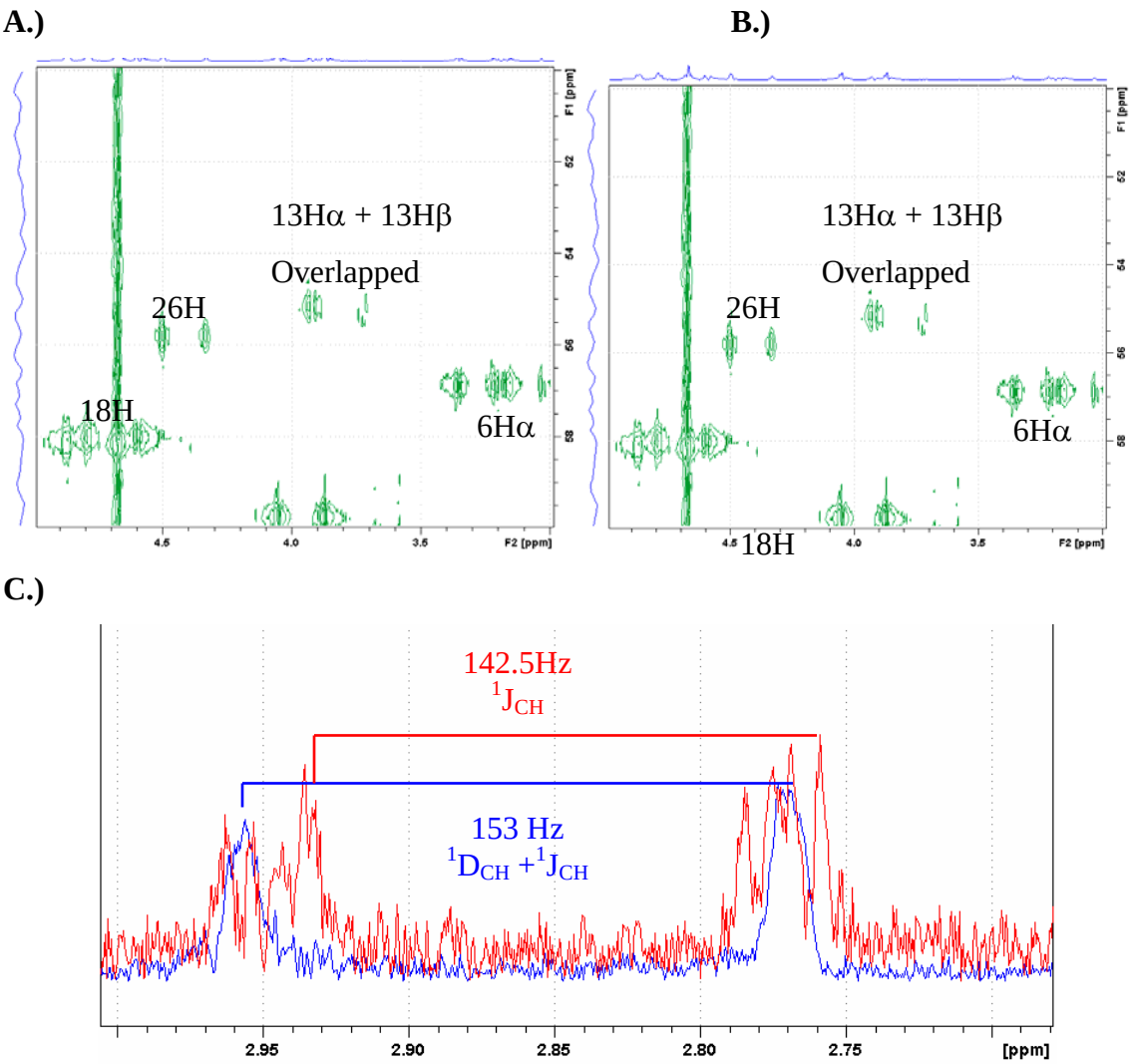

A.) The region from f2 3-5ppm and f1 50-60 ppm of the unaligned F2 coupled HSQC of **1**. B.) Identical spectral region of HSQC from the 10mg/ml phage aligned sample. C.) Overlays of one dimensional slices of the 11Ha resonance form the unaligned HSQC spectrum (red) and the same slice from the aligned HSQC (blue). Note the loss of the fine structure of the blue peaks making it impossible to determine the $^{1}D_{CH}+^{1}J_{CH}$ value to the ~1Hz accuracy required. All spectra were obtained on a Bruker 800 MHz NMR equipped with a cryoprobe.

Figure 23. Sample F2-HSQC NMR Spectra

Table 4. RDC Values for CH bonds in 1 as Measured in the F2 Coupled HSQC

Resonance	F2 Dimension Couplings			
	$^1J_{CH} + {}^1D_{CH}$ (Hz)	$^1J_{CH}$ (Hz)	$^1D_{CH}$ (Hz)	Error
3H-3C	144.8	143.8	0.9	> 1Hz
4Ha-4C	137.5	140.0	-2.5	> 1Hz
4Hb-4C	133.2	133.4	-.02	>1Hz
6Hb-4C	146.1	141.3	4.8	> 1Hz
11Ha-11C	153.5	142.5	11.0	> 1Hz
11Hb-11C	147.2	133.2	14.0	> 1Hz
18H-18C	152.4	146.0	6.4	> 1Hz
19Ha-19C	137.5	140.0	-2.5	> 1Hz
19Hb-19C	138.5	134.1	4.4	> 1Hz
21Ha-21C	148.0	142.8	5.2	> 1Hz
21Hb-21C	156.9	143.3	13.6	>1 Hz
26H-26C	129.0	151.9	-22.9	> 1Hz

4.4 F1 (^{13}C) DIMENSION MEASUREMENT OF RDC DATA

To achieve better spectral resolution the ^{1}H-^{13}C coupled HSQC pulse sequence was modified to eliminate the 180^o pulse on the ^{1}H channel during the t1 evolution period and decoupling was performed during signal acquisition (2k data points in the F1dimension zero filed back to 2k for a resolution of 2.94 Hz/point and 4k data points in the F2 dimension). The collection of HSQC spectra in this manner allowed the measurement of the coupling values in the ^{13}C (F1) dimension where line broadening was diminished and had less of an impact upon RDC measurement (Figure 24). The coupling values were obtained from one dimensional slices of the two dimensional dataset (Table 5).

Table 5. Residual Dipolar Coupling Values Measured in F1 (^{13}C) Dimension

Resonance	F1 Dimension Coupling			
	$^{1}J_{CH} + {}^{1}D_{CH}$ (Hz)	$^{1}J_{CH}$ (Hz)	$^{1}D_{CH}$ (Hz)	Error
3H-3C	144.4	144.7	-0.28	±0.5 Hz
4Ha-4C +4Hb-4C	269.0	271.0	-1.99	±0.5 Hz
6Ha-6C + 6Hb-6C	292.1	287.6	4.57	±0.5 Hz
10H-10HC	152.3	147.3	5.00	±0.5 Hz
11Ha-11C + 11Hb-11C	310.3	296.6	13.74	±0.5 Hz
13Ha-13C + 13Hb-13C	299.3	276.9	22.35	±0.5 Hz
18H-18C	155.0	146.9	8.06	±0.5 Hz
19Ha-19C + 19Hb-19C	275.4	277.0	-1.62	±0.5 Hz
21Ha-21C + 21Hb-21C	301.3	297.7	3.58	±0.5 Hz
26H-26C	135.8	148.8	13.01	±0.5 Hz

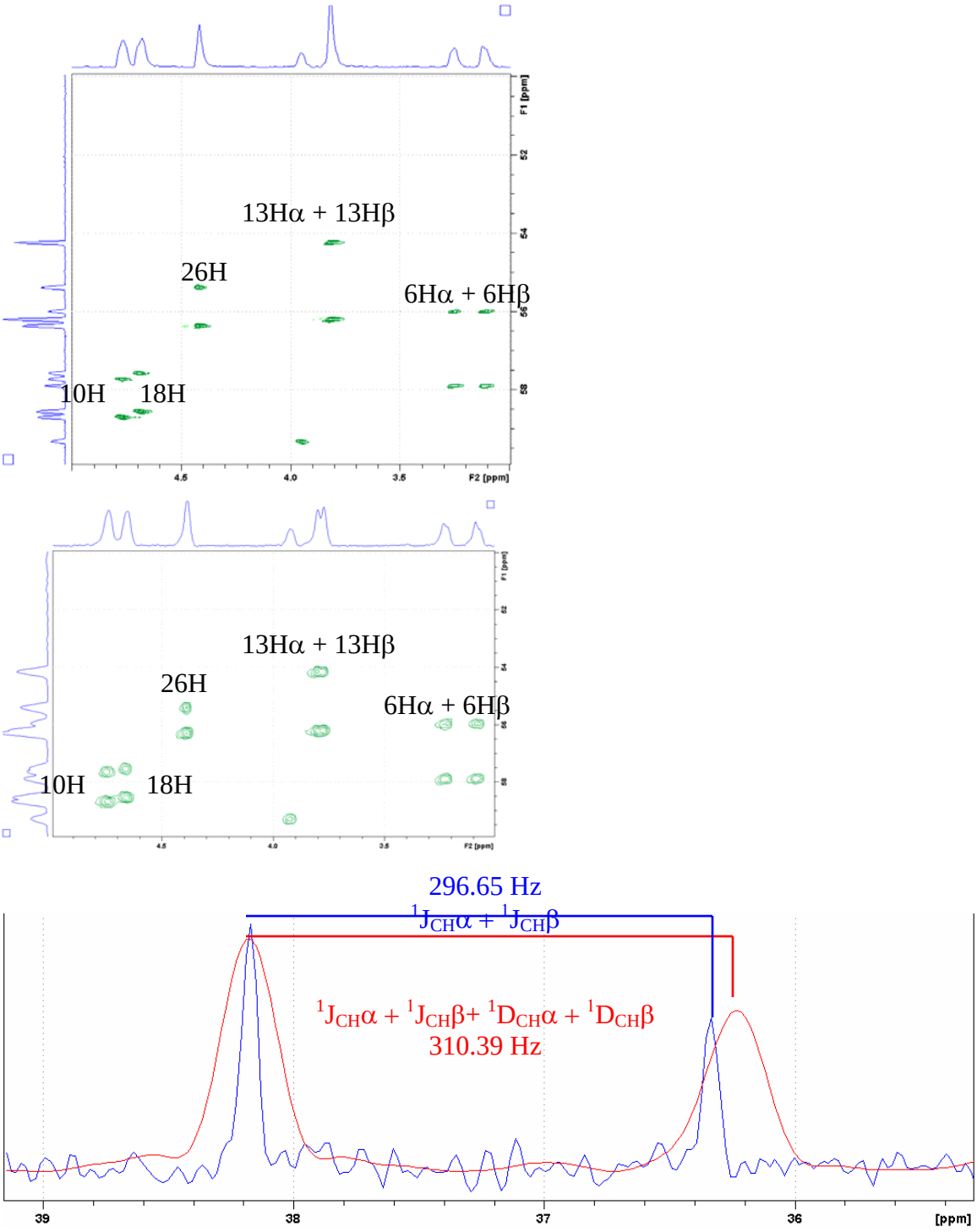

HSQC spectrum without phage solution added and with phages solution added, along with an overlay one a one dimensional slice of the 11Hb-11C resonance

Figure 24 Sample F1-HSQC NMR Spectra

4.5 RANKING OF CONFORMATIONAL SEARCH MODELS' FIT TO RDC DATA

As a first search of the conformational space of **1**, we generated a library of 30 plausible conformers representing structures that contained envelope conformation changes for all three pyrrolidine rings in **1**. This was carried out using a stochastic search[44] with the Amber 94[10] force field within the MOE[9] molecular modeling package. The lowest energy structure from the AMBER 94 force field prediction in MOE was submitted to DFT refinement, as were seven other models. Within this eight member library of structures were models that contained the most reasonable conformations of the three pyrrolidine rings of **1**. From the modeling done with the AMBER 94 force field, each pyrrolidine ring was found to exist in two envelope conformations, and the envelope changes were the most likely conformational changes in **1**.

A.

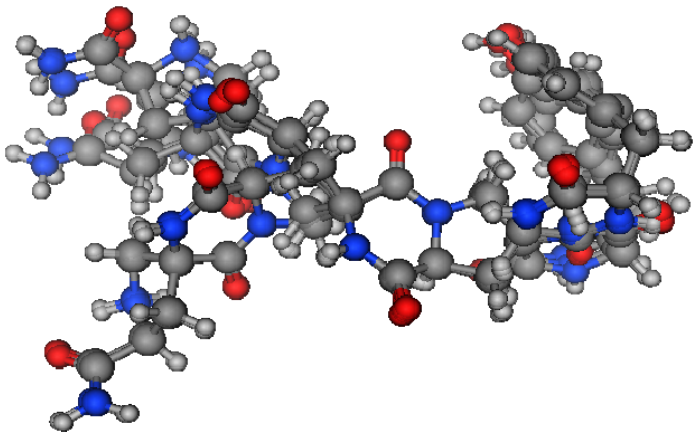

B.

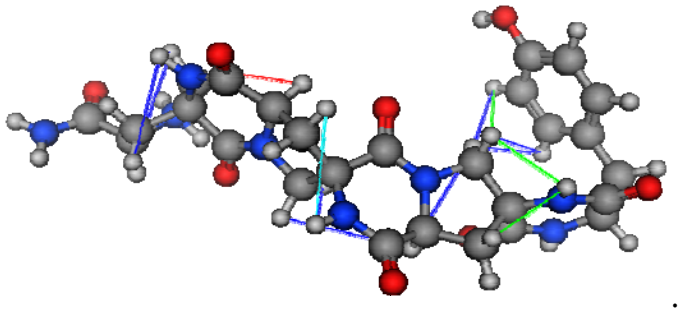

Figure 25 DFT Models of 1

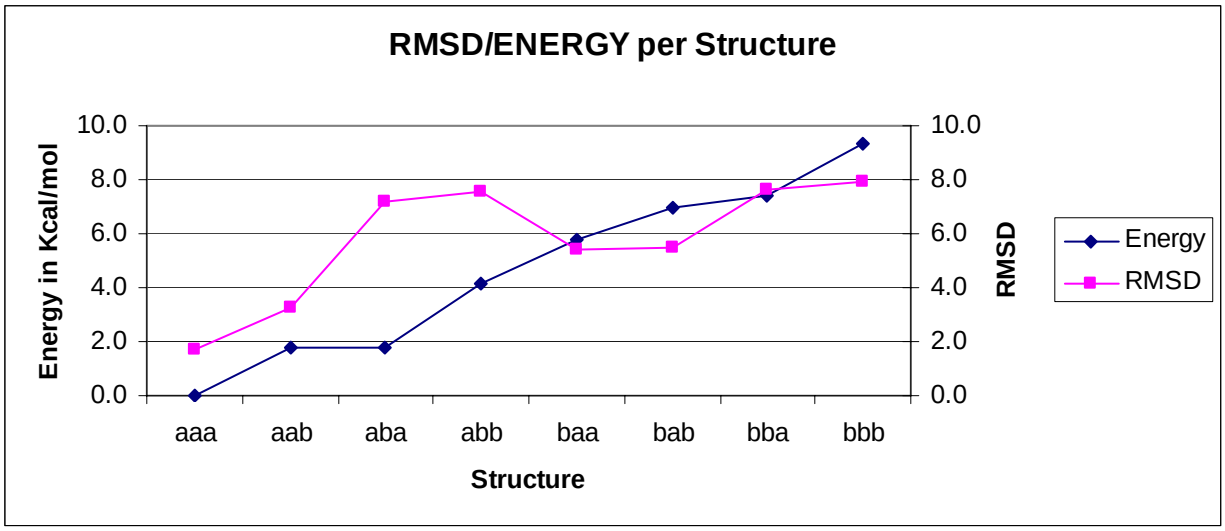

Figure 26 Relative Energy of DFT Refined Structures and RMSD Fit to RDC Data

The structures in the library were named corresponding to the lowest energy AMBER 94 structure: the lowest structure was labeled "aaa", the structure which contained a change in the envelope of the pyrrolidine ring containing C5 was labeled baa. Similar names were given to the other conformers used in the DFT calculations, where each change of a pyrrolidine ring conformation containing C5, C10 or C20 was noted in the as a change from the letter a to b in the three letter code respectively (as an example the flipped conformation at C10 only would be labeled "aba").

The eight DFT optimized structures are shown overlaid in Figure 25a. Figure 25b shows the best fit DFT model structure (RMSD = 1.82, Figure 26). This model was also calculated by DFT calculations to be the lowest energy conformer of **1**. A graph of the correlation of measured RDC values to those calculated from the DFT best fit structure is seen in Figure 27.

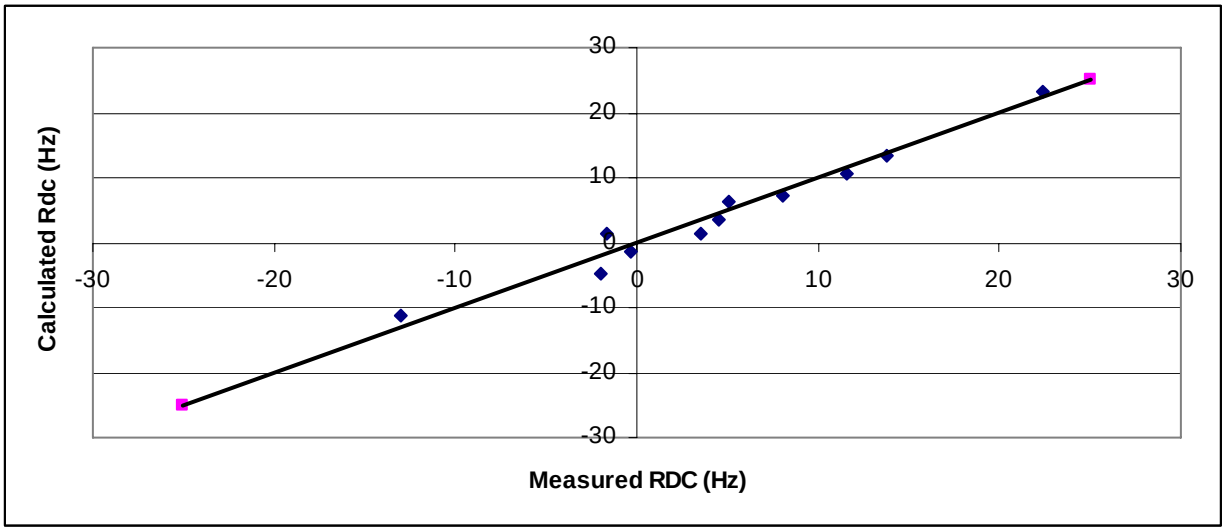

Figure 27 Correlation Chart of Measured versus Calculated RDC Values for Best Fit DFT Structure

4.6 COMPARISON TO ROESY DATA

The best bit conformer structure as determined by residual dipolar coupling shown in Figure 25b is overlaid with ROESY correlations observed in the spectrum of **1.** The observed correlations are consistent with the RDC best fit structure.

The ROESY spectrum of **1** displayed correlations between the N8 amide proton and one each of the geminal C4 and C6 hydrogen atoms. This relationship allowed the facial assignment of the geminal C4 and C6 hydrogen atoms, as the amide N8 stereochemistry was set prior to incorporation into the oligomer. The geminal C4 and C6 hydrogen atoms that had ROESY correlations with the N8 amide proton also were observed to have transanular ROESY correlations with each other. The observed correlations indicated that the pyrrolidine ring containing C4 and C6 was in the envelope conformation seen in Figure 28a. This conformation corresponds to the conformation of this ring in the lowest energy model. A model of the flipped conformation of same pyrrolidine ring can be seen in Figure 28b. This conformation of the pyrrolidine ring was only seen in models of **1** which did not fit well to the ROESY or RDC data, and were calculated to be higher in energy than the best fit model. In Figure 28b, there appears to be a closer approach of the N8 amide proton and the C2 carbonyl. We have reasoned this

approach may increase the steric interaction of these groups making this envelope a higher energy conformation.

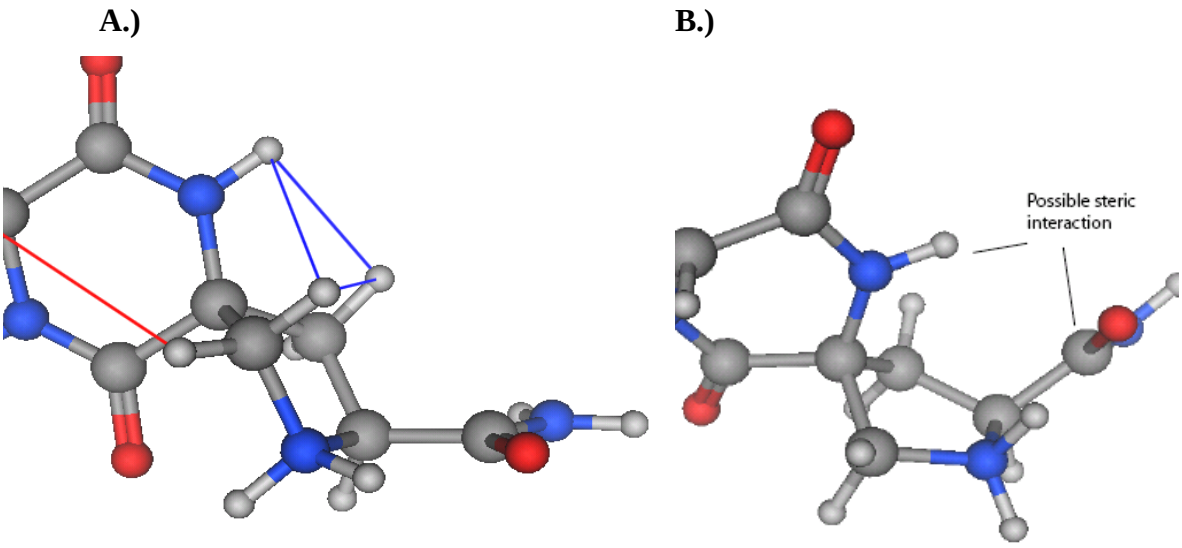

A.) A model of the preferred conformation of a pyrrolidine ring of a pro4(2S4S) monomer in **2** with ROESY correlations overlaid. B.) A model of the "b" conformation of the pyrrolidine ring of a pro4(2S4S) monomer.

Figure 28. Conformations of the Pyrrolidine Ring in Pro4(2S4S) monomer

A similar set of correlations was observed in the ROESY spectrum of **1** for the pyrrolidine ring containing C11 and C13. We again interpreted these results to indicate the pyrrolidine ring containing these atoms appeared to prefer to reside in an envelope conformation which limited steric interaction between the N16 amide proton and the C10 carbonyl. These conformational findings were also consistent with ROESY data collected on other bis peptides[4-8].

4.7 CONCLUSIONS

We were able to use HSQC NMR experiments to measure residual dipolar coupling values for the ^{13}C-^{1}H bonded atoms in the backbone of **1**. Our calculations showed that the lowest energy conformation calculated by DFT had the greatest correlation to the RDC values measured for **1**; the measured and calculated RDC values for the best fit DFT model, "aaa", of **1**

had an RMSD of 1.82. The models calculated to have the next lowest energies, “aab” and “aba”, had RMSD fit values of 3.27 and 7.20 respectively. In solution, compound **1** will be dynamic however our experiments suggest that it spends most of its time in the “aaa” conformation which is the lowest energy conformation according to DFT calculations and the conformation most consistent with the observed RDCs.

The intent of this project was to determine if RDC measurements in conjunction with molecular modeling could be used to aid in the solution structure determination of bis-peptide **1**. We feel confident that since the measured RDC values in **1** included data about the internuclear vectors of all C-H bonds in the polycyclic backbone of **1**, we have been able to identify a probable solution phase structure of **1.** Our interpretation is reinforced by the fact that this model is also consistent with the ROESY correlations observed in **1**.

The benefits of RDCs are that they provide additional NMR constraints for the structure determination of bis-peptide oligomers. RDC constraints are complementary to ROESY constraints in that they provide information on the angular relationship between C-H bonds within a molecule while ROESY constraints provide distance information between pairs of hydrogen atoms that are physically close to each other. In this way, RDCs provide more “global” structural information complementing the more “local” structural information provided by ROESY correlations. As we synthesize longer, more complex bis-peptides the likelihood of overlapped resonances or ambiguous ROESY correlations will increase. The use of RDC constraints to supplement ROESY constraints will allow the structure determination of larger bis-peptides.

4.8 NMR STUDY OF THE BIS-PEPTIDE SEQUENCE *PIP5(2S5R)-PIP5(2R5S)-PRO4(2S4S)*-TYR

We designed a curved scaffold to be used for bifunctional catalyst development. Our approach is to develop curved scaffolds that can hold two functional groups, one on each end of the oligomer, close to each other in space. The scaffold consisted of the monomer sequence *pip5(2S5R)-pip5(2R5S)-pro4(2S4S)*-Tyr[7], **2** (Figure 29). It was necessary to determine the

sequence's solution structure to ensure its curved conformation. To accomplish this, traditional two dimensional NMR correlation experiments were employed and compared to computer models of the oligomer generated using a stochastic conformational search[44] with the MOE[9] molecular modeling program utilizing the AMBER 94[10] force field. I also helped initiate the determination of the solution structure of this molecule using residual dipolar couplings.

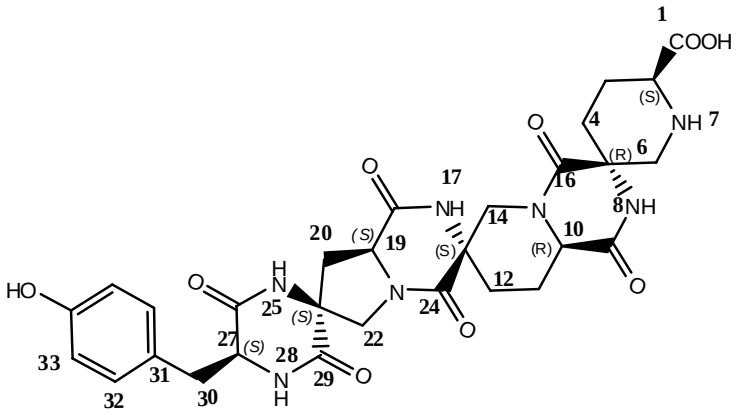

2

Figure 29. ChemicalStructure of the *pip5(2S5R)-pip5(2R5S)-pro4(2S4S)*-Tyr Sequence

4.9 ASSIGNMENT OF ^{1}H AND ^{13}C RESONANCES IN 2

The first step in the determination of the structure of **2** was to assign all of the ^{1}H and ^{13}C resonances. This determination included the assignment of diastereotopic methylene hydrogens. A solution of **2** (10.4 mM) was prepared in 10% D_2O in H_2O, buffered to pH 3.45 with acetic acid-d_4/ ammonium acetate-d_7 buffer. The collection of TOCSY (total correlation spectroscopy), HMBC (heteronuclear multiple bond correlation spectroscopy), and ROESY (rotating frame Overhauser enhancement spectroscopy) spectra was performed at $4^{o}C$ to shift the residual water peak downfield and away from the spectral region where the monomers' α protons generally appear (approx. 4.6 ppm).

The TOCSY spectrum allowed the assignment of protons to the spin systems within **2** (Figure 30), while the HMBC spectrum allowed the assignment of the C-H and C-C connectivity

of the monomers. Additionally the HMBC allowed the inter-residue connectivity to be established through the multiple bond correlations of the diketopiperazine amide protons.

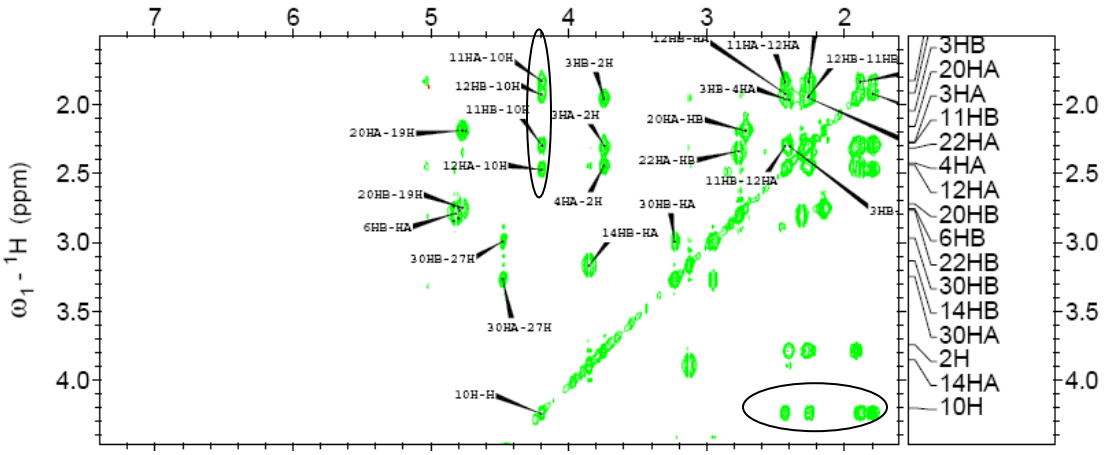

A section of the TOCSY spectrum of **2**. Note the correlations to 10H, where correlations are seen to protons on both C11 and C12. This is an example of one full spin system showing correlations between all members, not just those atoms within three bonds as is observed in COSY-type experiments.

Figure 30. TOCSY Spectrum of 2

The assignment of all H-C correlations within individual residues was accomplished through the portions of the HMBC spectrum shown in Figure 31a and Figure 31b and modeled in Figure 32c (full spectra included in Appendix). The spectra in Figure 32a and Figure 32b show the correlations of the diketopiperazine amide bonds. As can be seen in in the three dimensional rendering of **2** in Figure 32c, each amide proton contained within the diketopiperazine rings was correlated to at least four carbon atoms, for example the N8 proton was correlated to C5, C9, C10 and C16. The C5 and C16 carbon atoms were contained in the *pip5*(2S5R) monomer, while the C9 and C10 carbon atoms were contained in the *pip5*(2R5S) monomer. By combining the assignment of the correlations within the monomer residues with the correlations of the amide protons in the diketopiperazine linkages, network of C-H correlations could be established for **2** from C1 throughout the molecule and into the tyrosine ring (Figure 33). This network of connections assigned all carbon and hydrogen resonances with **2**, but did not allow the assignment of diastereotopic protons.

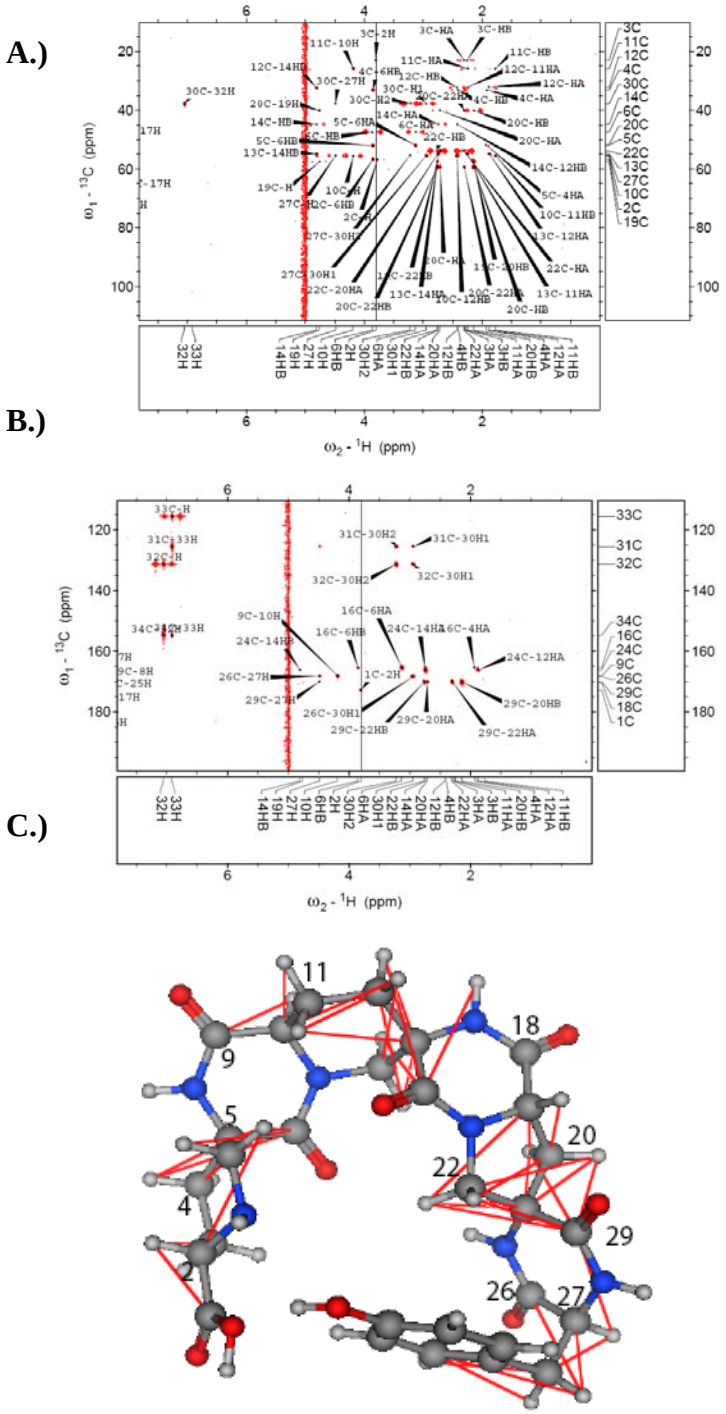

A.) Section of the HMBC spectrum of **2** highlighting the methylene region of the spectrum. B.) Section of HMBC spectrum of **2** highlighting the carbonyl region of the spectrum. C.) Overlay of intra-residue HMBC correlations with theoretical model.

Figure 31. HMBC Spectra Showing Intra-residue Connectivity

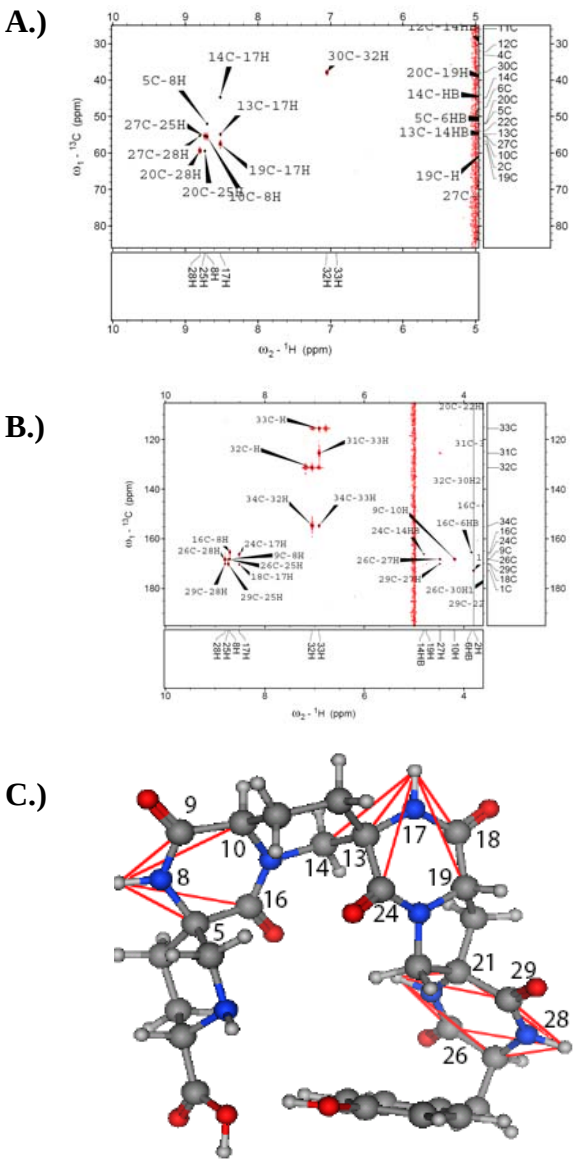

A and B) Sections of HMBC spectrum of 2 highlighting inter-residue correlations. C.) Overlay of inter-residue HMBC correlations with theoretical model.

Figure 32. HMBC Spectra Showing Inter-residue Connectivity

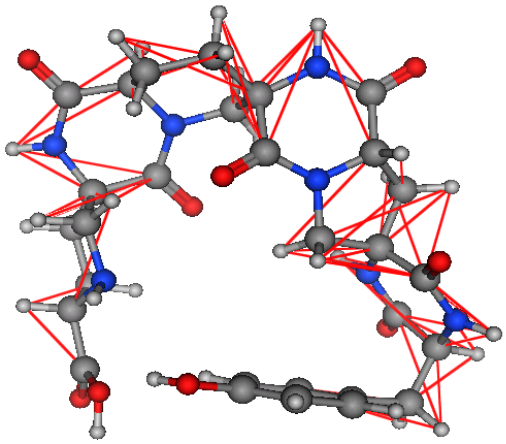

Figure 33. Network of HMBC Correlations used to Assign the ^{1}H and ^{13}C Resonances of 2

4.10 ASSIGNMENT OF THE DIASTEREOTOPIC PROTONS ON METHYLENE GROUPS

The assignment of the methylene protons within **2** was accomplished using ROESY spectroscopy and the absolute stereochemistry of each monomer, which was established in the synthesis of **2**. The known stereochemistry within the monomers was used to assign correlations in the ROESY spectrum (Figure 34a) to the geminal methylene hydrogen atoms of each piperidine or pyrrolidine ring in **2** (Figure 34b). Figure 35 shows the *pip5(2S5R)* monomer of **2** with ROESY correlations from the N8 amide proton overlaid. From the *pip5*(2S4R) monomer stereochemistry, we knew that the diketopiperazine amide hydrogen atom on N8 was on the same face of the piperidine ring as the hydrogen atom on C2. Strong correlations were observed between the N8 hydrogen atom and only one hydrogen atom each on C6 and C4 (Figure 35). We inferred that this C6 hydrogen atom was on the same face of the piperidine ring as the N8 hydrogen atom, and it was termed $C6H_a$; the correlated geminal C4 hydrogen atom was assigned to the same face of the ring and was termed $C4H_a$. One C3 hydrogen atom was observed to have a weak correlation to the N8 hydrogen atom leading us to assign it to the same face as $C6H_a$ and $C4H_a$. A similar network of ROESY correlations between the geminal hydrogen atoms on the

monomer rings and the amide hydrogen atoms of the diketopiperazine rings, or the correlations between the geminal hydrogen atoms and the hydrogen atom on either C10 or C19, were used to assign all of the methylene hydrogen atoms within **2**.

A.) **B.)**

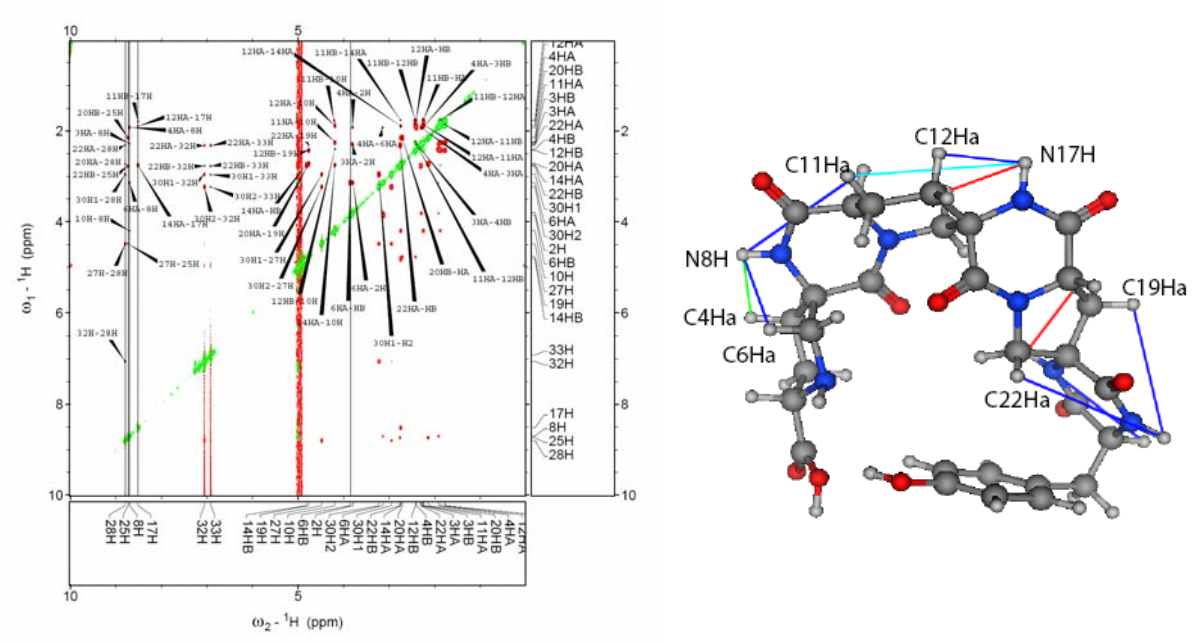

A) ROESY spectrum of **2** B.) ROESY correlations of the diketopiperazine amide hydrogen atoms and methylene hydrogen atoms in **2** are overlaid on the lowest energy conformer of **2** as predicted by the AMBER 94 force field.

Figure 34. ROESY Spectrum and Overlay of Certain Correlations with a Model of 2

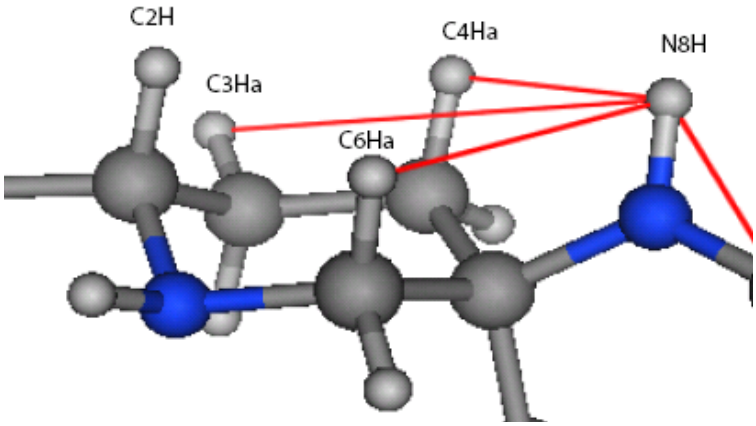

Figure 35. Overlay of ROESY Correlations with *Pip4*(2S5R) Monomer in 2

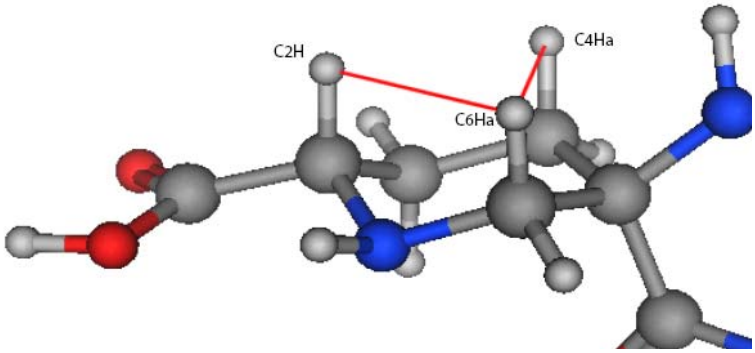

Figure 36. ROESY Correlations Overlaid with *Pip4*(2S5R) Monomer in 2

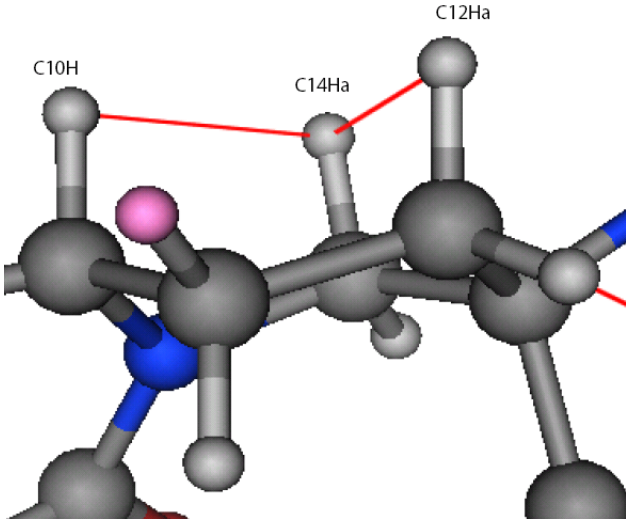

Figure 37. ROESY Correlations Overlaid with *Pip4*(2R5S) Monomer in 2

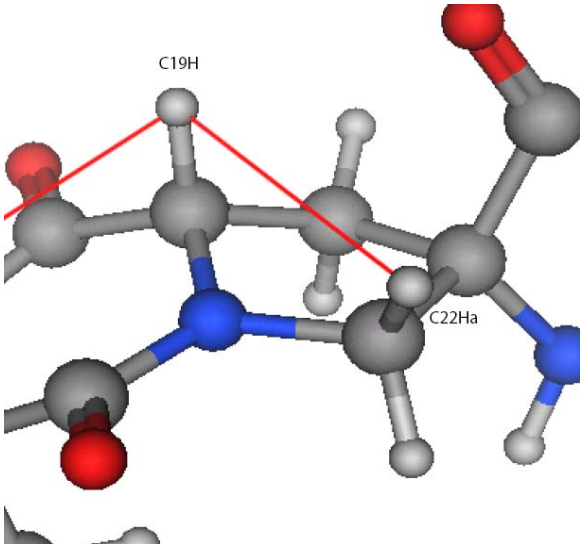

Figure 38. ROESY Correlations Overlaid on a Model of the Pro4(2S4S) Monomer in 2

4.11 DETERMINATION OF THE CONFORMATION OF 2 BY ROESY SPECTROSCOPY

With the methylene hydrogen atoms assigned, the shape of the molecule could be interpreted from the intra and inter-residue ROESY correlations by comparison with model structures. The comparison of ROESY correlations with MOE/AMBER 94 derived conformers of **2** was undertaken to determine which conformer was most consistent with the NMR data.

A correlation between the C2 hydrogen atom and C6Ha in the ROESy spectrum of **2** (Figure 36) were interpreted as indicating a 1,3 diaxial relationship between these protons. The C6Ha and C4Ha hydrogen atoms were correlated in the spectrum and were interpreted to be diaxial. This observation was consistent with the piperidine ring of the *pip5*(2S5R) residue residing in the chair conformation shown in Figure 36. Similarly, a network of correlations between the C10 hydrogen atom with one each of the geminal C12 and C14 protons indicated the chair conformation for the *pip5*(2R5S) monomer as shown in Figure 37.

The conformation of the *pro4*(2S4S) residue was inferred using the correlation of C19H with C22Ha to be the conformation displayed in Figure 38. ROESY correlations between the aryl protons of the tyrosine residue and both C22 protons indicated that the aromatic ring was rotated to be in proximity to C22 of the *pro4*(2S4S) monomer (Figure 39).

A.) **B.)**

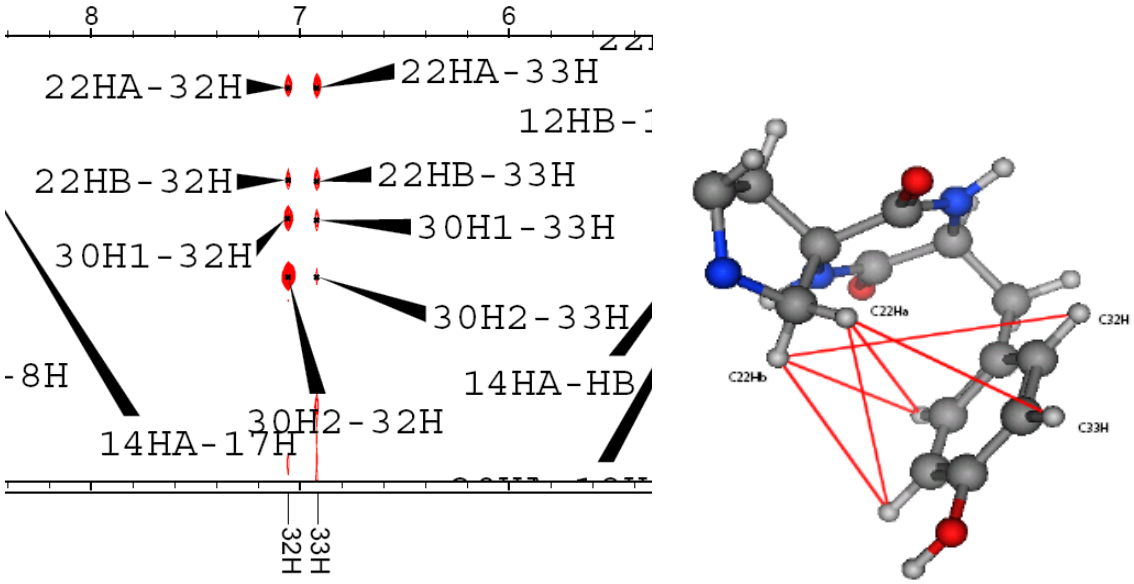

A.) A section of the ROESY spectrum of **2** demonstrating the interactions of the tyrosine aryl protons with the protons on C22. B.) An overlay of the ROESY interactions with the lowest energy conformer of **2**.

Figure 39. ROESY Spectrum Section Showing Tyrosine Interactions with C22 Protons

4.12 CONCLUSIONS

The conformer of **2** found to be most consistent with the NMR data was the conformer predicted by MOE/AMBER 94 to be the thermodynamically favored structure (Figure 40), and was consistent with previous data collected on other bis-peptides[5,6].

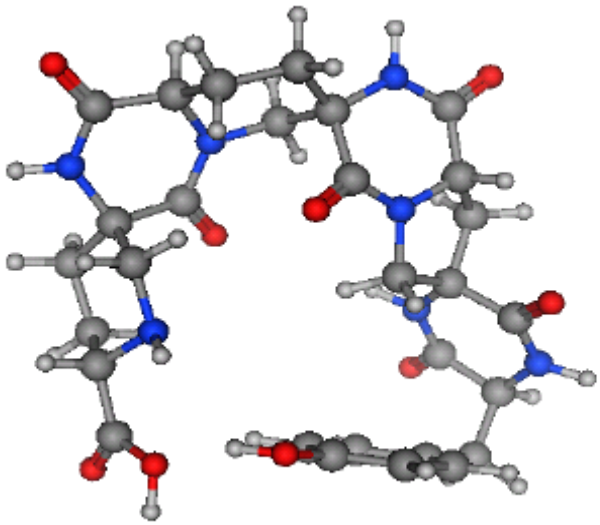

Figure 40. Solution Phase Structure of 2 Determined by ROESY Spectroscopy

The data was most consistent with the *pip5* monomers preferring a chair conformation that places the methine proton of the piperidine ring in a pseudo-axial position. This conformation limits the 1,3-diaxial interaction between the carbonyl group attached to the methine carbon and axial protons within the monomer ring. As an example, the C2 hydrogen atom of the *pip5*(2S4R) monomer is in the axial position in the solution phase structure of **2**.

The limitation of the use of only ROESY correlations to determine a solution structure is highlighted by the interpretation of the *pro4*(2S4S) residue pyrrolidine ring conformation. Only one ROESY correlation was available from the spectrum to interpret the conformation of the pyrrolidine ring. The use of residual dipolar coupling could determine additional constrains on the conformation of this ring allowing a greater confidence in the conformational assignment.

Bis-peptide oligomer **2** was designed to contain a tight curve that placed the ends of the oligomer in close proximity. The solution phase structure we have determined for **2** contains just such a tight curve**.** Our determination of the curved conformation of **2** has led us to further investigate the potential catalytic properties of this molecule, as the close proximity of the two ends of the oligomer may allow its use as a scaffold for bifunctional catalysis.

4.13 EXPERIMENTAL METHODS

Example of preparation of Pro4SS-Pro4RR-Pro4SS-Tyr (1)

Rink Amide AM resin (Novabiochem, 200-400 mesh, 0.63 mmol/g loading), 33.1 mg, was swollen in DMF overnight. The resin was washed with DMF three times and Fmoc deprotected with a solution of 20% piperidine in DMF for 30 minutes. The resin was washed, for five minutes each step, twice with DMF, twice with isopropanol, three times with DMF and once with DCM. Preactivation of the Pro4SS monomer (2 eq with respect to resin loading) was done with 2 eq. O-(7-Azabenzotiazol-1-yl)-N,N,N',N'-tetramethyluronium hexafluorophosphate (HATU) (Aldrich) and 4eq. diisopropylethylamine (DIPEA) in 330 μL of 20%DCM in DMF for five minutes before introduction to the resin. The coupling solution was allowed to react with the resin bound amine for 1 hour. The resin was washed according to the procedure above, and the coupling procedure was repeated with the same monomer.

After washing the resin, Fmoc deprotection was done with 20% piperidine in DMF. The resin was again washed as above and the next residue, Pro4RR, was coupled to the resin as above. This was repeated until the sequence had been formed.

After the terminal tyrosine residue was coupled, the resin was Fmoc deprotected and washed with DMF, acetic acid, DCM, methanol, DCM, then methanol. Drying of the resin was accomplished by placing it under vacuum overnight. Cleavage of the dried resin was performed with 95% trifluoroacetic acid (TFA), 2.5% triispropylsilane, and 2.5% water (total volume 1 mL) for two hours. The cleavage solution was removed and the resin washed with additional TFA. The combined cleavage solution and wash solution was dried down to solid with a stream of dry N_2.

The residue was dissolved in 1 mL of 20% piperidine in 1-methyl-2-pyrrolidinone (NMP) and was incubated for 3 days at room temperature to allow closure of the diketopiperazine rings. Closure was monitored by LCMS with a one-half hour gradient of 0-25% acetonitrile in water with 0.1% formic acid added.

After closure was complete the NMP solution was diluted in 40 mL of diethyl ether to precipitate the product. Centrifugation at 3200 RPM for 30 min. concentrated the precipitate, allowed the ether to be decanted from the tube and the precipitate to be dissolved in 1 mL of water with 0.1% TFA added. This solution was HPLC purified on a Varian Pro Star Preparatory

HPLC system with an Xterra Prep MS C18 5 μm diameter column (6.5 mL/min flow rate, 0-25% gradient over 30 minutes of acetonitrile in water with 0.1% formic acid added) and dried down to a white powder in a Savant Speed Vac SC110. The yield of product was determined by UV absorbance of the tyrosine residue at 274 nm to be 10.2 μmol (48.8% yield based on resin loading). HRMS –Q-Tof : $[M+H]^+$ calcd for $C_{27}H_{31}N_8O_8$ 595.2265; found 595.2268.

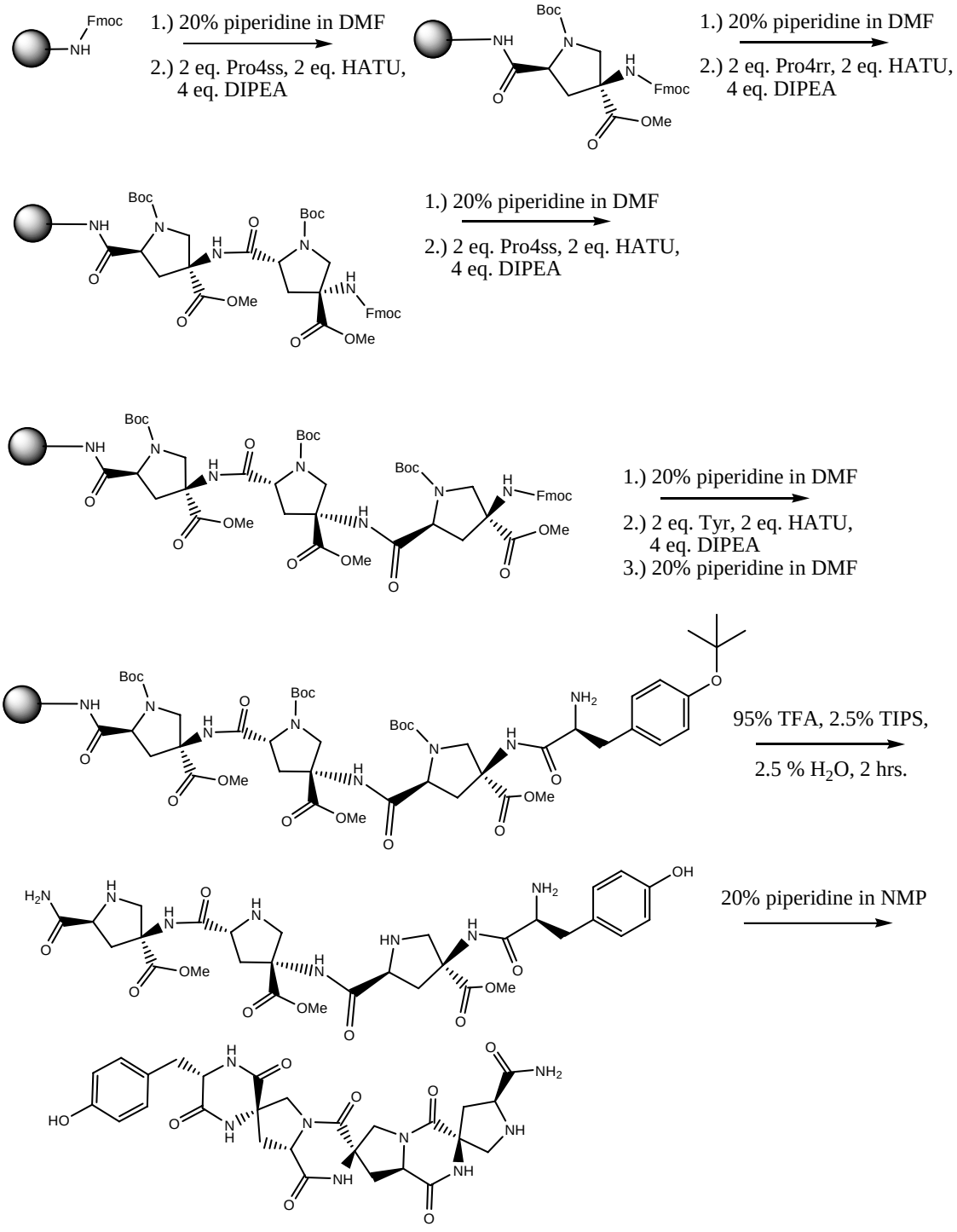

NMR Sample preparation for complete assignment

A portion of the sample was brought up in 400 uL of 20 mM acetate buffered 10% D_2O in H_2O (pH 3.49) and placed in a Shigemi NMR tube for spectral collection. An aliquot of 2 μL from the NMR sample was diluted up 50 μL and tested for absorbance at 274 nm. The concentration of the sample was 8.5 mmol/L. This sample was used to establish the identity of individual resonances through HMBC, TOCSy and ROESy experiments obtained at 277 K on a Bruker DRX 600 MHz instrument.

Example Spectra of Assignment

TOCSy

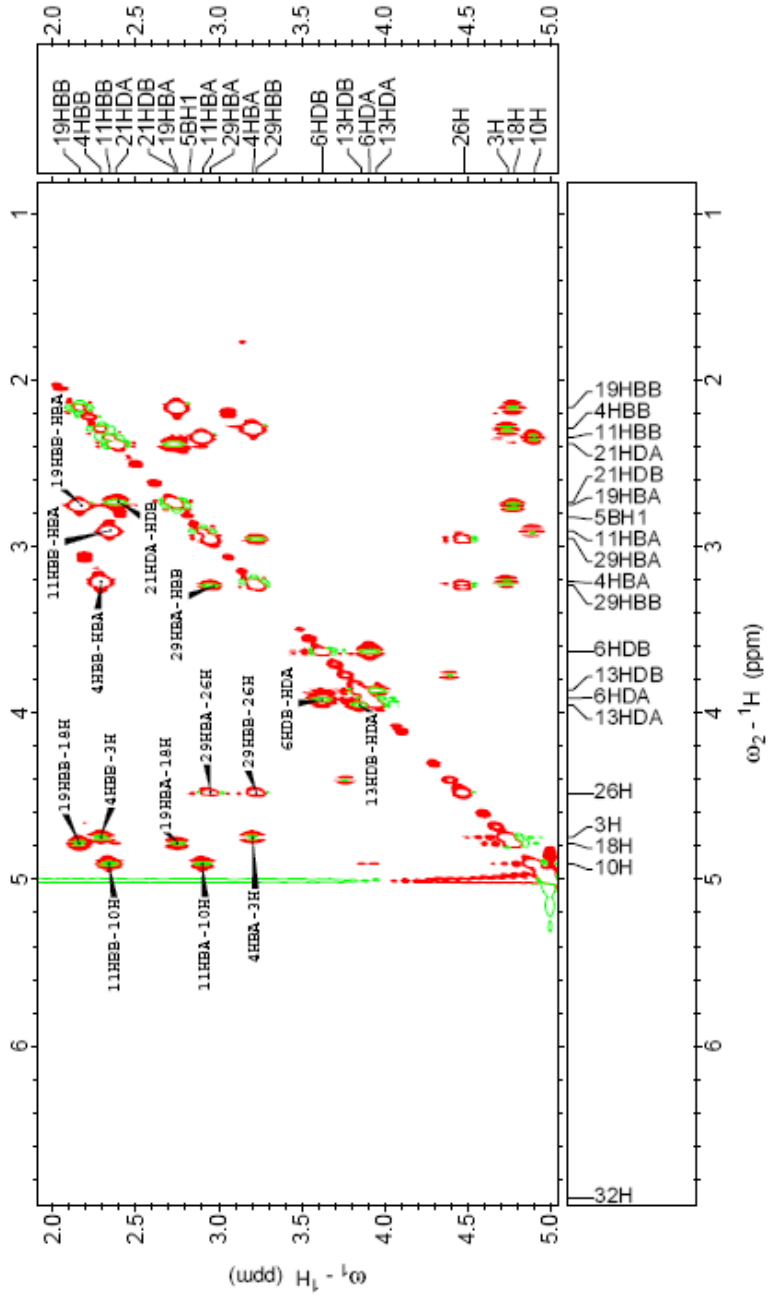

ROESy

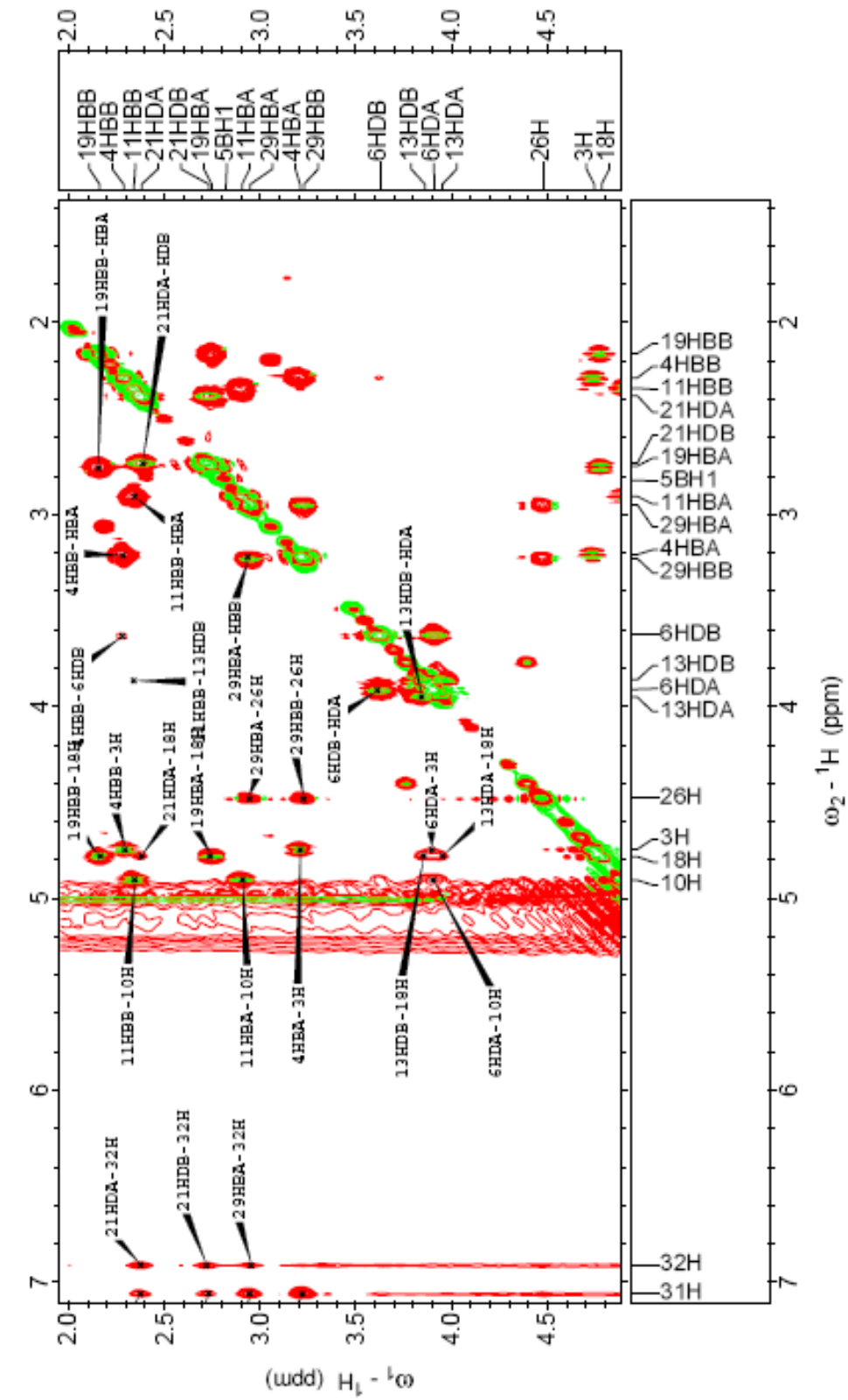
19HBB
4HBB
11HBB
21HDA
21HDB
19HBA
5BH1
11HBA
29HBA
4HBA
29HBB
6HDB
13HDB
6HDA
13HDA
26H
3H
18H
19HBB-HBA
21HDA-HDB
4HBB-HBA
11HBB-HBA
29HBA-HBB
13HDB-HDA
29HBA-26H
29HBB-26H
6HDB-HDA
21HDA-18H
6HDA-3H
13HDA-18H
11HBB-10H
11HBA-10H
4HBA-3H
13HDB-18H
6HDA-10H
21HDA-32H
21HDB-32H
29HBA-32H
10H
31H
32H
ω1 - 1H (ppm)
ω2 - 1H (ppm)

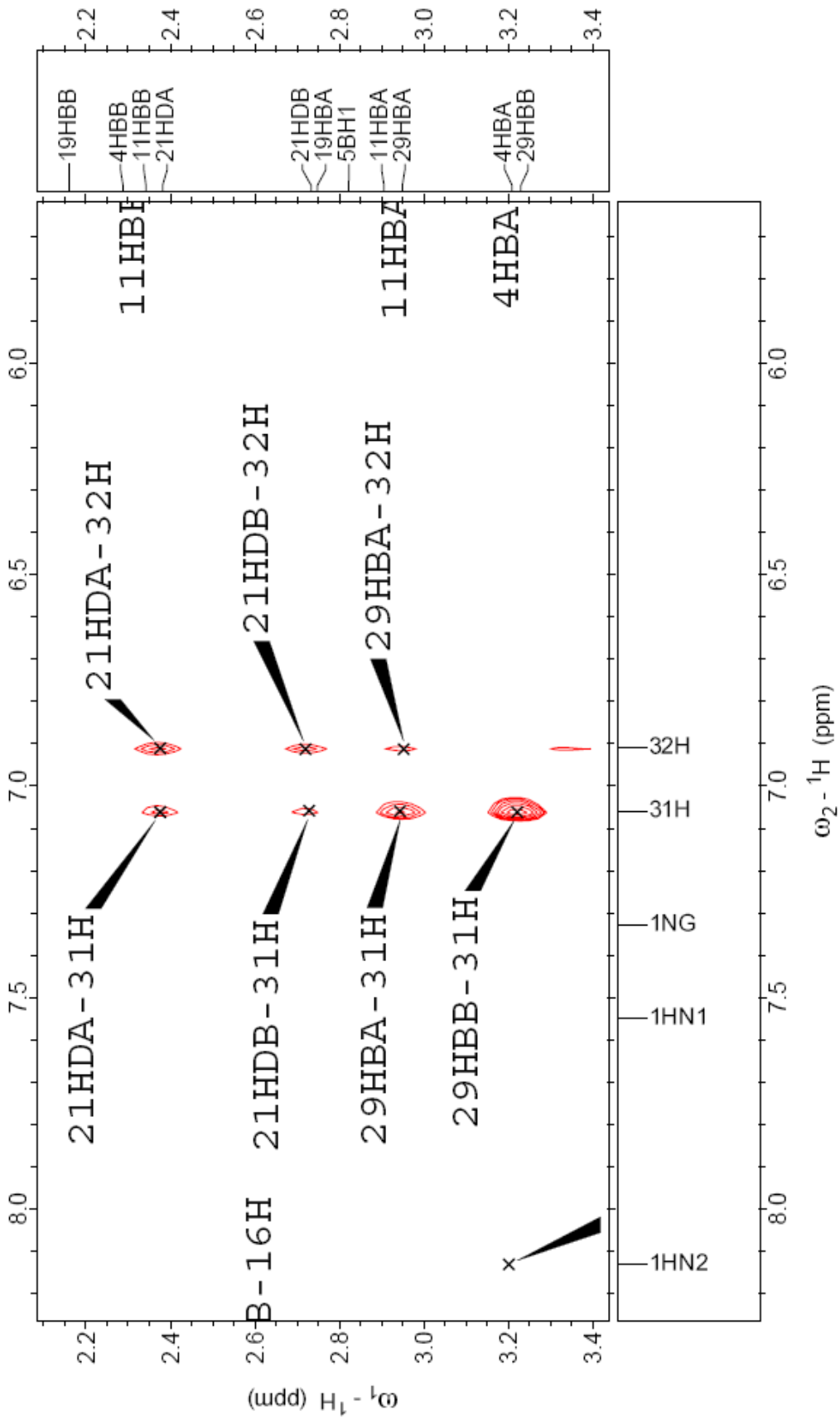
19HBB
4HBB
11HBB
21HDA
21HDB
19HBA
5BH1
11HBA
29HBA
4HBA
29HBB
11HBB
11HBA
4HBA
21HDA-32H
21HDB-32H
29HBA-32H
21HDA-31H
21HDB-31H
29HBA-31H
29HBB-31H
B-16H
32H
31H
1NG
1HN1
1HN2
ω1 - 1H (ppm)
ω2 - 1H (ppm)

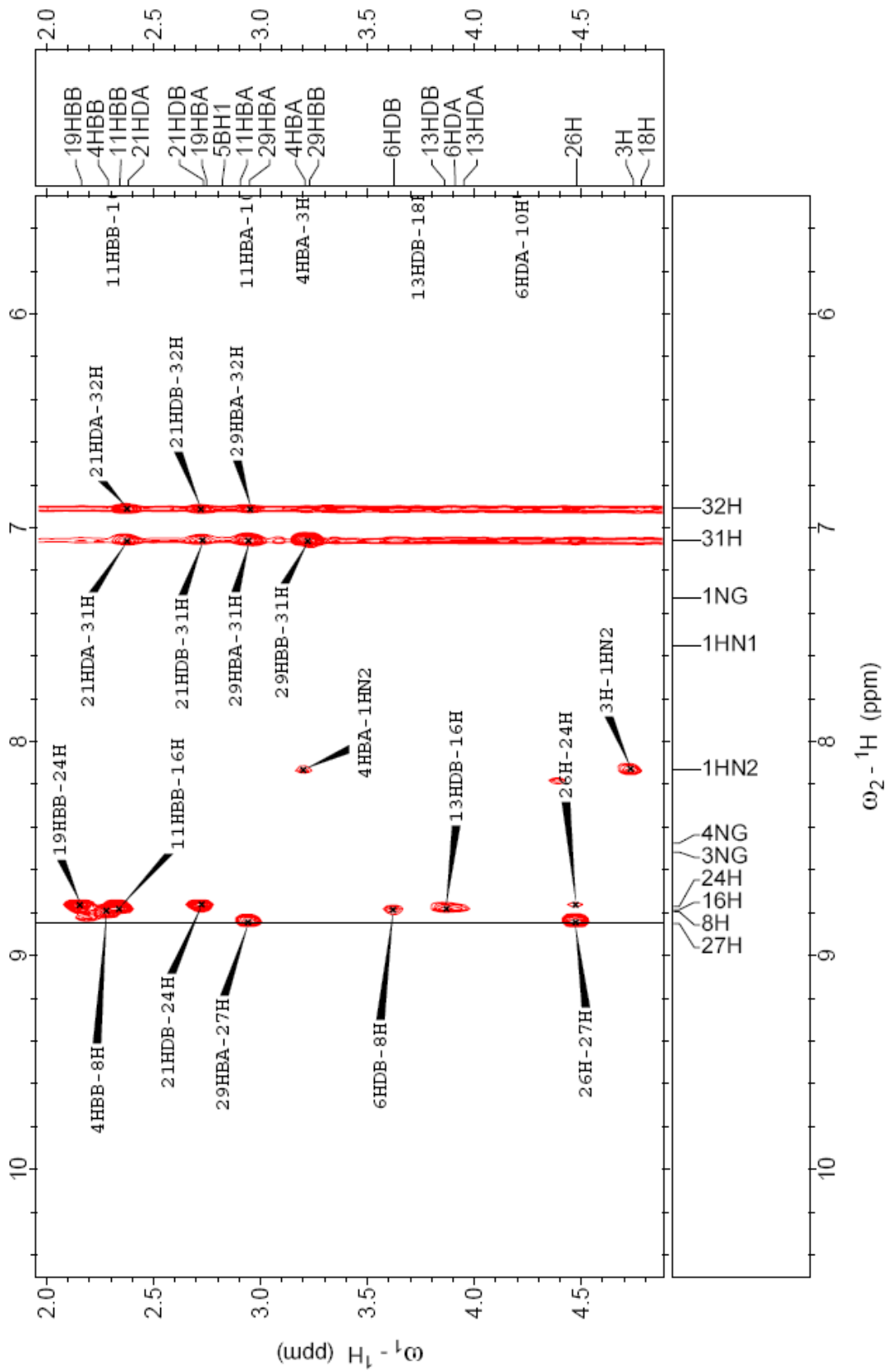
19HBB
4HBB
11HBB
21HDA
21HDB
19HBA
5BH1
11HBA
29HBA
4HBA
29HBB
6HDB
13HDB
6HDA
13HDA
26H
3H
18H
11HBB-1
11HBA-1
4HBA-3H
13HDB-18
6HDA-10H
21HDA-32H
21HDB-32H
29HBA-32H
21HDA-31H
21HDB-31H
29HBA-31H
29HBB-31H
4HBA-1HN2
13HDB-16H
26H-24H
3H-1HN2
19HBB-24H
11HBB-16H
4HBB-8H
21HDB-24H
29HBA-27H
6HDB-8H
26H-27H
32H
31H
1NG
1HN1
1HN2
4NG
3NG
24H
16H
8H
27H
ω_1 - ^{1}H (ppm)
ω_2 - ^{1}H (ppm)

HMBC

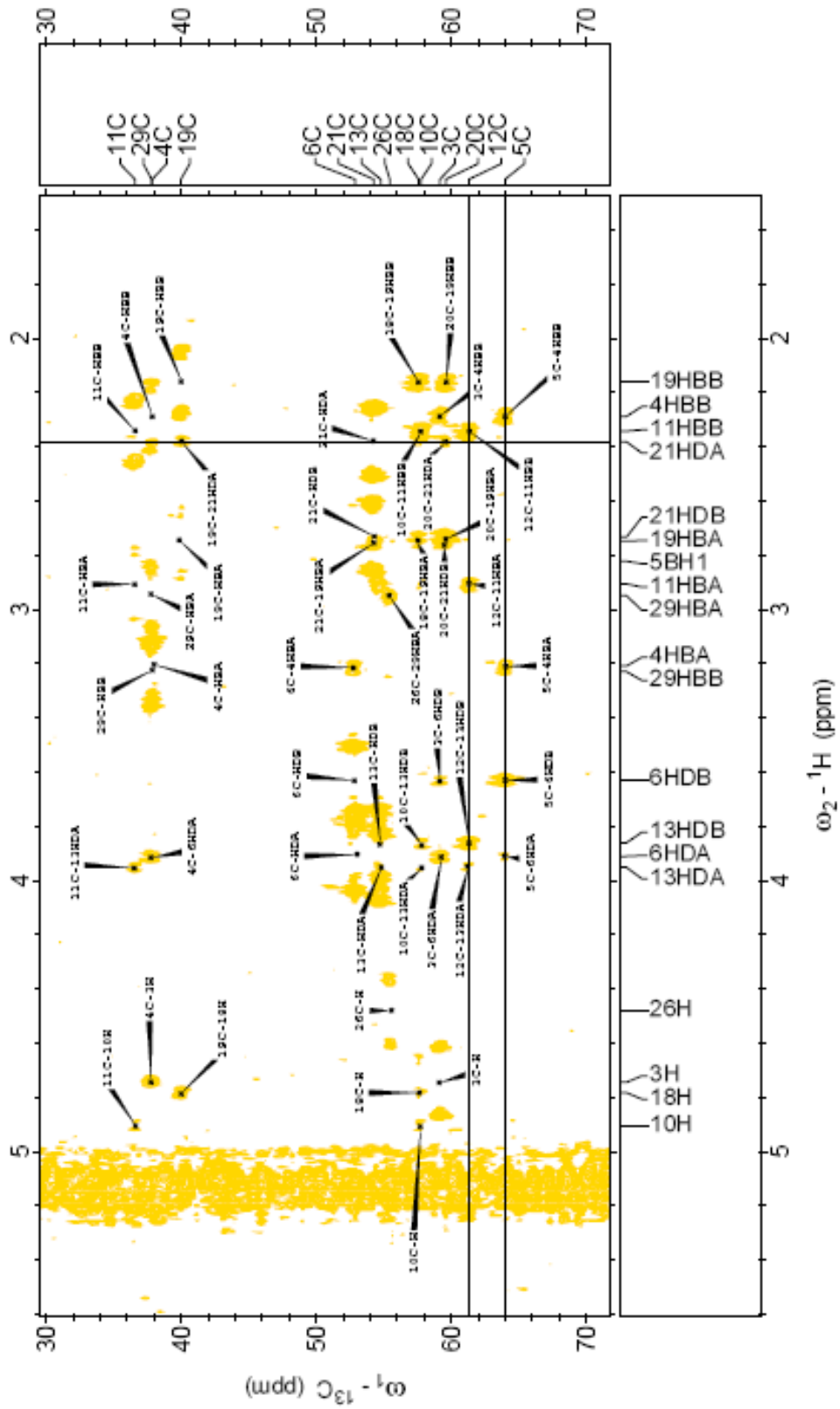
11C
29C
4C
19C
6C
21C
13C
26C
18C
10C
3C
20C
12C
5C
19HBB
4HBB
11HBB
21HDA
21HDB
19HBA
5BH1
11HBA
29HBA
4HBA
29HBB
6HDB
13HDB
6HDA
13HDA
26H
3H
18H
10H
ω1 - 13C (ppm)
ω2 - 1H (ppm)

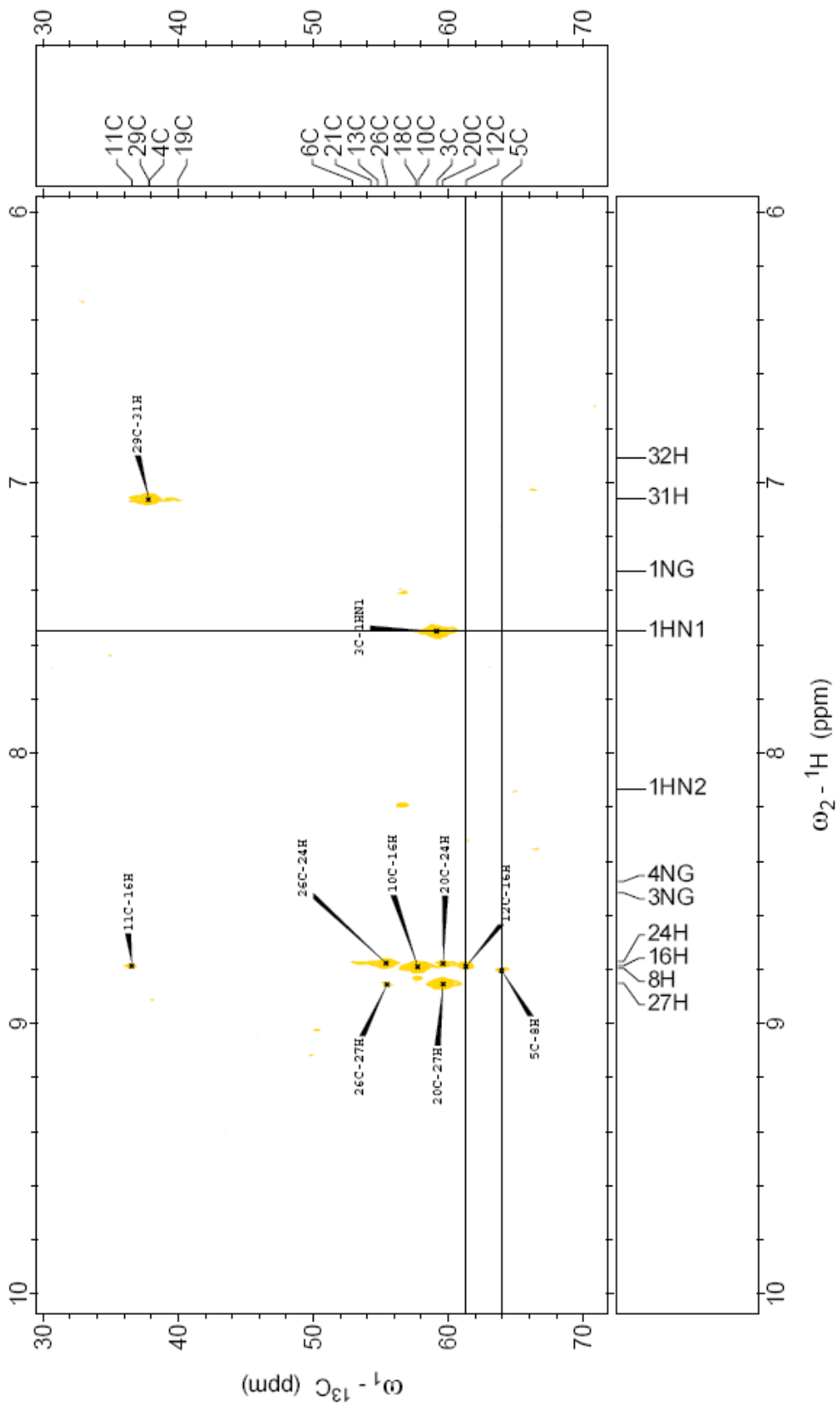
11C
29C
4C
19C
6C
21C
13C
26C
18C
10C
3C
20C
12C
5C
29C-31H
3C-1HN1
11C-16H
26C-24H
10C-16H
20C-24H
12C-16H
26C-27H
20C-27H
5C-8H
32H
31H
1NG
1HN1
1HN2
4NG
3NG
24H
16H
8H
27H
ω1 - 13C (ppm)
ω2 - 1H (ppm)

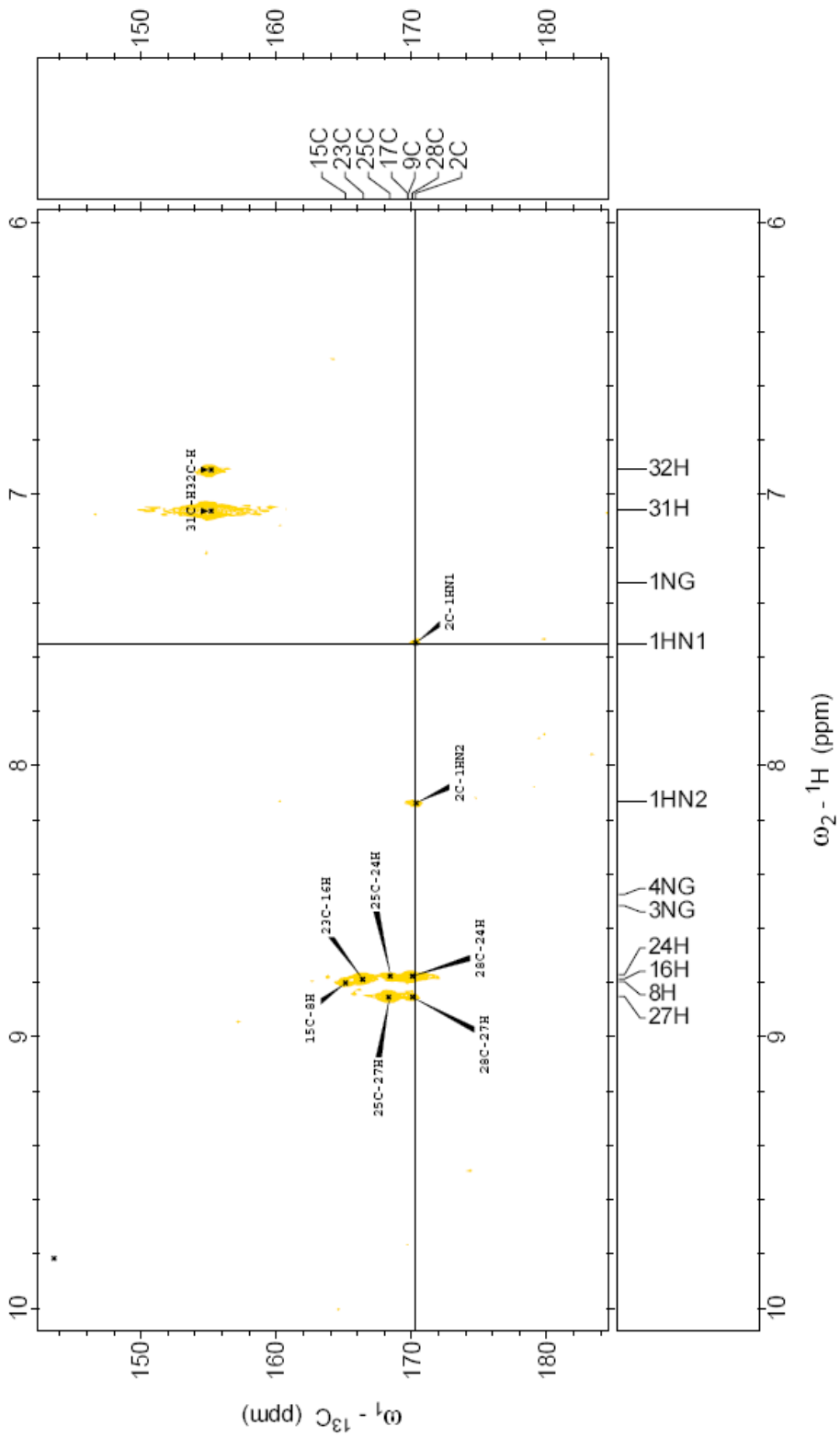
15C
23C
25C
17C
9C
28C
2C
31C-H32C-H
2C-1HN1
2C-1HN2
23C-16H
25C-24H
28C-24H
15C-8H
28C-27H
25C-27H
32H
31H
1NG
1HN1
1HN2
4NG
3NG
24H
16H
8H
27H
ω1 - 13C (ppm)
ω2 - 1H (ppm)

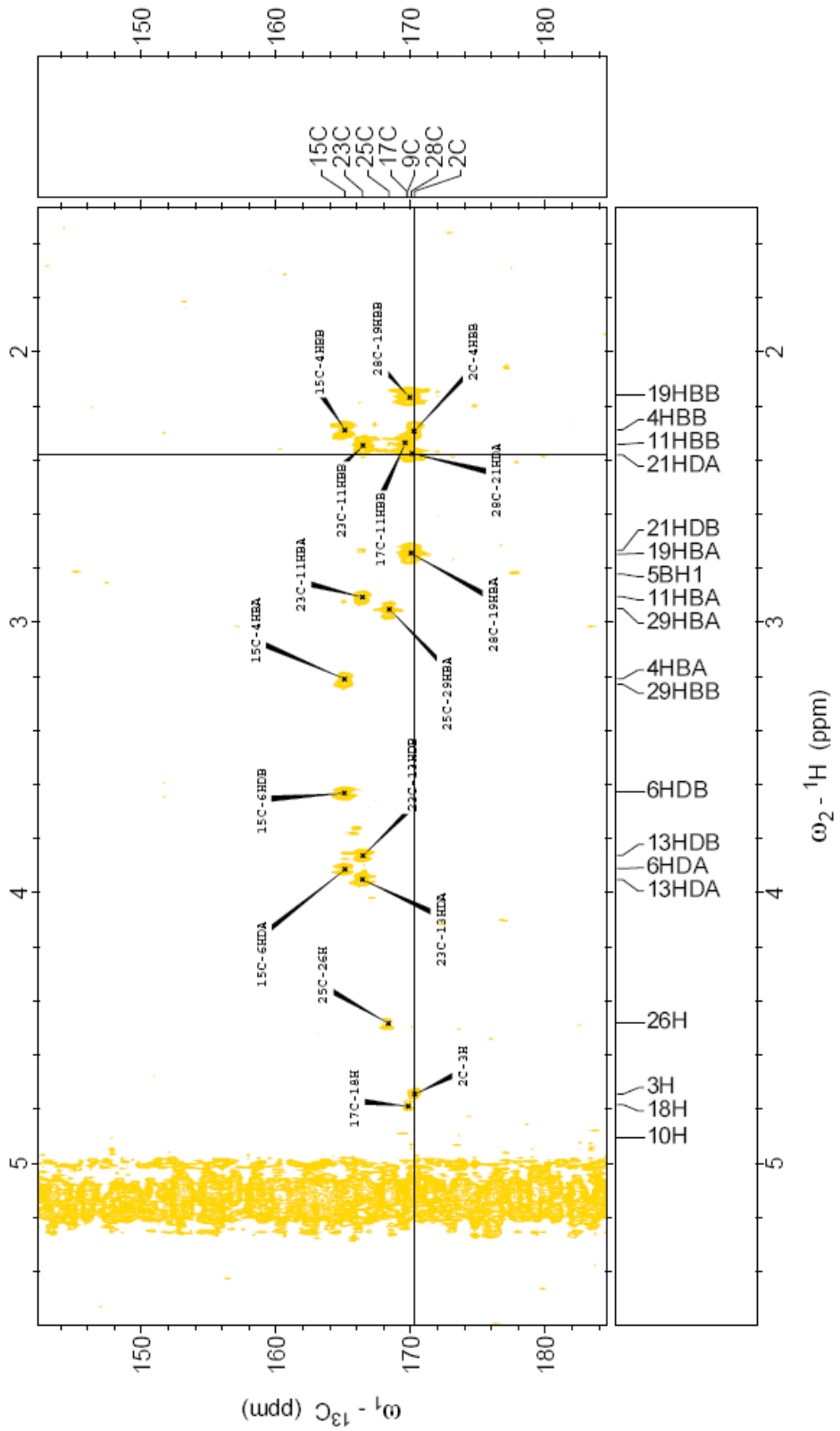
15C
23C
25C
17C
9C
28C
2C
19HBB
4HBB
11HBB
21HDA
21HDB
19HBA
5BH1
11HBA
29HBA
4HBA
29HBB
6HDB
13HDB
6HDA
13HDA
26H
3H
18H
10H
ω_1 - ^{13}C (ppm)
ω_2 - ^{1}H (ppm)

Unaligned NMR sample preparation (F2 coupled)

A portion of the sample was brought up in 350 uL of 50 mM phosphate buffered D_2O (pD 7.49) and placed in a Shigemi NMR tube. The analyte concentration of this sample was 4.6 mM. This sample was used to determine the $^1J_{CH}$ coupling constants as measured in the F2 dimension of an HSQC experiment on a Bruker 800MHz NMR with a cryoprobe and sample temperature of 298 K. The data was collected at 16K data points in the F2 dimension and 256 points in the F1. The introduction of coupling was achieved by setting the decoupling pulse strength during signal acquisition to 120 dB.

Dialysis of phage

Pf1 Magnetic Resonance Cosolvent Solution (pf1 phage 54mg/ml in 10 mM phosphate buffered H_2O, pH 7.6) was purchased from Asla Biotech. To obtain aligned spectra in D_2O, samples of the phage solution were dialyzed with pD 7.49 50 mM phosphate buffered D_2O. 200 μL of the supplied phage solution was placed in a Millipore Biomax 10K NMWL Membrane Filter and diluted to 1.5 mL with buffer. The filtration device was placed in a 40 mL Falcon tube and Centrifuged at 3200 rpm for 4 hours. The residual phage was resuspended with an additional 1.5 ml of buffer and centrifuged for four hours. The residual phage was diluted with a volume of buffered D_2O sufficient to give a 50 mg/ml solution. Final concentration of phage was determined by UV absorbance at 270 nm and was found to be 45.5 mg/mL.

Aligned NMR sample preparation (F2 coupled)

An amount of dialyzed phage solution sufficient to achieve a 10 mg/ml solution of phage (98 μL) was added to the 350 μL sample of analyte to give a 3.6 mM analyte concentration and a second F2 dimension coupled HSQC spectrum was collected at 298 K (16K data points F2, 256 F1).

Collection of F1 coupled HSQC spectra

The deletion of the 180 degree, ^1H channel pulse during the incremented delay period allowed for $^1J_{CH}$ coupling values to be viewed in the F1 (carbon) dimension of the spectrum. A sample of the trimer was dissolved in 350 μL of 50 mM phosphate buffered (pD 7.49) D2O.

This sample was determined to be 4.2 mM in analyte. The HSQC spectrum was obtained on a Bruker DRX 600MHZ instrument equipped with a cryoprobe and a sample temperature of 298K. The spectrum was collected with 4K data points in the F2 dimension and 2K data points in the F1 dimension. For methine groups the splitting was equivalent to the $^{1}J_{CH}$ value, while for methylene groups the splitting was equivalent to the sum of both $^{1}J_{CH}$ values.

Deuterium oxide dialyzed phage alignment media, 76 μL of 45.5 mg/mL concentration was added to this sample to give a final analyte concentration of 3.4 mM and a phage concentration of 10mg/mL. This sample was used for the measurement of the summed $^{1}J_{CH}$ and $^{1}D_{CH}$ values.

Group	Atom	Nuc	Chemical Shift
1	C	13C	172.85
18	C	13C	170.366
29	C	13C	170.094
26	C	13C	168.334
9	C	13C	168.131
24	C	13C	166.182
16	C	13C	165.397
34	C	13C	154.764
32	C	13C	131.363
31	C	13C	125.516
33	C	13C	115.548
19	C	13C	57.519
2	C	13C	56.722
10	C	13C	55.478
27	C	13C	55.33
13	C	13C	54.852
22	C	13C	53.864
5	C	13C	51.924
20	C	13C	51.643
6	C	13C	47.426
14	C	13C	44.766
30	C	13C	37.772

4	C	13C	33.104
12	C	13C	32.205
11	C	13C	25.839
3	C	13C	22.981
28	H	1H	8.799
25	H	1H	8.736
8	H	1H	8.702
17	H	1H	8.517
32	H	1H	7.055
33	H	1H	6.918
14	HB	1H	4.814
19	H	1H	4.765
27	H	1H	4.485
10	H	1H	4.194
6	HB	1H	3.858
2	H	1H	3.799
30	H2	1H	3.227
6	HA	1H	3.137
30	H1	1H	2.952
22	HB	1H	2.766
14	HA	1H	2.747
20	HA	1H	2.715
12	HB	1H	2.425
4	HB	1H	2.404
22	HA	1H	2.313
3	HA	1H	2.293
3	HB	1H	2.263
11	HA	1H	2.248
20	HB	1H	2.144
4	HA	1H	1.928
12	HA	1H	1.879
11	HB	1H	1.773

All values are relative to TMS

Pro4ss-Pro4rr-Pro4ss-Y

Group	Atom	Nuc	Shift
2	C	13C	170.314
28	C	13C	170.055
17	C	13C	169.719
25	C	13C	168.392
23	C	13C	166.442
15	C	13C	165.119
31	C	13C	131.486
32	C	13C	125.297
5	C	13C	63.996
12	C	13C	61.319
20	C	13C	59.596
3	C	13C	59.171
10	C	13C	57.775
18	C	13C	57.596
26	C	13C	55.461
13	C	13C	54.786
21	C	13C	54.276
6	C	13C	52.887
19	C	13C	39.988
4	C	13C	37.863
29	C	13C	37.825
11	C	13C	36.584
27	H	1H	8.85
8	H	1H	8.793
16	H	1H	8.786
24	H	1H	8.771
1	HN2	1H	8.134
1	HN1	1H	7.55
31	H	1H	7.059
32	H	1H	6.91
10	H	1H	4.905
18	H	1H	4.782
3	H	1H	4.745
26	H	1H	4.479

13	HA	1H	3.95
6	HA	1H	3.911
13	HB	1H	3.863
6	HB	1H	3.627
29	H2	1H	3.229
4	HA	1H	3.209
29	H1	1H	2.949
11	HA	1H	2.906
19	HA	1H	2.748
21	HB	1H	2.732
21	HA	1H	2.38
11	HB	1H	2.341
4	HB	1H	2.288
19	HB	1H	2.162

All values are relative to TMS

4.2

Synthesis of 4.2 was performed by Christopher Morgan

NMR Sample preparation for complete assignment

2 was dissolved in 400 uL of 20 mM acetate buffered 10% D_2O in H_2O (pH 3.49) and placed in a Shigemi NMR tube for spectral collection. An aliquot of 2 μL from the NMR sample was diluted up 50 μL and tested for absorbance at 274 nm. The concentration of the sample was 10.3 mmol/L. This sample was used to establish the identity of individual resonances through HMBC, TOCSy and ROESy experiments obtained at 277 K on a Bruker DRX 600 MHz instrument.

BIBLIOGRAPHY

(1) Roco, M. C.; Bainbridge, W. S. *Societal Implications of Nanoscience and Nanotechnology*; Kluwer Academic Publishers: Boston, 2001.

(2) Gellman, S. H. *Acc. Chem. Res.* **1998**, *31*, 173-180.

(3) Hill, D. J.; Mio, M. J.; Prince, R. B.; Hughes, T. S.; Moore, J. S. *Chem Rev* **2001**, *101*, 3893-4012.

(4) Habay, S. A.; Schafmeister, C. E. *Org Lett* **2004**, *6*, 3369-3371.

(5) Gupta, S.; Das, B. C.; Schafmeister, C. E. *Org Lett* **2005**, *7*, 2861-2864.

(6) Levins, C. G.; Schafmeister, C. E. *J Am Chem Soc* **2003**, *125*, 4702-4703.

(7) Levins, C. G.; Schafmeister, C. E. *J Org Chem* **2005**, *70*, 9002-9008.

(8) Levins, C. G.; Brown, Z. Z.; Schafmeister, C. E. *Org Lett* **2006**, *8*, 2807-2810.

(9) 2005.06 ed.; Chemical Computing Group, Inc: Montreal, Canada, 2005.

(10) Cornell, W. D.; Cieplak, P.; Bayly, C. I.; Gould, I. R.; Merz, K. M. J.; Ferguson, D. M.; Spellmeyer, D. C.; Fox, T.; Caldwell, J. W.; Kollman, P. A. *J Am Chem Soc* **1995**, *117*, 5179-5197.

(11) Bucherer, H. T.; Steiner, W. J. *J. Prakt. Chem./Chem-Ztg.* **1934**, *140*, 129-150.

(12) Bucherer, H. T.; Fischbeck, H. T. *J. Prakt. Chem./Chem-Ztg.* **1934**, *140*, 69.

(13) Rapoport, H.; Lubell, W. D. *J. Am. Chem. Soc.* **1987**, *109*, 236-239.

(14) Sharma, R.; Lubell, W. D. *J. Org. Chem.* **1996**, *61*, 202-209.

(15) Jamison, T. F.; Lubell, W. D.; Dener, J. M.; Kirshe, M. J.; Rapoport, H. *Org. Synth., CV 9*, 103.

(16) Lubell, W. D.; Rapoport, H. *J. Am. Chem. Soc.* **1987**, *109*, 236-239.

(17) Corey, E. J.; Link, J. O. *J. Am. Chem. Soc.* **1991**, *114*, 1906-1908.

(18) Dominguez, C.; Ezquerra, J.; Baker, S. R.; Borrelly, S.; Prieto, L.; Espada, M.; Pedregal, C. *Tet. Lett.* **1998**, *39*, 9305-9308.

(19) Katritzky, A. R.; Todadze, E.; Angrish, P.; Draghici, B. *J. Org. Chem.* **2007**, *72*, 5794-5801.

(20) Humphrey, J. M.; Chamberlin, A. R. *Chem. Rev.* **1997**, *97*, 2243-2266.

(21) Pellicciari, R.; al, e. *Med Chem Res* **1992**, *2*, 491.

(22) Maruoka, K.; Concepcion, A. B.; Yamamoto, H. *J. Org. Chem.* **1994**, *59*, 4725-4726.

(23) Edward, J. T.; Jitrangsri, C. *Canadian Journal of Chemistry* **1975**, *53*, 3339-3350.

(24) Azumaya, I.; Aebi, R.; Kubik, S.; Rebek, J., Jr. *Proc. Natl. Acad. Sci. U. S. A.* **1995**, *92*, 12013-12016.

(25) Gupta, S.; Macala, M.; Schafmeister, C. E. *J Org Chem* **2006**, *71*, 8691-8695.

(26) Bothner-By, A. A.; Stephens, R. L.; Lee, J.-M.; Warren, C. D.; Jeanloz, R. W. *J Am Chem Soc* **1984**, *106*, 811-813.
(27) Bax, A.; Davis, D. G. *J. Magn. Reson.* **1985**, *63*, 207-213.
(28) Pornsuwan, S.; Bird, G.; Schafmeister, C. E.; Saxena, S. *J Am Chem Soc* **2006**, *128*, 3876-3877.
(29) Klochkov, A. V.; Khairutdinov, B. I.; Tagirov, M. S.; Klochkov, V. V. *Magn. Reson. Chem.* **2005**, *43*, 948-951.
(30) Mangoni, A.; Esposito, V.; Randazzo, A. *Chem Commun (Camb)* **2003**, 154-155.
(31) Thiele, C. M.; Berger, S. *Org Lett* **2003**, *5*, 705-708.
(32) Thiele, C. M. *J Org Chem* **2004**, *69*, 7403-7413.
(33) Yan, J.; Kline, A. D.; Mo, H.; Shapiro, M. J.; Zartler, E. R. *J Org Chem* **2003**, *68*, 1786-1795.
(34) Yan, J.; Delaglio, F.; Kaerner, A.; Kline, A. D.; Mo, H.; Shapiro, M. J.; Smitka, T. A.; Stephenson, G. A.; Zartler, E. R. *J Am Chem Soc* **2004**, *126*, 5008-5017.
(35) Tjandra, N.; Bax, A. *Science* **1997**, *278*, 1111-1114.
(36) Azurmendi, H. F.; Martin-Pastor, M.; Bush, C. A. *Biopolymers* **2002**, *63*, 89-98.
(37) Martin-Pastor, M.; Bush, C. A. *Biopolymers* **2000**, *54*, 235-248.
(38) Sanders, C. R., 2nd; Schwonek, J. P. *Biochemistry* **1992**, *31*, 8898-8905.
(39) Hansen, M. R.; Mueller, L.; Pardi, A. *Nat. Struct. Biol.* **1998**, *5*, 1065-1074.
(40) Tycko, R.; Blanco, F. J.; Ishhii, Y. *J Am Chem Soc* **2000**, *122*, 9340-9341.
(41) Bax, A. *Protein Sci* **2003**, *12*, 1-16.
(42) Homayoun, V.; Prestegard, J. H. *J. Mag. Res.* **2004**, *167*, 228-241.
(43) Bax, A.; Zweckstetter, M. *J Am Chem Soc* **2000**, *122*, 3791-3792.
(44) Ferguson, D. M.; Raber, D. J. *J Am Chem Soc* **1989**, *111*, 4371-4378.